4-[^{18}F]Fluoroiodobenzene and its applications in palladium-mediated Sonogashira cross coupling reactions.

by

Jenilee Dawn Way

A thesis submitted in partial fulfillment of the requirements for the degree of

Master of Science

in

Experimental Oncology

Department of Oncology

University of Alberta

© Jenilee Dawn Way, 2014

Abstract

4-[^{18}F]Fluoroiodobenzene and its applications in palladium-mediated Sonogashira cross coupling reactions.

Way, Jenilee[1]; Wang, Monica[1]; Wuest, Melinda[1]; Bergmann, Cody[1]; Hamann, Ingrit[1]; Wuest, Frank[1*]

[1] *University of Alberta, Department of Oncology, Edmonton, Alberta, Canada*

The ongoing demand for novel ^{18}F-labelled radiotracers is frequently accompanied with the need to develop novel radiolabelling techniques. Synthesizing radiotracers should preferentially involve rapid, selective and functional group-tolerating reactions. In this line, the use of catalysts such as enzymes or transition metal complexes has proved to be particularly valuable for rapid and efficient syntheses of a wide variety of ^{18}F-radiolabelled compounds.

Here we present a four-chapter Masters thesis:

Chapter 2 starts with a review of palladium-mediated cross-coupling reactions in radiochemistry[1]. Showing the utility and versatility of various Pd-mediated chemical reactions as applicable to the synthesis of radiolabelled PET imaging probes. From this review we will be focusing on the use of the Sonogashira reaction, which involves the reaction between 4-[^{18}F]fluoroiodobenzene ([^{18}F]FIB) along with a terminal alkyne in order to create a new carbon-carbon bond.

Chapter 3 outlines the use [^{18}F]FIB in the Sonogashira cross-coupling reaction as it provides the ability to produce large amounts of this prosthetic group in a

reliable and robust manner. In line with this, we created a fully automated synthesis of [^{18}F]FIB[2], achieving 89 ± 10 % (n=7) decay-corrected radiochemical yields within a reaction time of 59 ± 2 min including HPLC purification. Allowing for up to 6.4 GBq of [^{18}F]FIB to be produced from 10.4 GBq of n.c.a. [^{18}F]fluoride, with a radiochemical purity greater than 97 % and a specific activity greater than 40 GBq/μmol.

In chapter 4, we demonstrate the applicability of the Sonogashira cross-coupling reaction using ASU produced [^{18}F]FIB to a simple amino acid of propargylglycine in order to produce the novel ^{18}F-labelled amino acid radiotracer of 2-amino-5-(4-[^{18}F]fluorophenyl)pent-4-ynoic acid ([^{18}F]FPhPA)[3]. This C-C bond forming reaction is optimized in terms of the Pd-complexes, solvents, reaction temperatures, reaction times and amounts of propargylglycine and triethylamine used. After complete optimization and HPLC purification [^{18}F]FPhPA could be obtained in 42 ± 10% (n=11) decay-corrected radiochemical yields within 56 ± 5 min based on 4-[^{18}F]fluoroiodobenzene. Overall 480 MBq of D/L-[^{18}F]FPhPA could be isolated in high radiochemical purity of greater 95% starting from 1200 MBq of 4-[^{18}F]fluoroiodobenzene.

[^{18}F]FPhPA was also analyzed in both *in vivo* and *in vitro* with EMT6 cells, as compared to the current clinical standard amino acid radiotracer of [^{18}F]FET. Overall as a PET imaging agent L-[^{18}F]FPhPA gave a maximum standardized uptake value (SUV) of 1.35 after 60 min p.i. which was higher than that of the

comparable L-[^{18}F]FET (SUV_{60min} 1.22) in BALB/c mice bearing subcutaneous EMT6 tumors.

Finally, chapter 5 illustrates the expanded application of this methodology from a single acid to a larger 9 amino acid peptide as the Sonogashira reaction with [^{18}F]FIB is further tested in terms of applicability to biomolecules. Here the reaction of [^{18}F]FIB with a model bombesin peptide, is tested in terms of Pd-complexes, solvents, reaction temperatures, reaction times, and peptide concentration. After complete optimization [^{18}F]FBpBBN could be achieved with a 71 ± 4% radiochemical yield after a 35 min reaction time, including HPLC purification. The specific activity of [^{18}F]FBpBBN was calculated to be 625 ± 334 GBq/μmol (n=3). Overall showing the utility of this method in radiolabelling a biological molecules of interest, as optimized this reaction proceeds at room temperature in as little as 10 minutes.

Overall, an innovative and useful method is demonstrated which can lead to the ^{18}F-radiolabelling of biomolecules using aqueous reaction conditions with a palladium mediated cross-coupling reaction.

References: [1] Way *et al. Curr. Org. Chem.*, **2013**, *17*, 2138-2152.

[2] Way *et al. J. Labelled Compds. Radiopharm.*, **2014**, *57*, 104-109.

[3] Way *et al. Nucl. Med Biol.*, **2014**, *41*, 660-669.

Preface

Chapter 2:

*Way, J. D.; Bouvet, V.; and Wuest, F. Synthesis of 4-[^{18}F]fluorohalobenzenes and palladium-mediated cross-coupling reactions for the synthesis of ^{18}F-labelled radiotracers. *Current Organic Chemistry*, **2013**, *17*, 2138-2152.

Contributions: Dr. Bouvet was responsible for the preparation of the 1st half of the review article and I was responsible for the preparation of the 2nd half of the review article. This entails everything proceeding **section 1.4** Transition metal chemistry was prepared by myself. Permission was obtained from Dr. Bouvet for the use of his section of the review.

Chapter 3:

*Way, J. D. and Wuest, F. Automated radiosynthesis of no-carrier-added 4-[^{18}F]fluoroiodobenzene: a versatile building block in ^{18}F radiochemistry. *Journal of Labelled Compounds & Radiopharmaceuticals,* **2014**, *57*, 104-109.

Contributions: I was responsible for all of the experimental work in this publication.

Chapter 4:

*Way, J. D.; Wang, M.; Wuest, M.; and Wuest, F. Synthesis and evaluation of 2-amino-5-(4-[^{18}F]fluorophenyl)pent-4-ynoic acid ([^{18}F]FPhPA): A novel ^{18}F-labelled amino acid for oncologic PET imaging. *Nuclear Medicine and Biology*, **2014**, *41,* 660-669.

Contributions: I completed all testing of reaction parameters for the Sonogashira reaction along with any radiochemistry. I also did perform a few cell uptake studies, but Monica Wang performed the majority of the *in vitro* work. Also, Dr. Ingrit Hamann performed the western blot work and Dr. Melinda Wuest performed the *in vivo* PET imaging. Permission was obtained from all involved for this inclusion of this work in my thesis.

Dedication

I dedicate this work to my family, which supported me through the long stressful workdays. Especially my husband Sion Woodfield for his loving support and also my two puppies Lucy Way and Dexter Way. Also, I would like to dedicate this to my Mom and Dad; Kathy and Eugene Way to which I would not be here today and whom I will always love dearly.

Love, Jenilee

Acknowledgements

I would firstly like to thank the support of my supervisor Dr. Frank Wuest for all the help and guidance he provided with my Master's work. Also I would like to acknowledge the rest of the Wuest group as well, especially Monica Wang, Melinda Wuest, Cody Bergmann to which this work would not have been able to be completed without their expertise in cell biology, PET imaging and peptide synthesis.

Next, I would like to thank Dr. John Wilson, David Clendening and Blake Lazurko from the Edmonton PET Center for radionuclide production and excellent technical support.

Also, I would like to thank my committee members of Dr. John Wilson, Dr. Carlos Velasquez, and Dr. Frank Wuest for support and guidance in preparation of this thesis.

I also gratefully acknowledge the Dianne and Irving Kipnes Foundation and the National Science and Engineering Research Council of Canada (NSERC) for supporting this work.

Table of contents

Abstract……... ii

Preface……. v

Dedication……vii

Acknowledgements……. viii

Table of contents…….……ix

List of tables…… xvi

List of figures…….. xvii

Abbreviations…….. xxiv

Chapter 1 – Introduction……... 1

1.1. Positron emission tomography……... 1

1.2. PET radionuclides……...…2

1.3. Radiochemistry with fluoride-18..……..…4

1.4. Hypothesis and rationale……..... 4

1.5. References…….. 6

Chapter 2 – Synthesis of 4-[^{18}F]fluorohalobenzenes and palladium-mediated cross-coupling reactions for the synthesis of ^{18}F-labelled radiotracers……..… 11

2.1. Introduction…… 11

2.2. Synthesis of 4-[^{18}F]bromofluorobenzene and 4-[^{18}F]fluoro-iodobenzene……..... 14

2.2.1. [^{18}F]Fluorine recoil chemistry…… 17

2.2.2. Direct electrophilic aromatic radiofluorination……..…… 18

2.2.3. Direct nucleophilic aromatic radiofluorination……..… 19

2.2.3.1. Balz-Schiemann reaction……21

2.2.3.2. The Wallach reaction……..……21

2.2.3.3. Applications of [^{18}F]KF……..22

2.2.3.4. Iodyl leaving group…….……22

2.2.3.5. Trimethylammonium leaving group……..……..…23

2.2.3.6. Nitro leaving group…….……23

2.2.4. DNAR followed by decarbonylation……..……23

2.2.5. Iodonium salts as labeling precursors for the preparation of 4-[^{18}F]fluorohalobenzenes……..……25

2.2.6. Sulfonium salts……...…… 27

2.2.7. Application of new technologies…… 28

2.2.7.1. Iodonium salts with microwave activation…….……29

2.2.7.2. Microfluidic technology……..… 30

2.2.8. Summary……..…31

2.3. Application of 4-[^{18}F]fluorohalobenzenes in palladium-mediated cross-coupling reactions…….…… 31

2.3.1. Stille reactions with 4-[^{18}F]fluorohalobenzenes……..… 31

2.3.2. Suzuki reactions with 4-[^{18}F]fluorohalobenzenes……..… 35

2.3.3. Sonogashira reaction with [^{18}F]fluorohalobenzenes……...……36

2.3.4. Buchwald *N*-arylation reactions with 4-[^{18}F]fluorohalobenzenes…..37

2.4. Novel developments……...…… 39

2.4.1. Palladium-mediated nucleophilic radiofluorinations……..39

2.4.2. Electrophilic late-stage radiofluorinations……..41

2.5. Conclusions……...……. 43

2.6. Acknowledgements…… 44

2.7. References…… 44

Chapter 3 – Automated radiosynthesis of no-carrier added 4-[^{18}F]fluoroiodobenzene: A versatile building block in ^{18}F-radiochemistry…….……52

3.1. Introduction…… 52

3.2. Experimental……...……54

3.2.1. General……54

3.2.2. Preparation of kryptofix 2.2.2. solution……..……54

3.2.3. Manual synthesis of 4-[^{18}F]fluoroiodobenzene ([^{18}F]FIB)…… 55

3.2.4. Fully automated synthesis of 4-[^{18}F]fluoroiodobenzene ([^{18}F]FIB)...55

3.2.5. HLPC purification of 4-[^{18}F]fluoroiodobenzene ([^{18}F]FIB).....56

3.3. Results and discussion……57

3.3.1. Optimization of reaction parameters for manual synthesis of 4-[^{18}F]fluoroiodobenzene……...… 57

3.3.1.1. Influence of solvent on radiosynthesis of [^{18}F]FIB…… 58

3.3.1.2. Influence of temperature on radiosynthesis of [^{18}F]FIB……..…59

3.3.1.3. Influence of reaction time on radiosynthesis of 4-[^{18}F]FIB……..… 60

3.3.1.4. Influence of labelling precursor amount on radiosynthesis of 4-[^{18}F]FIB……...…… 61

3.3.1.5. Influence of solid phase extraction (SPE) cartridges on radiosynthesis of [^{18}F]FIB……..…… 61

3.3.1.6. Summary of optimized reaction parameters for the manual synthesis of [^{18}F]FIB……..… 62

3.3.2. Automated synthesis of [^{18}F]FIB……62

3.3.3. HLPC purification of 4-[^{18}F]fluoroiodobenzene ([^{18}F]FIB).....63

3.4. Conclusions…… 64

3.5. Acknowledgements…….……...…… 64

3.6. Conflict of Interest…….……64

3.7. References……..…… 65

Chapter 4 – Synthesis and evaluation of 2-amino-5-(4-[^{18}F]fluorophenyl)pent-4-ynoic acid ([^{18}F]FPhPA): A novel ^{18}F-labelled amino acid for oncologic PET imaging……..…… 67

4.1. Introduction…… 67

4.2. Materials and methods……69

4.2.1. General……69

4.2.2. Chemistry..... 71

4.2.2.1. General procedure for the synthesis of D/L-FPhPA, L-FPhPA, and L-FPhPA.....71

4.2.2.2. D/L-(2-amino-5-(4-[^{19}F]fluorophenyl)pent-4-ynoic acid) (D/L-FPhPA).....72

4.2.2.3. Synthesis of L-(2-amino-5-(4-[^{19}F]fluorophenyl)pent-4-ynoic acid) (L-FPhPA).....72

4.2.2.4. Synthesis of D-(2-amino-5-(4-[^{19}F]fluorophenyl)pent-4-ynoic acid) (D-FPhPA).....72

4.2.3. Radiochemistry……..……73

4.2.3.1. Syntheses of 4-[^{18}F]fluoroiodobenzene ([^{18}F]FIB) and *O*-(2-[^{18}F]fluoroethyl-L-tyrosine ([^{18}F]FET)……..73

4.2.3.2. Formulation of 4-[^{18}F]fluoroiodobenzene ([^{18}F]FIB) for use in cross-coupling reactions..... 73

4.2.3.3. Manual synthesis of 2-amino-5-(4-[^{18}F]fluorophenyl) pent-4-ynoic acid ([^{18}F]FPhPA)..... 73

4.2.3.4. HLPC purification of [^{18}F]FPhPA.....74

4.2.3.5. Formulation of [^{18}F]FPhPA solutions for use in cell and small animal PET studies..... 74

4.2.4. Pharmacology and radiopharmacology……..…… 75

4.2.4.1. Cell cultures…….……...……75

4.2.4.2. Western blot for detection of amino acid transporter expression…...76

4.2.4.3. Cellular uptake studies…….……...……77

4.2.4.4. Cellular uptake inhibition studies……...…… 78

4.2.4.5. Determination of lipophilicity (logP)…… 78

4.2.4.6. Small animal PET imaging studies…….……78

4.2.4.7. Data analysis……...……80

4.3. Results……...……. 80

4.3.1. Chemistry……...….……80

4.3.2. Radiochemistry……...……80

4.3.3. Determination of logP…… 85

4.3.4. Cell uptake studies…….……..…85

4.3.5. Radiotracer uptake competitive inhibition experiments……..…86

4.3.6. Characterization of LAT1, ASCT1 and ASCT2 expression in EMT6 cells…….…… 89

4.3.7. Small animal PET studies……...……90

4.4. Discussion……...……94

4.5. Conclusion……..…… 100

4.6. Acknowledgments……..…… 101

4.7. References……..… 101

Chapter 5 - Sonogashira reaction with 4-[^{18}F]fluoroiodobenzene for ^{18}F-labelling of peptides……..……106

5.1. Introduction…… 106

5.2. Results…… 109

5.2.1. Synthesis of labeling precursor pBBN and reference compound [^{19}F]FBpBBN……...…109

5.2.2. Radiochemistry……...…111

5.2.3. Determination of IC_{50} of [^{18}F]FBpBBN…….…… 116

5.2.4. Determination of logP of [^{18}F]FBpBBN…….117

5.3. Discussion……..….117

5.4. Conclusion……..… 119

5.5. Materials and methods……..……..…120

5.5.1. General……120

5.5.2. Chemistry.....121

5.5.2.1. Resin synthesis of propargylglycine-bombesin derivative (pBBN)... 121

5.5.2.2. General manual procedure for the synthesis of [^{19}F]FBpBBN.....121

5.5.2.3. On-resin synthesis of [^{19}F]FBpBBN.....122

5.4.3. Radiochemistry.....123

5.4.3.1. Syntheses of 4-[^{18}F]fluoroiodobenzene ([^{18}F]FIB)…… 123

5.4.3.2. Formulation of 4-[^{18}F]fluoroiodobenzene ([^{18}F]FIB) for use in cross-coupling reactions..... 123

5.5.3.3. Manual synthesis of [^{18}F]FBpBBN..... 123

5.4.3.4. TLC analysis of [^{18}F]FBpBBN……..…124

5.5.3.5. HLPC purification of [^{18}F]FBpBBN..... 124

5.6. References..... 125

Chapter 6 - Summary and outlook……129

6.1. Summary…….…129

6.2. Outlook……... 133

6.3. References……..… 133

Appendix……..……...……. 134

Bibliography……..……...156

List of tables

Table 2.1. Yields for the direct electrophilic aromatic radiofluorinations... 19

Table 2.2. Yields for the direct nucleophilic aromatic radiofluorinations…20

Table 2.3. Yields for the use of iodonium salts in the synthesis of fluorohalobenzenes…….....26

Table 2.4. Summary of synthesis approached for ^{18}F-labelled fluorohalobenzenes……..30

Table 2.5. Sonogashira reaction with 4-[^{18}F]fluoroiodobenzene……..… 37

Table 2.6. Buchwald *N*-arylation with 4-[^{18}F]fluorohalobenzenes……..… 39

Table 2.7. Radiofluorination of Pd-aryl complexes **42** with electrophilic fluorination reagent **41**…… 42

Table 4.1. Influence of reaction conditions and parameters on the synthesis of D/L-[^{18}F]FPhPA……..……82

Table 5.1. Selection of various methods for peptide labeling with ^{18}F…… 107

Table 5.2. Summary of results for the Sonogashira reaction of [^{18}F]FIB with pBBN…….……. 112

Table 7.1. Area under the UV trace for various [^{18}F]FIB production syntheses……..……139

Table 7.2. Area under the UV trace for various [^{18}F]FPhPA production syntheses……..……147

Table 7.3. Area under the UV trace for various [^{18}F]FBpBBN production syntheses……..154

List of figures

Figure 1.1. Principle of PET……..…… 1

Figure 1.2. Representative examples of drugs containing fluorophenyl groups..... 3

Figure 2.1. Typical catalytic cycle for palladium-mediated cross-coupling reactions……...……12

Figure 2.2. Representative examples of fluorophenyl containing drugs……14

Figure 2.3. Synthetic pathways to achieve the synthesis of fluorohalobenzenes……..……16

Figure 2.4. DEAR for the synthesis of fluorohalobenzenes……..…… 18

Figure 2.5. DNAR for the synthesis of fluorohalobenzenes……..…20

Figure 2.6. Direct nucleophilic aromatic radiofluorinations starting for triazene…… 21

Figure 2.7. Direct nucleophilic aromatic radiofluorinations followed by decarbonylation……...…… 24

Figure 2.8. Iodonium salts for the synthesis of fluorohalobenzenes.…… 25

Figure 2.9. Sulfonium salts for the synthesis of fluorohalobenzenes…… 28

Figure 2.10. Microwave devices with iodonium salts…….…… 28

Figure 2.11. Iodonium salts with microwave activation……..……29

Figure 2.12. Iodonium salts with microfluidic technology……..……31

Figure 2.13. Stille cross coupling reactions of fluorohalobenzenes…… 32

Figure 2.14. Stille cross coupling reaction yielding a nicotinic acetylcholine receptor binding ligand…….…… 33

Figure 2.15. Stille cross coupling reaction yielding 4-[^{18F}]fluoro-phenylallylamine…….…..... 33

Figure 2.16. Stille cross coupling reaction yielding uridine based compounds……...……34

Figure 2.17. Stille cross coupling reactions yielding various COX-2 inhibitor compounds……35

Figure 2.18. Suzuki cross coupling reaction to synthesize biphenyl derivatives……36

Figure 2.19. Buchwald *N*-arylation to yield a serotonin HT_{2A} receptor antagonist…….……38

Figure 2.20. Examples of biaryl monophosphine ligands used in PMNR…...40

Figure 2.21. Palladium mediated nucleophilic radiofluorination reaction scheme…….…… 40

Figure 2.22. Palladium mediated nucleophilic radiofluorination of aromatic compounds……...……40

Figure 2.23. Palldium catalyzed nucleophilic fluorination of aryl triflates.… 41

Figure 2.24. Electrophilic late stage radiofluorination reaction scheme……. 42

Figure 3.1. Scheme of the automated synthesis unit for the synthesis of 4-[^{18}F]fluoroiodobenzene…… 56

Figure 3.2. Synthetic procedure for the radiosynthesis of 4-[^{18}F]fluoroiodobenzene **3**…….…… 57

Figure 3.3. Comparison of DMF and CH_3CN as solvents for the ^{18}F-radio-labelling of (4-iodophenyl)diphenylsulfonium triflate……58

Figure 3.4. Influence of reaction temperature (n=3), reaction time (n=3) and concentration of labeling precursor 1 (n=1) on radiochemical yield[a] of 4-[^{18}F]fluoroiodobenzene……..…… 60

Figure 3.5. HPLC trace of 4-[^{18}F]fluoroiodobenzene as produced from the ASU…….…… 63

Figure 3.6. HPLC purified [^{18}F]FIB along with [^{19}F]FIB…….…… 63

Figure 4.1. Selection of ^{18}F-labelled amino acids…….…… 68

Figure 4.2. Synthesis of D/L-FPhPA, D-FPhPA, and L-FPhPA……..… 80

Figure 4.3. General reaction scheme for the preparation of [^{18}F]FPhPA….. 81

Figure 4.4. Cell uptake of D/L-[^{18}F]FPhPA, D-[^{18}F]FPhPA, and L-[^{18}F]FPhPA in EMT6 cells…….. 85

Figure 4.5. Competitive inhibition studies of L-[^{18}F]FPhPA with MeAIB, BCH and L-Ser. Each bar represents the mean±SEM (n=6). * P<.05; *** P<.001……..... 86

Figure 4.6. Competitive inhibition studies of L-[^{18}F]FPhPA with system ASC inhibitors L-Ser and L-Gln. Each bar represents the mean±SEM (n=6). *** P<.001…….…….....89

Figure 4.7. Qualitative detection of LAT1, ASCT1 and ASCT2 in murine EMT6 cells. EMT6 murine cells were grown to near confluence, washed with PBS and lysed in CelLytic™ M. LAT1, ASCT1 and ASCT2 were detected by Western blotting and immuno-detection using specific antibodies. α-Tubulin staining was used as loading control……...…… 90

Figure 4.8. Representative PET images displayed as maximum-intensity projections (MIPs) of EMT6 tumor bearing mice at 10 min, 30 min and 60 min after injection (4-5 MBq in 100-120 mL of saline) of L-[^{18}F]FPhPA (top) and L-[^{18}F]FET (bottom, taken from literature 16). Isoflurane was used for anesthesia of the mice……...…… 91

Figure 4.9. Time-activity curves (TACs) reflecting the kinetics of L-[^{18}F]FPhPA (purple) and L-[^{18}F]FET (black) in tumor and muscle (A), heart (B), brain (C) and kidneys (D). Data are given as SUV from three different experiments with each radiolabelled amino acid…….…… 92

Figure 5.1. Structure of peptides pBBN and [^{19}F]FBpBBN……..… 110

Figure 5.2. Radiolabelling of [^{18}F]FIB with pBBN to yield [^{18}F]FBpBBN.. 111

Figure 5.3. Colorimetric ligand substitution of $Pd(OAc)_2$ with tppts…… 115

Figure 5.4. HPLC of purified [^{18}F]FBpBBN (bottom) and co-injected cold reference (top)……..……116

Figure 6.1. Synthetic procedure for the production of [^{18}F]FIB…… 130

Figure 6.2. Synthetic procedure for the production of [^{18}F]FPhPA……...131

Figure 6.3. Synthetic procedure for the production of [^{18}F]FBpBBN……... 132

Figure 7.1. ^{1}H-NMR of [^{19}F]FPhPA……..… 134

Figure 7.2. ^{13}C-NMR of [^{19}F]FPhPA…….… 135

Figure 7.3. ^{19}F-NMR of [^{19}F]FPhPA…….… 135

Figure 7.4. LR-MS of [^{19}F]FPhPA cold reference compound……..…136

Figure 7.5. HR-MS of [^{19}F]FPhPA cold reference compound.....136

Figure 7.6. HR-MS of [^{19}F]FBpBBN cold reference compound.....137

Figure 7.7. LR-MS of [^{19}F]FBpBBN cold reference compound..... 137

Figure 7.8. HPLC purification of [^{19}F]FBpBBN cold reference compound..... 138

Figure 7.9. TLC analysis for the synthesis of 4-[^{18}F]fluoroiodobenzene….. 138

Figure 7.10. Specific activity curve for [^{19}F]fluoroiodobenzene…….139

Figure 7.11. TLC analysis for the synthesis of 4-[^{18}F]FPhPA…….140

Figure 7.12. Secondary TLC analysis for the synthesis of 4-[^{18}F]FPhPA...…140

Figure 7.13. HPLC purification of [^{18}F]FPhPA.....141

Figure 7.14. Chiral separation of D-propargylglycine…….…141

Figure 7.15. Chiral separation of L-propargylglycine……. 142

Figure 7.16. Chiral separation of L-[^{18}F]FPhPA……..... 142

Figure 7.17. Chiral separation of D-[^{18}F]FPhPA……..…... 142

Figure 7.18. Chiral separation of D/L-[^{18}F]FPhPA…….……... 143

Figure 7.19. Palladium type versus yield for the synthesis of [^{18}F]FPhPA (n=3)…… 143

Figure 7.20. Propargylglycine concentration type versus yield for the synthesis of [^{18}F]FPhPA (n=3)…… 144

Figure 7.21. Solvent versus yield for the synthesis of [^{18}F]FPhPA (n=3)……...…. 144

Figure 7.22. Palladium mass versus yield for the synthesis of [^{18}F]FPhPA (n=3)…… 145

Figure 7.23. Copper mass versus yield for the synthesis of [^{18}F]FPhPA (n=3)…… 145

Figure 7.24. Triethylamine volume versus yield for the synthesis of [^{18}F]FPhPA (n=3)…… 145

Figure 7.25. Temperature versus yield for the synthesis of [^{18}F]FPhPA (n=3)…… 146

Figure 7.26. Time versus yield for the synthesis of [^{18}F]FPhPA (n=3)……... 146

Figure 7.27. HPLC radiotrace of [^{18}F]FPhPA……..... 146

Figure 7.28. Specific activity curve of [^{18}F]FPhPA…….....147

Figure 7.29. LogD of [^{18}F]FPhPA over the pH range of 0 to 14……..... 148

Figure 7.30. TLC analysis for the synthesis of 4-[^{18}F]FBpBBN……..… 148

Figure 7.31. Secondary TLC analysis for the synthesis of 4-[^{18}F]FBpBBN……... 149

Figure 7.32. HPLC purification of [^{18}F]FBpBBN..... 149

Figure 7.33. Recoverable radiochemical yield versus palladium catalyst for the synthesis of [^{18}F]FBpBBN (n=3)……150

Figure 7.34. Recoverable rcy. versus peptide concentration for the synthesis of [^{18}F]FBpBBN (n=3)…… 150

Figure 7.35. Recoverable rcy. versus temperature and solvent for the synthesis of [^{18}F]FBpBBN (n=3)…… 151

Figure 7.36. Recoverable rcy. versus palladium catalyst mass for the synthesis of [^{18}F]FBpBBN (n=3)…… 151

Figure 7.37. Recoverable rcy. versus water soluble palladium catalyst for the synthesis of [^{18}F]FBpBBN (n=3)……152

Figure 7.38. Recoverable rcy. versus time of reaction for the synthesis of [^{18}F]FBpBBN (n=3)…… 152

Figure 7.39. Recoverable rcy. versus temperature and base of reaction for the synthesis of [^{18}F]FBpBBN (n=3)……... 153

Figure 7.40. Rcy. versus CuI, Pd and base of reaction for the synthesis of [^{18}F]FBpBBN (n=3)…… 153

Figure 7.41. Specific activity curve of [^{18}F]FBpBBN…..... 154

Figure 7.42. LogD of [^{18}F]FBpBBN over the pH range of 0 to 14……..…155

Abbreviations

(2,2,6,6-tetramethylpiperidin-1-yl)oxidanyl	TEMPO
3-[^{18}F]fluoro-cyclobutyl-1-carboxylic acid	[^{18}F]FACBC
[^{18}F]acetyl hypofluoride	[^{18}F]AcOF
[^{18}F]fluoride to aluminum bond	Al-^{18}F
[^{18}F]fluoride to boron bond	B-^{18}F
[^{18}F]fluoride to silicon bond	Si-^{18}F
[^{18}F]fluorobenzyl-propargylglycine modified bombesin	[^{18}F]FBpBBN
^{18}F-fluoro-ethyl-tyrosine	[^{18}F]FET
2-(methylamino)isobutyric acid	MeAIB
2-[^{18}F]fluoro-5-hydroxy-L-tyrosine	[^{18}F]Fdopa
2-amino-2-norbornanecarboxylic acid	ANCA
2-amino-5-(4-[^{18}F]fluorophenyl)pent-4-ynoic acid	[^{18}F]FPhPA
2-aminobicyclo-(2,2,1)-heptane-2-carboxylic acid	BCH
2-deoxy-2-[^{18}F]fluoro-D-glucose	[^{18}F]FDG
2-dimensional	2D
3-(1-[^{18}F]fluoromethyl)-L-alanine	L-[^{18}F]FMA
3-dimensional	3D
3,3',3"-phosphanetriyltris trisodium salt	tppts
4-[^{18}F]fluoroiodobenzene	[^{18}F]FIB
4, 7, 13, 16, 21, 24-hexaoxa-1, 10-diazabicycle [8.8.8] hexacosane	K_{222}
acetonitrile	CH_3CN
amine	NH_2
aryl-fluoride bond	Ar-F
automated Synthesis Unit	ASU
becquerel	Bq
benzyl	Bn
bicinchoninic acid	BCA
Bis(triphenylphosphine)palladium(II) dichloride	$PdCl_2(PPh_3)_2$
bovine serum albumin	BSA
canadian council on animal care	CCAC
carbon-11	^{11}C
carbon-carbon	C-C
carbon-nitrogen	C-N
carbonyl	CHO
cesium carbonate	Cs_2CO_3
cesium fluoride	CsF
copper-64	^{64}Cu
copper(I) iodide	CuI
curie	CI
cyclooxygenase-2	COX-2

degrees celcius	°C
diisopropylethylamine	DIPEA
dimethyl sulfoxide	DMSO
direct electrophilic aromatic radiofluorination	DEAR
direct nucleophilic aromatic radiofluorination	DNAR
fetal bovine serum	FBS
fluorine-18	^{18}F
gallium-68	^{68}Ga
gastrin-releasing peptide receptors	GRPRs
good manufacturing practice	GMP
half life	$t_{1/2}$
high performance liquid chromatography	HPLC
high resolution mass spectroscopy	HRMS
horseradish peroxidase	HRP
hydrochloric acid	HCl
immunoglobulin	IgG
internal system of units	SI
iodyl	IO_2
lipophilicity	logP
maximum a posteriori	MAP
median inhibition concentration	IC50
microwave	μ-wave
minutes	min
N-succinimidyl-4-[^{18}F]fluorobenzoate	[^{18}F]SFB
N,N-dimethylformamide	DMF
no-carrier-added	n.c.a
nuclear magnetic resonance	NMR
palladium	Pd
palladium (0) 3,3',3"-phosphanetriyltris trisodium salt	$Pd(tppts)_4$
palladium (II) nitrate	$Pd(NO_3)_2$
palladium-mediated nucleophilic radiofluorination	PMNR
palladium(II) acetate	$Pd(OAc)_2$
phosphate buffered saline	PBS
polyvinylidene fluoride	PVDF
positron emission tomography	PET
positron emission tomography/x-ray computerized tomography	PET/CT
potassium [^{18}F]fluoride	[^{18}F]KF
potassium acetate	KOAc
potassium carbonate	K_2CO_3
potassium phosphate	K_3PO_4
propargylglycine modified bombesin	pBBN
quaternary methyl ammonium cartridge	QMA

radio-immunoprecipitation assay	RIPA
reactor 1	R1
regions of interest	ROI
retention factor	R_f
retention time	t_R
reverse osmosis/ deionized water system	RO/DIS
sodium dodecyl sulfate	SDS
sodium hydroxide	NaOH
sodium tert-butoxide	NaO^tBu
solid phase extraction	SPE
standardized uptake values	SUV
system ASC amino acid transporter 1	ASCT1
system ASC amino acid transporter 2	ASCT2
system L amino acid transporter 1	LAT1
tetrafluoroborate	BF_4^-
tetrahydrofuran	THF
tetrakis(triphenylphosphine)palladium(0)	$Pd(PPh_3)_4$
thin layer chromatography	TLC
thiol	SH
time	t
time-activity curves	TAC
tri(o-tolyl)phosphine	$P(o\text{-}tol)_3$
triethylamine	TEA
trifluoroacetic acid	TFA
triphenylarsine	$AsPh_3$
tris buffered saline with tween® 20	TBST
tris(dibenzylideneacetone)dipalladium(0)	$Pd_2(dba)_3$
ultraviolet	UV
vial 1	V1
vial 2	V2
vial 3	V3
vial 4	V4
vial 5	V5
vial 6	V6

Chapter 1

Introduction

Jenilee Way

1.1. Positron emission tomography (PET)

Positron emission tomography (PET) is a functional molecular imaging technology, which provides quantitative information on biochemical and physiological processes at the cellular and molecular level in intact organisms over time. PET has found numerous applications in cardiology[1,2], neurology[3,4], oncology[5-7], including the molecular imaging of inflammation[8-12] and fever[13,14]. PET imaging relies upon the simultaneous detection of two 180° photons resulting from positron-electron annihilation. In a typical PET study the PET radiotracer, a compound labelled with a short-lived positron emitter, is injected intravenously into a human or animal.

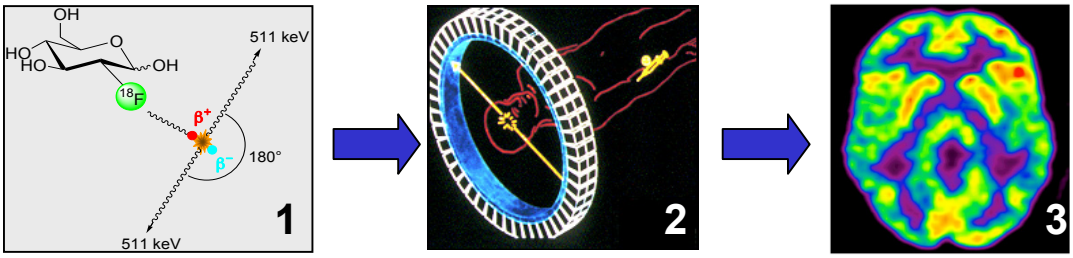

Figure 1.1. Principle of PET.

Tissue concentrations of the radiotracer are measured over time, and these data are combined with information on plasma probe concentration of the radiotracer to assay metabolism. Mathematical methods for the evaluation of PET

measurements within the framework of compartment models are well established. The result is an image, which reflects the 3-dimensional distribution of the radiotracer[15]. The basic principle of PET is summarized in *Figure 1.1*., where (1) A positron emitting radionuclide (e.g. ^{18}F) is incorporated into a biologically active compound to give a PET radiotracer (e.g. [^{18}F]FDG), which is intravenously administered and distributed within the body. (2) Two 511 keV photons, generated by the positron annihilation, are electronically detected as coincidence events along the line of response (LOR) by a PET scanner. (3) Measurement of the integral of activity along sets of LORs provides projection data, which produce tomographic images of the radiotracer distribution after photon attenuation correction and computer-assisted reconstruction.

1.2. PET radionuclides

When it comes to PET imaging the selection of the appropriate radionuclide is often critical. There are several factors, which need to be considered including, spatial resolution, half-life, effective dose, isotope availability, and ease of radiochemistry. Several PET radionuclides commonly employed are fluorine-18 [^{18}F], carbon-11 [^{11}C], gallium-68 [^{68}Ga], and copper-64 [^{64}Cu][16]. Fluorine-18 and gallium-68 have half-lives in the one to two hour range compared to carbon-11 which has a half-life of just 20 min, resulting in a more challenging radiochemistry. Copper-64 has a longer half-life of 12.4 h making it suitable for longer imaging protocols with higher molecular weight compounds like antibodies, but also increasing its effective dose to the patient[16]. Fluorine-18 and gallium-68 result in comparable effective doses, but ^{18}F possesses the best spatial

resolution of all PET radionuclides[16]. Fluorine-18 can be produced via a small biomedical cyclotron, whereas ^{68}Ga is available through a ^{68}Ge/^{68}Ga generator. The ease of production on small biomedical cyclotrons, the high spatial resolution, and the favorable 109.8 min half-life make ^{18}F a very important PET radionuclide for development of ^{18}F-labelled compounds for molecular imaging purposes.

The preferred focus on ^{18}F as radionuclide for the development of PET radiotracers is due to two major reasons: (1) Possibility of substitution of hydrogen atom with a fluorine atom in a monovalent bioisosteric replacement as well as the prevalence of a broad variety of fluorinated pharmaceuticals in medicine today[17]. (2) 4-Fluorophenyl groups are a very common pharmaceutical structural motif and have been shown to be beneficial in drug design[18]. Some examples of fluorophenyl containing drugs are displayed in *Figure 1.2*.

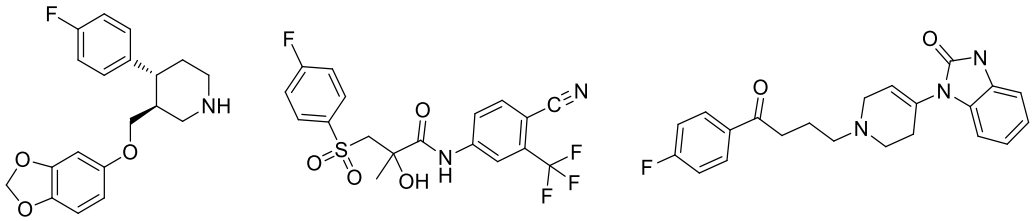

Figure 1.2. Representative examples of drugs containing fluorophenyl groups.

Since the use of potential ^{18}F-radiotracers is thus in high demand, development of novel radiolabelling tools is important. Advances in novel radiolabelling techniques, especially with ^{18}F, will further expand the arsenal of available PET radiotracers for molecular imaging purposes.

1.3. Radiochemistry with fluorine-18

The success of PET depends greatly on the availability of suitable radiolabelled molecular probes, often referred to as radiotracers[19]. Yet despite the recent advancements in radionuclide production[20], automation of radiotracer synthesis[21,22], and significant improvement of PET scanner instrumentation[23-26], including small animal PET-scanners[27], the design and synthesis of novel PET radiotracers remains a special challenge. Specifically ^{18}F-labelled radiotracers have long been used allowing for the diagnosis for many diseases including cancer[28]. Some recent novel strategies for [^{18}F]fluoride radiochemistry include examples such as electrophillic ^{18}F-fluorinations, strain-promoted copper free click chemistry, and transition metal chemistry reations[29]. Even further some ^{18}F-radiochemsitry has been seen using building blocks or an indirect method for radiofluorination[30].

1.4. Hypothesis and rationale

The flexibility behind carbon-carbon bond forming reactions allows for the preparation of structurally diverse compounds starting from smaller prosthetic groups or building blocks. In this line, various transition metal-mediated cross-coupling reactions using halobenzenes are particularly interesting reactions for the preparation of fluorophenyl-containing compounds. Therefore, the ability to produce a large amount of ^{18}F-labelled halobenzenes in a routine and automated system would greatly impact the ability to produce further molecules with such C-C bond forming chemistry. One important halobenzene is 4-[^{18}F]fluoroiodo-benzene ([^{18}F]FIB), which over the last decades, has been synthesized through

various methodologies including direct nucleophilic aromatic radiofluorination, iodonium salts and sulfonium salts as radiolabelling precursors. Most recently, the use of triarylsulfonium salts has been shown to produce [^{18}F]FIB from a commercially available starting material[31]. That makes this reaction scheme quite promising for the preparation of 4-[^{18}F]fluorohalobenzenes.

We hypothesize that [^{18}F]FIB as a ^{18}F-labelled building block can be applied to the Sonogashira cross-coupling reactions with compounds representing different levels of structural complexity. We want to test our hypothesis with the synthesis of small molecules like amino acids, and larger, more complex compounds like peptides. Moreover, the proposed radiochemistry should proceed under mild and aqueous conditions compatible with functional and structural integrity of delicate biomolecules like amino acids and peptides.

We propose the following goals for this thesis project:

1. Development of a fully automated synthesis for the preparation of [^{18}F]FIB.
2. Application of Sonogashira reaction with [^{18}F]FIB for the radiosynthesis of a ^{18}F-labelled amino acid.
3. Application of Sonogashira reaction with [^{18}F]FIB for the radiosynthesis of a ^{18}F-labelled peptide.

The first goal will be achieved by extending upon the work of Mu *et al.*[31] and using triarylsulfonium salts to achieve the fully optimized synthesis of [^{18}F]FIB compared to the manual synthesis as achieved by Mu *et al.*[31]. Allowing for large amounts of radiolabelled product to be easily and reliable generated.

Next, we will use [^{18}F]FIB in palladium-mediated cross couplings according to the Sonogashira reaction. Achieving the following two reactions:

(1) Application of [^{18}F]FIB for the synthesis of a ^{18}F-labelled amino acid starting from readily available propargylglycine as the labelling precursor. Various amino acid radiotracers have been used before in molecular imaging, and the novel ^{18}F-labelled amino acid will be used in both *in vivo* and *in vitro* experiments to assess the radiopharmacological profile in comparison with clinically relevant ^{18}F-labelled amino acid [^{18}F]FET.

(2) Optimized radiochemistry using [^{18}F]FIB will next be applied to a model peptide (bombesin derivative). We propose full optimization of the cross-coupling reaction with regard to mild and physiological reaction conditions.

1.4. References

1 Anagnostopoulos, C., Georgakopoulos, A., Pianou, N., Nekolla, S. G. (2013) Assessment of myocardial perfusion and viability by positron emission tomography. *Int. J. Cardiol. 167*, 1737-1749.

2 Millar, B. C., Prendergast, B. D., Alavi, A., Moore, J. E. (2013) ^{18}FDG-positron emission tomography (PET) has a role to play in the diagnosis and therapy of infective endocarditis and cardiac device infection. *Int. J. Cardiol. 167*, 1724-1736.

3 Keiding, S., Pavese, N. (2013) Brain metabolism in patients with hepatic encephalopathy studied by PET and MR. *Arch. Biochem. Biophys. 536*, 131-142.

4 Hayempour, B. J., Alavi, A. (2013) Neuroradiological advances detect abnormal neuroanatomy underlying neuropsychological impairments: the power of PET imaging. *Eur. J. Nucl. Med. Mol. Imaging. 40*, 1462-1468.

5 Strauss, L. G., Conti, P. S. (1991) The Applications of PET in clinical oncology. *J. Nucl. Med. 32*, 623-648.

6 Vicente, A. M. G., Castrejón, A. S. (2013) New perspectives of PET/CT in oncology. *Méd. Nucl. 37*, 88-92.

7 Fukuda, H., Kubota, K., Matsuzawa, T. (2013) Pioneering and fundamental achievements on the development of positron emission tomography in oncology. *Tohoku. J. Exp. Med. 230*, 155-169.

8 Sathekge, M., Maes, A., VandeWiele, C. (2013) FDG-PET imaging in HIV infection and tuberculosis. *Semin. Nucl. Med. 43*, 349-366.

9 Keidar, Z., Nitecki, S. (2013) FDG-PET in prosthetic graft infections. *Semin. Nucl. Med. 43*, 396-402.

10 Bierry, G., Dietemann, JL. (2013) Imaging evaluation of inflammation in the musculoskeletal system: current concepts and perspectives. *Skeletal Radiol*. *42*, 1347-1359.

11 Palestro, C. J. (2013) FDG-PET in musculoskeletal infections. *Semin. Nucl. Med. 43*, 367-376.

12 Erba, P. A., Sollini, M., Lazzeri, E., Mariani, G. (2013) FDG-PET in cardiac infections. *Semin. Nucl. Med. 43*, 377-395.

13 Vos, F. J., Bleeker-Rovers, C. P., Oyen, W. J. G. (2013) The use of FDG-PET/CT in patients with febrile neutropenia. *Semin. Nucl. Med. 43*, 340-348.

14 Kouijzer, I. J. E., Bleeker-Rovers, C. P., Oyen, W. J. G. (2013) FDG-PET in fever of unknown origin. *Semin. Nucl. Med. 43*, 333-339.

15 Valk, P. E., Delbeke, D., Bailey, D. L., Townsend, D. W., Maisey, M. N. (2006) *Positron emission tomography: clinical practice*. Springer-Verlag London Ltd.

16 Pagani, M., Stone-Elander, S., Larsson, S. A. (1997) Alternative positron emission tomography with non-conventional positron emitters: effects of their physical properties on image quality and potential clinical applications. *Eur. J. Nucl. Med. 24*, 1304-1327.

17 Ismail, F. M. D. (2002) Important fluorinated drugs in experimental and clinical use. *J. Fluorine Chem. 118*, 27-33.

18 Park, B. K., Kitteringham, N. R., O'Neill, P. M. Metabolism of fluorine-containing drugs. *Annu. Rev. Pharmacol. Toxicol*. *41*, 443.

19 Gillings, N. (2013) Radiotracers for positron emission tomography imaging. *Magn. Reson. Mater Phy*. *26*, 149-158.

20 Qaim, S. M. (2003) *Cyclotron production of medical radionuclides.* In: Vertes, A., Nagy, S., Klencsar, Z. Handbook of Nuclear Chemistry, Volume 4, Radiochemistry and Radiopharmaceutical Chemistry in Life Science. Kluwer Academic Publishers, 47-79.

21 Krasikova, R. (2007) Synthesis modules and automation in F-18 labelling. *Ernst Schering Res. Found Workshop. 62*, 289-316.

22 Lu, S. Y., Pike, V. W. (2007) Micro-reactors for PET tracer labelling. *Ernst Schering Res. Found Workshop. 62*, 271-287.

23 Blodgett, T. M., Meltzer, C. C., Townsend, D. W. (2007) PET/CT: form and function. *Radiology 242*, 360-385.

24 Surti, S., Kuhn, A., Werner, M. E., Perkins, A. E., Kolthammer, J., Karp, J. S. (2007) The benefit of time-of-flight in PET imaging: experimental and clinical results. *J. Nucl. Med. 48*, 471-480.

25 Surti, S., Karp, J. S., Popescu, L. M., Daube-Witherspoon, M. E., Werner, M. (2006) Investigation of time-of-flight benefit for fully 3-D PET. *IEEE Trans. Med. Imaging. 25*, 529-538.

26 Zaidi, H. (2006) Recent developments and future trends in nuclear medicine instrumentation. *Z. Med. Phys. 16*, 5-17.

27 Sossi, V., Ruth, T. J. (2005) Micropet imaging: *in vivo* biochemistry in small animals. *J. Neural Transm. 112*, 319-330.

28 Alauddin, M. M. (2012) Positron emission tomography (PET) imaging with ^{18}F-based radiotracers. *Am. J. Nucl. Med. Mol. Imaging. 2*, 55-76.

29 Littich, R., Scott, P. J. H. (2013) Novel strategies for fluorine-18 radiochemistry. *Angew. Chem. Int. Ed. 51*, 1106-1109.

30 Li, L., Hopkinson, M. N., Yona, R. L., Bejot, R., Bee, A. D., Gouverneur, V. (2011) Convergent ^{18}F radiosynthesis: a new dimension for radiolabelling. *Chem. Sci. 2*, 123-131.

31 Mu, L., Fischer, C. R., Holland, J. P., Becaud, J., Schubiger, P. A., Schibli, R., Ametamey, S. M., Graham, K., Stellfeld, T., Dinkelborg, L. M., Lehmann, L. (2012) ^{18}F-Radiolabelling of aromatic compounds using triarylsulfonium salts. *Eur. J. Org. Chem. 5*, 889-892.

Chapter 2

*Synthesis of 4-[^{18}F]fluorohalobenzenes and palladium-mediated cross-coupling reactions for the synthesis of ^{18}F-labelled radiotracers.**

Jenilee Way, Vincent Bouvet, Frank Wuest

2.1. Introduction

Positron emission tomography (PET) is a highly sensitive functional molecular imaging technology which allows visualization of biochemical processes in living subjects. The success of PET as the most sophisticated molecular imaging methodology stems largely from the availability of suitable radiolabelled molecular probes, also referred to as radiotracers.

Despite the recent progress in radionuclide production[1], automation of radiotracer synthesis[2,3], and significant improvement of PET scanner instrumentation[4-7], including small animal PET-scanners[8], the design and synthesis of novel PET radiotracers remains a special challenge.

Today's organic PET chemistry has evolved into a complex chemical science and special efforts are focused on radiosyntheses using the most prominent short-lived positron emitter fluorine-18 (^{18}F, $t_{1/2}$ = 109.8 min). The use of ^{18}F for the development of PET radiotracers offers several advantages. The relatively long half-life of almost 2 hours, the low positron range in tissue, and the ease of production in small biomedical cyclotrons make ^{18}F an almost ideal PET radionuclide for radiotracer development and molecular imaging. ^{18}F allows performance of extended multi-step synthesis procedures and the monitoring of

* *Curr. Org. Chem.*, **2013**; *17*: 2138-2152.

physiological and biochemical processes, applying scanning times of up to 4-6 hours with high spatial resolution. However, the use of ^{18}F implies also the adaptation of chemical synthesis procedures to the two hours half-life and to the extraordinary stoichiometry as a result of the commonly used tracer amounts of ^{18}F-labelled compounds. Hence, the synthesis of ^{18}F-labelled radiotracers should preferentially employ rapid, selective, and functional group-tolerating reactions. In this line, the use of catalysts such as enzymes or transition metal complexes has proved to be particularly efficient for rapid and efficient radiosyntheses of a wide variety of PET radiotracers.

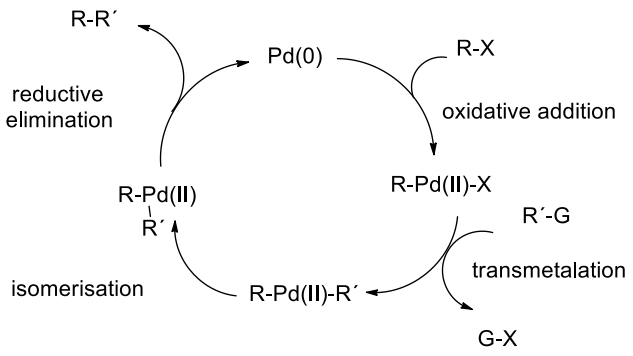

Figure 2.1. Typical catalytic cycle for palladium-mediated cross-coupling reactions.

In the last five decades organic chemists have developed a plethora of different transition metal-mediated cross-coupling reactions. Carbon-carbon bond-forming reactions are among the most important processes in organic chemistry. They are extensively employed in numerous areas of preparative organic chemistry ranging from the synthesis of complex natural products to supramolecular chemistry and material sciences. Many of the transition metal-mediated cross-coupling reactions follow a similar mechanistic scheme based on a catalytic cycle. The principle

reaction mechanism of the catalytic cycle is quite well understood. It involves an oxidative addition-transmetalation-reductive elimination reaction sequence. A typical catalytic cycle is given in *Figure 2.1.* as exemplified for palladium-mediated cross-coupling reactions.

Within the spectrum of transition metal-mediated reactions, reactions involving palladium complexes are particularly effective and versatile. Palladium complexes allow a number of selective transformations, especially distinct carbon-carbon and carbon-heteroatom bond formation processes. However, despite their undoubted success in pharmaceutical chemistry for the synthesis of several drugs, palladium-mediated cross-coupling reactions involving ^{18}F-labelled building blocks may still be considered as an exotic radiochemistry. The challenges to use palladium-mediated chemistry for radiosyntheses of organic PET radiotracers are as follows. The reaction times must be adapted to the short physical half-life of ^{18}F and special methods must be developed to enable rapid small-scale reactions and purification procedures of the complex reaction mixtures. However, during the last decade the situation has changed and several palladium-mediated cross-coupling reactions have entered the field of organic PET-chemistry. The application of palladium-mediated cross-coupling reactions has significantly expanded the number of available ^{18}F-labelled radiotracers for PET.

The present review addresses the utilization of various transition metal-mediated reactions for the synthesis of ^{18}F-labelled compounds. The first part of the review describes different methods for the preparation of 4-[^{18}F]bromofluorobenzene and 4-[^{18}F]fluoroiodobenzene as versatile ^{18}F-labelled building blocks for subsequent

palladium-mediated cross-coupling reactions. The second part will summarize applications of 4-[^{18}F]bromofluorobenzene and 4-[^{18}F]fluoroiodobenzene in Sonogashira reactions, Stille reactions, Suzuki reactions, and Buchwald *N*-arylation reactions.

The review will be concluded with a summary and an outlook on the future prospective of using palladium complexes for the synthesis of ^{18}F-labelled compounds as molecular probe development for PET imaging.

2.2. Synthesis of 4-[^{18}F]bromofluorobenzene and 4-[^{18}F]fluoroiodo-benzene

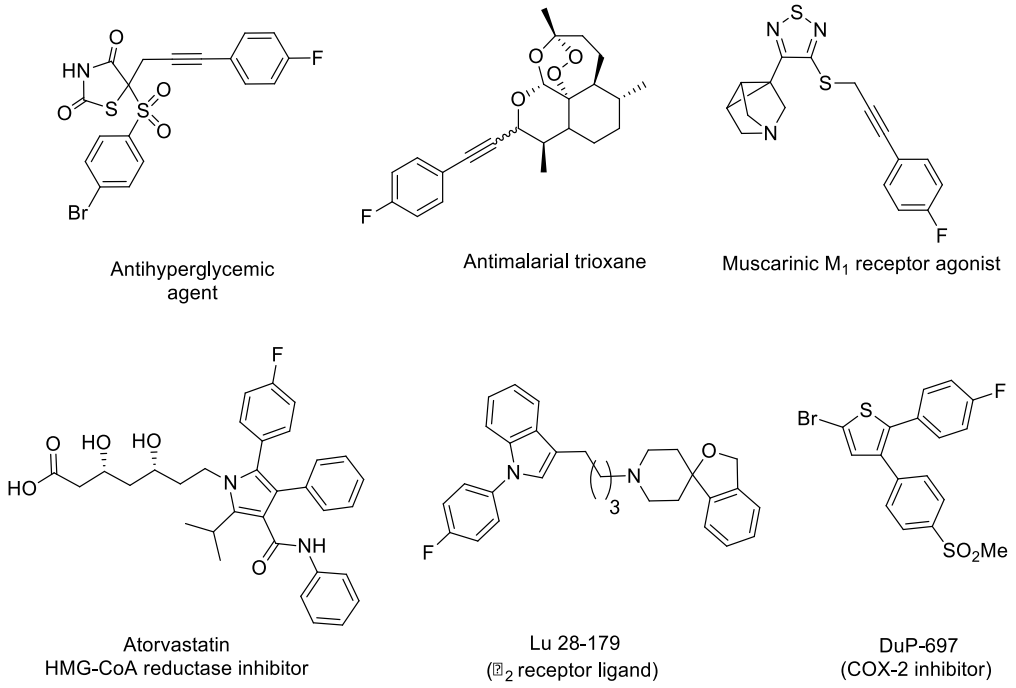

Figure 2.2. Representative examples of fluorophenyl containing drugs.

Transition metal-mediated cross-coupling reactions are powerful tools that have been applied for the synthesis of multiple biological targets using various

halobenzenes as electrophilic coupling partners. 4-Fluorophenyl groups are very popular structural motifs found in many fluorinated drugs, and the beneficial effect of fluorophenyl groups in drug design and development with regard to drug metabolism, in vivo activity and stability has been reviewed recently[9]. Moreover, the substitution of a hydrogen atom by a fluorine atom is one of the most commonly employed monovalent bioisosteric replacements. However, careful study of potential detrimental effects upon receptor binding and metabolic stability after bioisosteric replacement of hydrogen with fluorine is necessary. Representative examples of drugs containing a fluorophenyl group are given in *Figure 2.2*. Consequently, the design of 4-[^{18}F]fluorophenyl group-containing radiotracers should focus on cross-coupling reactions with 4-[^{18}F]fluoro-halobenzenes like 4-[^{18}F]bromofluorobenzene or 4-[^{18}F]fluoroiodobenzene as coupling partners.

Over the last two decades, various methodologies have been envisaged to prepare 4-[^{18}F]fluorohalobenzenes (*Figure 2.3.*). Early work focused on (1) hot atom recoil chemistry and (2) direct electrophilic radiofluorination. However, due to technical challenges, low radiochemical yields and low specific activity, researcher have explored the feasibility of (3) direct nucleophilic radiofluorination reactions starting from no-carrier-added (n.c.a.) [^{18}F]fluoride by screening multiple functional groups enabling a nucleophilic aromatic substitution as well as various leaving groups. Despite the plethora of optimization attempts, the overall radiochemical yields still required improvement. A significant breakthrough was achieved in 1998, when researchers applied a (4) direct nucleophilic aromatic

radiofluorination of nitrohalobenzaldehyde followed by decarbonylation using a Wilkinson catalyst to prepare 4[^{18}F]bromofluorobenzene. This methodology finally afforded satisfactory radiochemical yields while employing a remarkably simple experimental setup. Another approach, which was developed during the same time, was directed to the application of (5) diaryliodonium salts for aromatic radiofluorination with n.c.a. [^{18}F]fluoride.

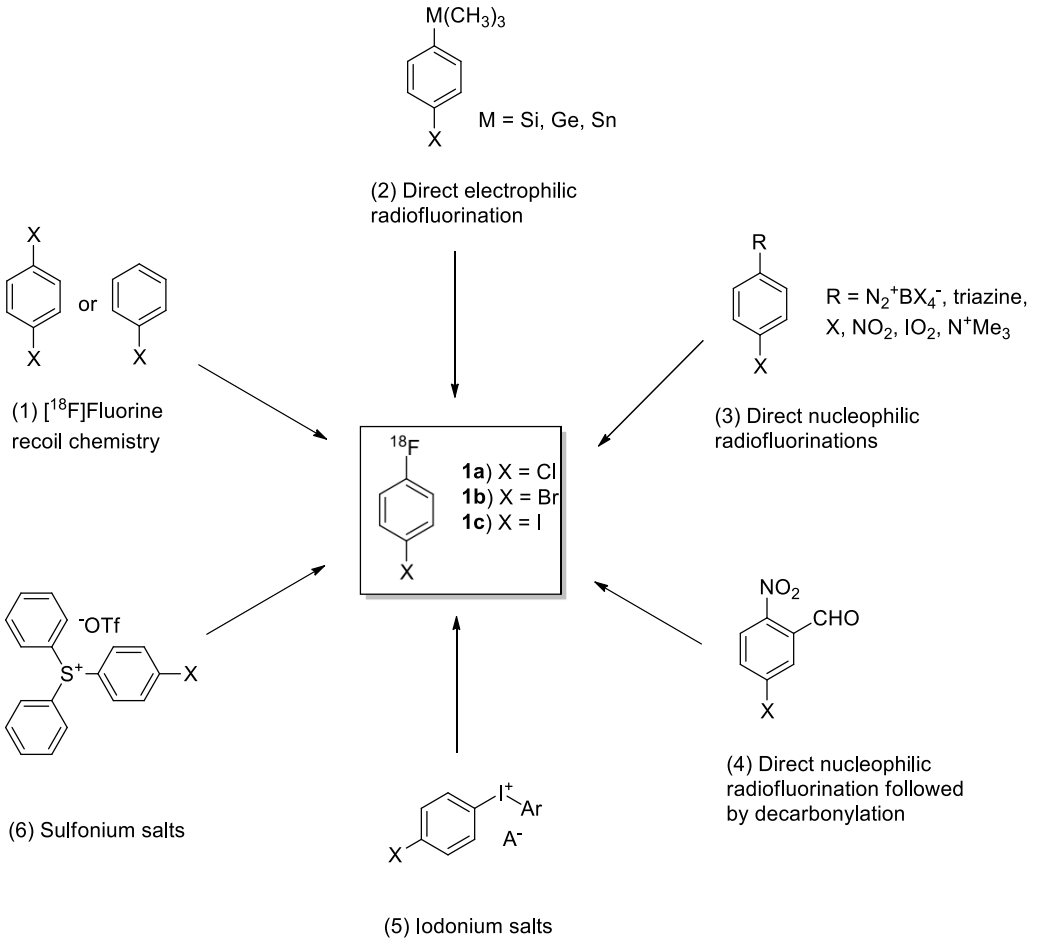

Figure 2.3. Synthetic pathways to achieve the synthesis of fluorohalobenzenes.

The iodonium salt-based procedure showed promising results for the radiosynthesis of non-activated or electron rich [^{18}F]fluoroaryl compounds. The

methodology has constantly been improved. Today, the availability of diaryliodonium salts has significantly improved, and their reactivity is much better understood making diaryliodonium salts highly suitable starting materials for the radiosynthesis of structurally diverse 4-[^{18}F]fluoroaryl-containing compounds.

More recently, the use of (6) triarylsulfonium salts have been reported as highly promising starting materials for the synthesis of [^{18}F]fluorohalobenzenes and other 4-[^{18}F]fluoroaryl-containing compounds starting from n.c.a. [^{18}F]fluoride. Some of the sulfonium salts are commercially available making this class of compound particularly attractive for the preparation of 4-[^{18}F]fluorohalobenzenes. Finally, in the past decade (7) several novel technologies beyond conventional thermal heating have been applied to the synthesis of 4-[^{18}F]fluorohalobenzenes. Technologies like microwave activation and micro-fluidic devices have further improved the radiochemical yield and extended the versatility of some previously described methodologies.

2.2.1. [^{18}F]Fluorine recoil chemistry

[^{18}F]Fluorine recoil chemistry was mainly studied in the mid 1970s and consisted of either gas phase or liquid phase reactions occurring in contact with the target. These experiments resulted in fluorine and hydrogen substitution to afford complex mixtures of compounds including radiolabelled fluorohalobenzenes[10]. 4-[^{18}F]chlorofluorobenzene (**1a**) was obtained in 6% radiochemical yield in either gas or liquid phase experiments and 4-[^{18}F]fluoroiodobenzene (**1c**) was obtained in 2%. However, the complex nature of the resulting reaction mixture and the low

radiochemical yields made this methodology impractical for the routine radiosynthesis of 4-[^{18}F]fluorohalobenzenes.

2.2.2. Direct electrophilic aromatic radiofluorination

In the mid 1980s, various direct electrophilic aromatic radiofluorination (DEAR) reactions were explored for the synthesis of 4-[^{18}F]fluorohalobenzenes.

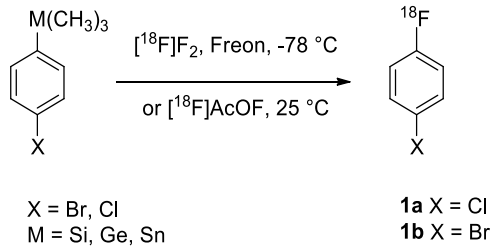

Figure 2.4. DEAR for the synthesis of fluorohalobenzenes.

The reactions used either [^{18}F]F_2 in Freon-11 at low temperatures of -78 °C or [^{18}F]acetyl hypofluoride ([^{18}F]AcOF) in acetic acid at 25 °C to perform various fluorodemetalation reactions to yield 4-[^{18}F]fluorohalobenzenes (*Figure 2.4./ Table 2.1.*). Fluorodesilylation reactions starting from (4-chlorophenyl)trimethylsilane (**2a**) or (4-bromophenyl)trimethylsilane (**2b**) afforded 4-[^{18}F]chlorofluorobenzene (**1a**) and 4-[^{18}F]bromofluorobenzene (**1b**) in 14% to 20% radiochemical yields, respectively[11,12].

Application of (4-bromophenyl)trimethylgermane (**2c**) and (4-bromophenyl) trimethylstannane (**2d**) resulted in improved radiochemical yields (35% and 25%) of 4-[^{18}F]bromofluorobenzene (**1b**) using either [^{18}F]F_2 or [^{18}F]acetyl hypofluoride as electrophilic radiofluorination agents[13]. However, the inevitable low specific activity of compounds **1a** and **1b** as typical for reactions involving

electrophilic [^{18}F]fluorine make this approach not suitable for the preparation of 4-[^{18}F]fluorohalobenzenes.

Compound	M	X	Product	Radiochemical yield
2a*	Si	Cl	1a	14%
2b*	Si	Br	1b	15-20%
2c*	Ge	Br	1b	25%
2d*	Sn	Br	1b	35%

Table 2.1. Yields for the direct electrophilic aromatic radiofluorinations.

**See Figure 2.4. for corresponding chemical structure.*

Application of (4-bromophenyl)trimethylgermane (**2c**) and (4-bromophenyl) trimethylstannane (**2d**) resulted in improved radiochemical yields (25% and 35%) of 4-[^{18}F]bromofluorobenzene (**1b**) using either [^{18}F]F_2 or [^{18}F]acetyl hypofluoride as electrophilic radiofluorination agents[13]. However, the inevitable low specific activity of compounds **1a** and **1b** as typical for reactions involving electrophilic [^{18}F]fluorine make this approach not suitable for the preparation of 4-[^{18}F]fluorohalobenzenes.

2.2.3. Direct nucleophilic aromatic radiofluorination

Direct nucleophilic aromatic substitution (DNAR) reactions are the most commonly applied approach for introducing n.c.a. [^{18}F]fluoride into aromatic rings. This type of reaction requires an activated aromatic system induced by electron-withdrawing groups such as CHO, CN, CO_2R, or NO_2, and a suitable

leaving group, preferentially at the *ortho*- or *para*-position. Preferred leaving groups are I, Br, Cl, F, NO_2, and N^+Me_3 (*Figure 2.5./ Table 2.2.*).

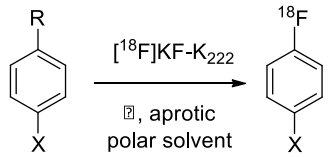

X = I, Br, Cl or F
R = $N_2^+BF_4^-$, triazine, I, Br, Cl, F, NO_2, IO_2, N^+Me_3

Figure 2.5. DNAR for the synthesis of fluorohalobenzenes.

Compound	R	X	Product	Radiochemical yield
3a	$N_2^+BF_4^-$	Br	1b	2-5%
3b	triazine	Br	1b	3-4%
3c	Br	Br	1b	1-2%
3d	IO_2	Cl	1a	2%
3e	N^+Me_3	Br	1b	8-12%
3f	N^+Me_3	I	1c	10-13%
3g	NO_2	Br	1b	2%
3h	NO_2	I	1c	2%

Table 2.2. Yields for the direct nucleophilic aromatic radiofluorinations.

The reactions are commonly carried out in aprotic polar solvents like dimethyl sulfoxide (DMSO), dimethylformamide (DMF), or acetonitrile (MeCN) at elevated temperature using the powerful nucleophilic radiofluorination agent [^{18}F]KF generated from cyclotron-produced n.c.a. [^{18}F]fluoride, kryptofix 222 (K_{222}) and potassium carbonate (K_2CO_3). *Figure 2.5.* illustrates the application of

nucleophilic aromatic radiofluorination reactions starting from various activated halobenzenes (**3a-h**) for the synthesis of 4-[^{18}F]fluorohalobenzenes (**1a-c**).

2.2.3.1. Balz-Schiemann reaction

Balz-Schiemann reaction (R = $N_2^+BF_4^-$) (**3a**) was carried out through thermal decomposition of diazonium salts in the presence of [^{18}F]KF and tetrafluoroborate (BF_4^-) to afford the corresponding 4-[^{18}F]fluorobromobenzene (**1b**). Radiochemical yields were low, ranging from 2 to 5%. The use of BF_4^- resulted in the formation of 4-[^{18}F] bromofluorobenzene at low specific radioactivity[14].

2.2.3.2. The Wallach reaction

The Wallach reaction (R = triazine) is a well know procedure to prepare [^{18}F]fluorobenzene derivatives by acidic decomposition of triazenes in the presence of [^{18}F]KF.

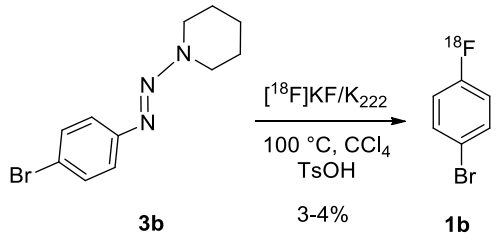

Figure 2.6. Direct nucleophilic aromatic radiofluorinations starting for triazene.

Even though a large variation of parameters were investigated (temperature, solvent, sulfonic acids, concentration) and the procedure was successfully applied to the synthesis of different aromatic ^{18}F-labelled compounds, the reaction afforded only low radiochemical yields of 3-4% as exemplified for the synthesis 4-[^{18}F]bromofluorobenzene starting from triazene (**3b**) (*Figure 2.6.*)[15,16].

However, undesired side reactions of the diazonium salts and triazenes, difficulties in purification, and the overall very low radiochemical yields make the Balz-Schiemann and Wallach reaction not suitable for the preparation of 4-[^{18}F]fluorohalobenzenes.

2.2.3.3. Applications of [^{18}F]KF

Application of several halogen exchange reactions using [^{18}F]KF have also been investigated to prepare 4-[^{18}F]fluorohalobenzenes. However, this type of reaction gave only very low radiochemical yields of 1-2% for the synthesis of 4-[^{18}F]bromofluorobenzene (**1b**) starting from 1,4-dibromobenzene (**3c**)[17,18]. Some reports in the literature also describe the preparation of 3-[^{18}F]bromofluorobenzene based on this method. 3-[^{18}F]Bromofluorobenzene could be prepared in 9% radiochemical yield[19].

2.2.3.4. Iodyl leaving group

Very few reports describe the use of the iodyl (IO_2) group as a leaving group for nucleophilic aromatic radiofluorinations. This methodology seems to give satisfactory results when labelling precursors are used which contain strong electron-withdrawing groups like CHO or NO_2 in the *para*-position of the aromatic ring. However, the presence of halogens like chlorine as activating groups significantly reduces the radiochemical yield. Starting from chlorine-containing labelling precursor (**3d**), only 2% of 4-[^{18}F]chlorofluorobenzene (**1a**) could be prepared[20].

2.2.3.5. Trimethylammonium leaving group

The use of the trimethylammonium group (**3e, 3f**) as leaving group in nucleophilic aromatic substitutions was also studied as a promising synthetic pathway to prepare 4-[^{18}F]fluoro-halobenzenes[21]. However, after detailed analysis of the reaction it was shown that only low radiochemical yields of 8-12% could be obtained for the synthesis of 4-[^{18}F]bromofluorobenzene (**1b**) and 4-[^{18}F]fluoroiodobenzene (**1c**)[17,22]. Comparable low radiochemical yields of about 3% were reported by Pike *et al.* when they studied the feasibility to incorporate n.c.a. [^{18}F]fluoride into the *meta*-position of aryl rings using corresponding trimethylammonium salts as labelling precursors[19].

2.2.3.6. Nitro leaving group

Numerous radiofluorination reactions demonstrated the usefulness of the nitro group as a suitable leaving group for nucleophilic aromatic substitutions with n.c.a. [^{18}F]fluoride. However, studies using 4-iodonitrobenzene and 4-bromonitrobenzene (**3g, 3h**) as labelling precursors for nucleophilic aromatic substitutions with n.c.a. [^{18}F]fluoride resulted mainly in the formation of 4-[^{18}F]fluoronitrobenzene (10 to 50%). Only very low amounts (<2%) of 4-[^{18}F]fluorohalobenzenes (**1b and 1c**) as the alternative reaction products were observed[23].

2.2.4. DNAR followed by decarbonylation

Numerous different methodologies have been tested to further optimize direct nucleophilic aromatic radiofluorinations with n.c.a. [^{18}F]fluoride. However, screening of multiple solvents and reaction temperature, and the testing of various

leaving groups as well as different sources of n.c.a. [^{18}F]fluoride gave only low radiochemical yields of the respective 4-[^{18}F]fluorohalobenzenes, when iodine- or bromine-containing aromatic rings were used as starting materials. The observed low radiochemical yields were mainly attributed to the weak activation of the aromatic ring for a nucleophilic aromatic substitution through the halogen (iodine or bromine). Therefore, the attachment of an additional strongly electron-withdrawing group and its subsequent removal after the nucleophilic aromatic substitution reaction with n.c.a. [^{18}F]fluoride was thought to be a feasible approach to significantly increase the radiochemical yield of 4-[^{18}F]fluorohalobenzenes. Among strong electron-withdrawing groups, the CHO group fulfills the requirements of inducing a strong activation effect on the aromatic ring towards a nucleophilic substitution while being easily removable from the aromatic ring through a decarbonylation reaction. An elegant methodology exploiting this activation-decarbonylation approach was developed by Forngren *et al.* and Allain-Barbier *et al.*.

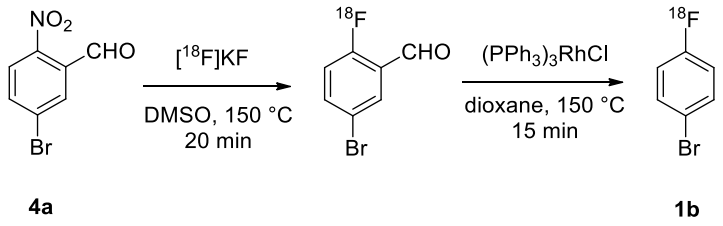

Figure 2.7. Direct nucleophilic aromatic radiofluorinations followed by decarbonylation.

They performed nucleophilic aromatic radiofluorinations with various nitro- and halogen-substituted benzaldehydes, with the CHO group in *ortho*-position of the nitro group (**4a**), followed by a decarbonylation reaction using Wilkinson catalyst

to afford the desired 4-[^{18}F]bromofluorobenzene (**1b**) (*Figure 2.7.*)[22,24]. Based on this two-step procedure, 4-[^{18}F]bromofluorobenzene (**1b**) could be prepared and isolated in radiochemical yields of 30 to 70%.

2.2.5. Iodonium salts as labelling precrsors for the preparation of 4-[^{18}F]fluorohalobenzenes

As previously mentioned aromatic nucleophilic substitutions using n.c.a. [^{18}F]fluoride suffer from low reactivity on poorly electron-deficient and electron-rich aromatic rings. In 1995, the use of diaryliodonium salts to incorporate n.c.a. [^{18}F]fluoride into arenes was introduced and provided an interesting solution to the problem (*Figure 2.8./ Table 2.3.*)[25,26].

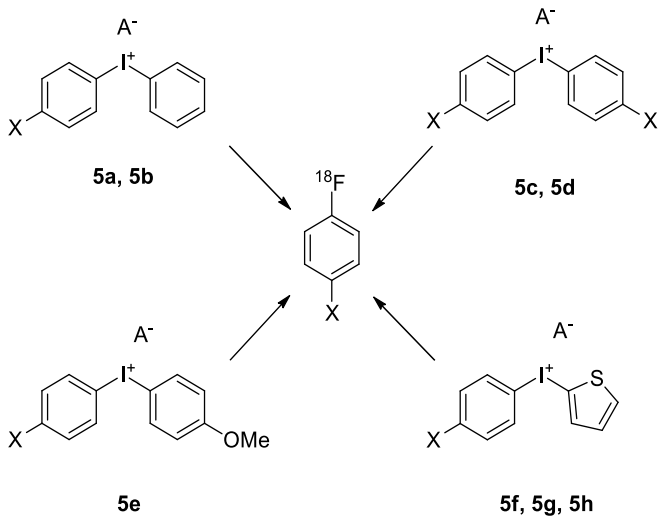

Figure 2.8. Iodonium salts for the synthesis of fluorohalobenzenes.

The reactivity of iodonium salts is controlled by two effects: (1) the so-called *ortho*-effect where an *ortho*-substituent on one of the arene rings directs the radiofluorination to occur on that ring and (2) the electronic effect where the radiofluorination occurs on the least electron-rich ring. Although there is much

debate on the reaction mechanism involving iodonium salts, the methodology is compatible with both electron-rich and electron-deficient arenes[27-30].

Compound	A^-	X	Product	Radiochemical yield
5a	OTs	Br	1b	34%
5b	OTs	I	1c	38%
5c	OTs	Br	1b	52%
5d	Br	Br	1b	65%
5e	OTs	Cl	1a	80%
5f	Br	Cl	1a	62%
5g	Br	Br	1b	70%
5h	Br	I	1c	60%

Table 2.3. Yields for the use of iodonium salts in the synthesis of fluorohalobenzenes.

Asymmetric bromodiphenyliodonium tosylate (**5a**) and iododiphenyliodonium tosylate (**5b**), respectively, afforded the desired 4-[^{18}F]fluorohalobenzenes (**1b** and **1c**) with 34% and 38% radiochemical yields whereas the symmetric dibromodiphenyliodonium tosylate (**5c**) afforded the desired 4-[^{18}F] bromofluorobenzene (**1b**) with 52% radiochemical yield. One of the major drawbacks of this methodology was the amount of labelling precursor needed for the reaction. This problem has apparently been solved by the use of radical scavenger such as TEMPO in order to stabilize the iodonium salt during the reaction[31,33]. Further investigations revealed that bromide anion seems to be the counter ion of choice[17,32,33]. Dibromodiphenyliodonium bromide (**5d**) afforded 4-

[^{18}F]bromofluorobenzene (**1b**) with 65% radiochemical yield[17]. In order to label electron-rich arenes the other aryl group must be electron-rich either by introducing an electron-donating group such as π-methoxy group[34], or by using a 2-thienyl ring[32,35]. Chlorophenyl(4-methoxyphenyl)iodonium tosylate (**5e**) afforded 4-[^{18}F]chlorofluorobenzene (**1a**) with 80% radiochemical yield. Reaction of halophenyl(2-thienyl)iodonium bromides (**5e, 5f and 5h**) with n.c.a. [^{18}F]fluoride gave 62% of chloro-derivative (**1a**), 70% of bromo-derivative (**1b**), and 60% of iodo-derivative (**1c**).

2.2.6. Sulfonium salts

Iodonium salts gave promising results for the synthesis of 4-[^{18}F]fluorohalobenzenes. However, reactions involving iodonium salts as labelling precursors still suffer from several drawbacks. They usually require harsh conditions (>130 °C) and fairly large quantities of labelling precursor for sufficient radiochemical yields. Moreover, preparation, handling and storage of iodonium salts also impose special challenges.

Recently, sulfonium salts were described as novel labelling precursors for the preparation of 4-[^{18}F]fluorohalobenzenes. The reaction can be performed under relatively mild conditions (80 °C) (*Figure 2.9.*), and a large variety of different sulfonium salts are commercially available. The commercial availability of (4-bromophenyl)diphenyl sulfonium and (4-iodophenyl)diphenylsulfonium trifluoro-methanesulfonate (**6a and 6b**) as well as the obtained high radiochemical yields (e.g. 4-[^{18}F]fluoroiodobenzene (**1c**), 91%), make sulfonium salts ideal starting materials for the preparation of 4-[^{18}F]fluorohalobenzenes[36,37].

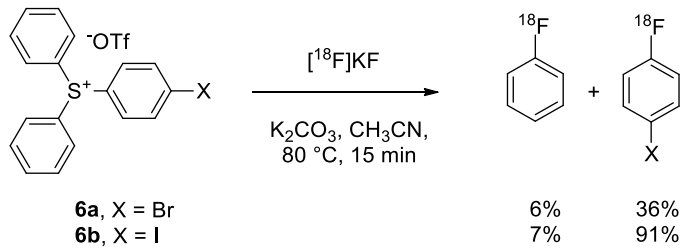

Figure 2.9. Sulfonium salts for the synthesis of fluorohalobenzenes.

2.2.7. Application of new technologies

Over the last the 15 years, various novel developments have been introduced into the synthesis of PET radiotracers. Such developments especially involve the use of microwave and microfluidic devices.

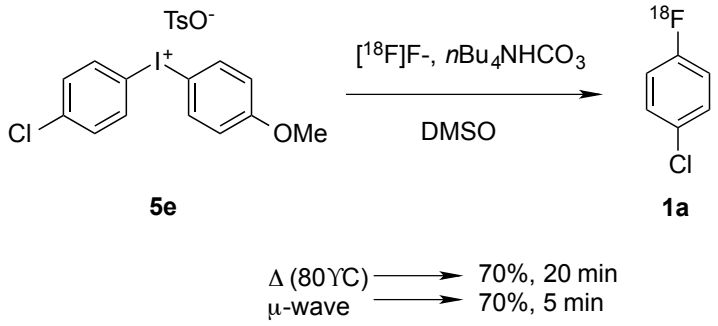

Figure 2.10. Microwave devices with iodonium salts.

Microwave devices improve heat transfer and usually drastically decrease reaction times while providing higher radiochemical yields. More recent applications of microfluidic technology exploit significantly improved mixing characteristics due to larger contact surfaces and microfluidic technology allows the performance of reactions in very small volumes at the μL scale. These characteristics result in faster reaction times, improved radiochemical yields, and significantly decreased labelling precursor amounts. Although both methodologies have been extensively

applied to radiochemistry with short-lived positron emitter fluorine-18, only very few examples have been reported in the literature for the synthesis of 4-[^{18}F]fluorohalobenzenes.

2.2.7.1. Iodonium salts with microwave activation

Three literature reports describe the use of microwave devices for the reaction of iodonium salts with n.c.a. [^{18}F]fluoride to obtain 4-[^{18}F]fluorohalobenzenes[17,34,38]. The reaction time could be reduced from 20 min to 5 min while retaining reasonable radiochemical yields of 70% (*Figure 2.10.*).

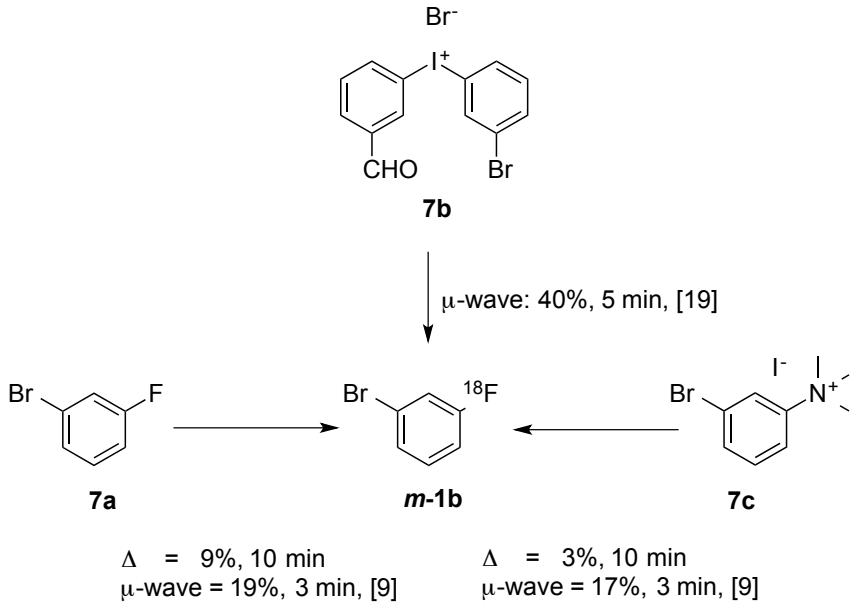

Figure 2.11. Iodonium salts with microwave activation.

The use of microwave activation also demonstrated the feasibility to prepare 3-[^{18}F] bromofluorobenzene in improved radiochemical yields of 17-19% compared to conventional heating radiochemical yields of 3-9% (*Figure 2.11.*)[19,33].

2.2.7.2. Microfluidic technology

Pike *et al.* described the use of microfluidic technology for the radiosynthesis of 2- and 3-substituted [^{18}F]fluorobenzene analogs using iodonium salts as labelling precursors (*Figure 2.12.*)[39,40]. It is noteworthy that the use of microfluidic technology seems to decrease the formation of radicals as side products and that application of TEMPO did not further improve the radiochemical yield in this experimental set up[40].

Precursor	Product	Reaction time (min)	Temperature (°C)	Solvent	Method	Radiochemical yield (%)
Low specific radioactivity						
1,4-Dichloro-benzene (N/A)	1a	N/A	N/A	N/A	1	6
1,4-Diiodo-benzene (N/A)	1c	N/A	N/A	N/A	1	2
2a (15 mg/mL)	1a	10	-78	Freon	2	14
2b (1 mg/mL)	1b	10	25	AcOH	2	15
2c (2 mg/mL)	1b	20	-78	Freon	2	25
2d (2 mg/mL)	1b	20	-78	Freon	2	35
High specific radioactivity						
3a (90 mg/mL)	1b	20	100	Dioxane	3	2-5
3b (60 mg/mL)	1b	15	100	CCl_4	3	4
3c (4.7 mg/mL)	1b	15	160	DMSO	3	2
3d (17 mg/mL)	1a	20	180	DMSO	3	2
3e (11 mg/mL)	1b	15	80	DMSO	3	12
3f (20 mg/mL)	1c	15	145	DMAA	3	13
3e, 3f (11 mg/mL)	1b, 1c	15	80	DMSO	3	<2
4a (10 mg/mL)	1b	40	140	DMSO	4	30-70
5a (15 mg/mL)	1b	40	100	DMF	5	34
5b (15 mg/mL)	1c	40	100	DMF	5	38
5c (15 mg/mL)	1b	40	100	DMF	5	52
5d (10 mg/mL)	1b	10	130	DMF	5	65
5e (10 mg/mL)	1a	20	80	DMSO	5	80
5f (20 mg/mL)	1a	45	130	DMF	5	62
5g (20 mg/mL)	1b	45	130	DMF	5	70
5h (20 mg/mL)	1c	45	130	DMF	5	60
6a (10 mg/mL)	1b	15	80	CH_3CN	6	36
6b (10 mg/mL)	1c	15	80	CH_3CN	6	91
7a (6 mg/mL)	m-1b	10	150	NMP	3	9
7a (6 mg/mL)	m-1b	3	μ-wave	NMP	3	19
7b (2 mg/mL)	m-1b	5	μ-wave	DMF/TEMPO	5	40
7c (6 mg/mL)	m-1b	10	150	NMP	3	3
7c (6 mg/mL)	m-1b	3	μ-wave	NMP	3	17
7d (4 mg/mL)	o-1b	4	μ-fluidic, 190	DMF	5	68

Table 2.4. Summary of synthesis approached for ^{18}F-labelled fluorohalobenzenes.

2.2.8. Summary

Table 2.4., summarizes all discussed approaches for the preparation of ^{18}F-labelled fluorohalobenzenes.

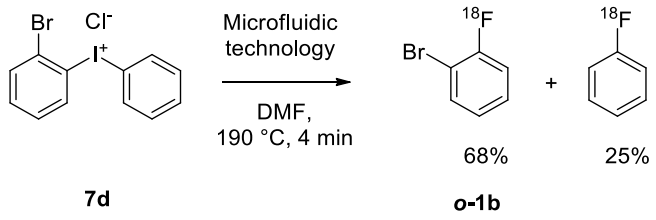

Figure 2.12. Iodonium salts with microfluidic technology.

2.3. Application of 4-[^{18}F]fluorohalobenzenes in palladium-mediated cross-coupling reactions

2.3.1. Stille reactions with 4-[^{18}F]fluorohalobenzenes

Palladium-mediated cross coupling reactions involving organostannanes, also referred to as the Stille reaction, were introduced into organic chemistry in 1979[41]. However, it took almost additional 20 years before the Stille reaction with 4-[^{18}F]fluorohalobenzenes was used for the radiosynthesis of ^{18}F-labelled compounds. One of the first examples was reported by Forngren *et al.* in 1998, when 4-[^{18}F]bromofluorobenzene (**1b**) was reacted with various organostannanes according to a Stille reaction[24]. Experiments were directed to the radiosynthesis of [^{18}F]fluvastatin. The authors tested various reaction conditions for the cross coupling of different organostannanes (**8a, 9a, 10a and 11a**) with 4-[^{18}F]bromofluorobenzene (**1b**) to give the corresponding 4-[^{18}F]fluorophenyl group-containing compounds **8b**, **9b**, **10b** and **11b.** High radiochemical yields greater than 80% were achieved for compounds **8b**, **9b** and **10b**, whereas a

significant lower radiochemical yield of 15% was obtained for compound **11b** (*Figure 2.13.*).

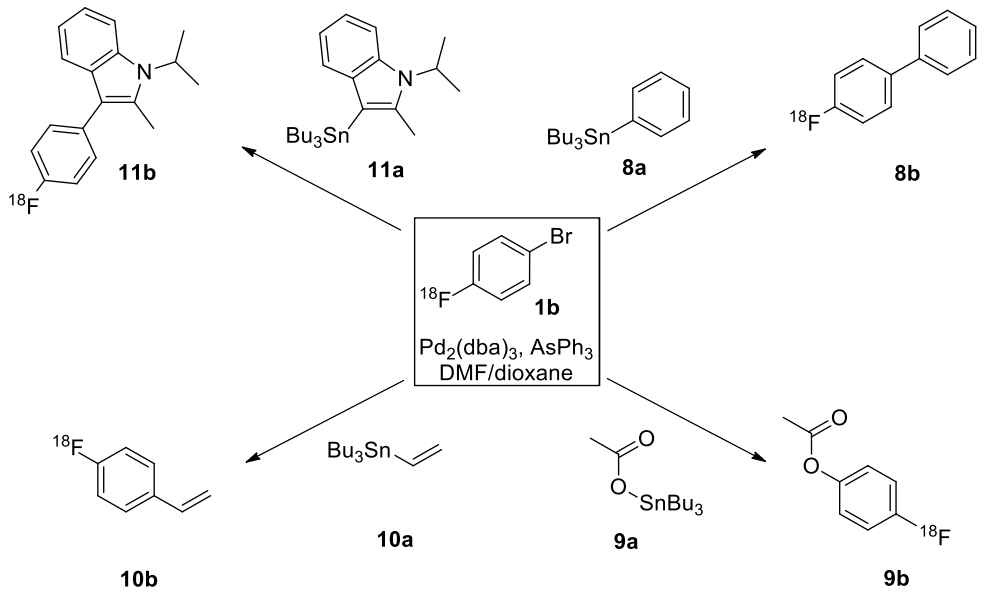

Figure 2.13: Stille cross coupling reactions of fluorohalobenzenes.

Another example of a Stille reaction in ^{18}F chemistry was described for the radiosynthesis of the nicotinic acetylcholine receptor binding ligand 9-(4'-[^{18}F]fluorophenyl)cytisine (**12c**) through coupling of 9-trimethylstannylcytisine (**12a**) with 4-[^{18}F]bromofluorobenzene (**1b**)[42]. The authors screened various reaction conditions and optimal reaction conditions were based on the use of dioxane as the solvent and $PdCl_2(PPh_3)_2$ as the palladium complex. Cross coupling of stannane (**12a**) with 4-[^{18}F]bromofluorobenzene (**1b**) afforded intermediate (**12b**) in 56-74% radiochemical yield before denitrosation. The total synthesis time was 150 min, and the final radiochemical yield was 6-10% (*Figure 2.14.*).

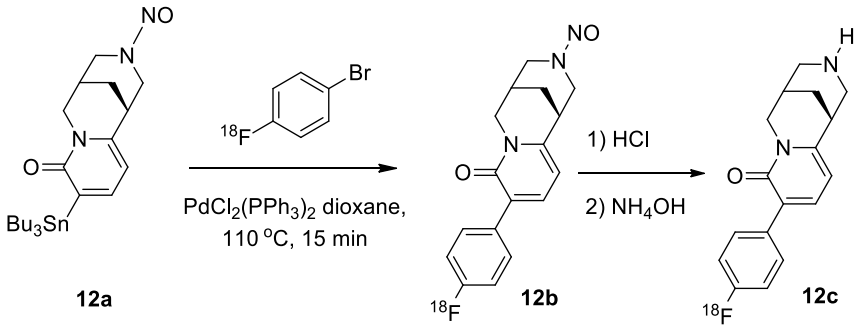

Figure 2.14. Stille cross coupling reaction yielding a nicotinic acetylcholine receptor binding ligand.

Barbier *et al.* applied the Stille reaction with 4-[^{18}F]bromofluorobenzene (**1b**) and 4-[^{18}F] fluoroiodobenzene (**1c**) for the synthesis of 4-[^{18}F]fluorophenylallylamine (**13b**) (*Figure 2.15.*)[22].

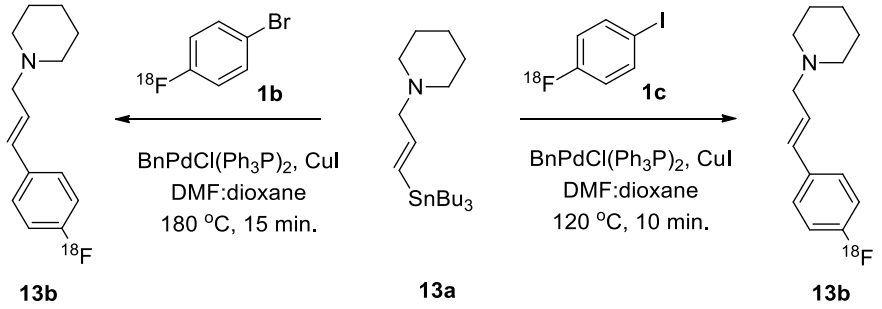

Figure 2.15. Stille cross coupling reaction yielding 4-[^{18F}]fluorophenylallylamine.

The reaction was performed at elevated temperature of 180 °C in a 1:1 mixture of DMF and dioxane as the solvent. Tributylstannylamine (**13a**) was reacted with 4-[^{18}F]bromofluorobenzene (**1b**) in the presence BnPdCl(Ph_3P)$_2$ as the palladium source and CuI as an additive. The reaction was completed in 15 min and the desired cross-coupled compound (**13b**) was isolated in radiochemical yields of 41%. Reaction of tributylstannylamine (**13a**) with 4-[^{18}F]fluoroiodobenzene (**1c**) under comparable reaction conditions except for lower temperature (120 °C) and

faster reaction time (10 min) afforded compound (**13b**) in radiochemical yields of 90%. This example illustrates the superior properties of 4-[^{18}F]fluoroiodobenzene (**1c**) as the coupling partner.

In a series of reports Wuest *et al.* described the synthesis of various 4-[^{18}F]fluorophenyl group-containing compounds according to a Stille reaction protocol[43,44]. Reaction of 4-[^{18}F]fluoroiodobenzene (**1c**) with 5-tributylstannyl-2',3',5'-triacetyl-uridine (**14a**) and 5-tributylstannyl-3',5'-diacetyl-deoxyuridine (**15a**) afforded 5-(4'-[^{18}F]fluorophenyl)uridine (**14b**) and 5-(4'-[^{18}F]fluorophenyl) deoxyuridine (**15b**), respectively. Reaction conditions were optimized through screening of various reaction parameters like solvent, temperature, catalyst, and co-ligand. Optimized reaction conditions (65 °C for 20 min, $Pd_2(dba)_3$ as catalyst, CuI as additive, $AsPh_3$ as co-ligand, and DMF/dioxane (1:1) as the solvent) gave the respective cross-coupling products in radiochemical yields of up to 69% (*Figure 2.16.*).

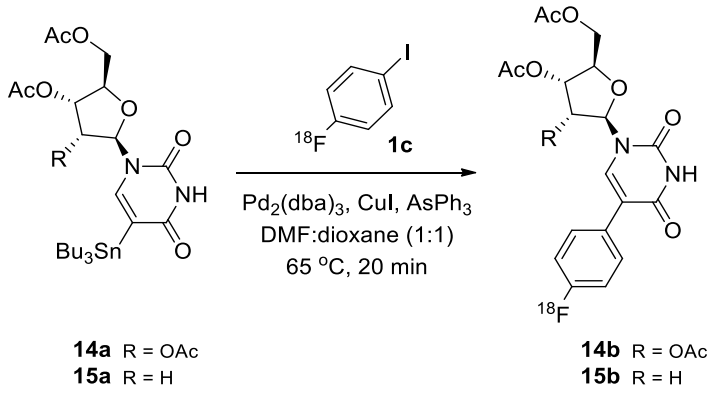

Figure 2.16. Stille cross coupling reaction yielding uridine based compounds.

Another series of reactions involving 4-[^{18}F]fluoroiodobenzene (**1c**) as the coupling partner in the Stille reactions was focused on the preparation of various COX-2 inhibitors[44]. The reaction depicted in *Figure 2.17*.

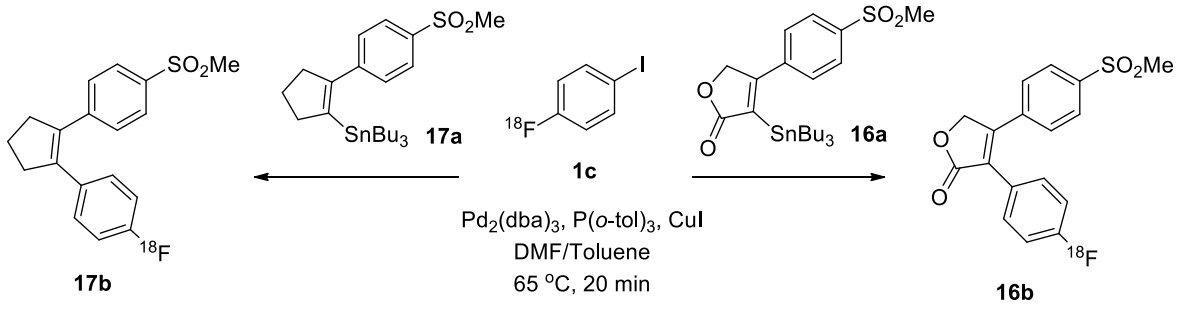

Figure 2.17. Stille cross coupling reactions yielding various COX-2 inhibitor compounds.

Optimized reaction conditions (DMF-toluene as the solvent, 65 °C for 20 min, $Pd_2(dba)_3$ as palladium source, CuI as additive, and $P(o\text{-tol})_3$ as co-ligand) gave cross-coupled products **16b** and **17b** in radiochemical yields of 93% and 68%, respectively.

2.3.2. Suzuki reactions with 4-[^{18}F]fluorohalobenzenes

An alternative to the Stille reaction is the palladium-mediated cross-coupling reaction of boronic acids and boronic esters with electrophiles, also referred to as the Suzuki reaction. The mild reaction conditions, the extensive functional group compatibility, and the lack of toxic tin by-products make the Suzuki reaction an attractive alternative to the frequently employed Stille reaction. The Suzuki reaction follows the principle catalytic cycle for palladium-mediated cross-coupling reactions. However, the reaction requires the presence of a base to activate the organoboron compound to enhance the transmetalation step[45].

The Suzuki reaction was implemented into ^{18}F chemistry in 2006, when Steiniger *et al.* reported the synthesis of various ^{18}F-labelled biphenyls through coupling of aryl boronic acid derivatives with 4-[^{18}F]fluroiodobenzene (**1c**)[46]. The reaction was optimized in a model reaction through screening various palladium sources ($Pd(PPh_3)_4$, $Pd_2(dba)_3$, $PdCl_2(PPh_3)_2$, $Pd(OAc)_2$), auxiliary bases (Cs_2CO_3, K_3PO_4, KOAc) and solvents. Optimized reaction conditions ($Pd_2(dba)_3$, Cs_2CO_3, CH_3CN) gave the desired biphenyl (**17b**) in high radiochemical yields of up to 95% after 5 min at 60 °C (*Figure 2.18.*).

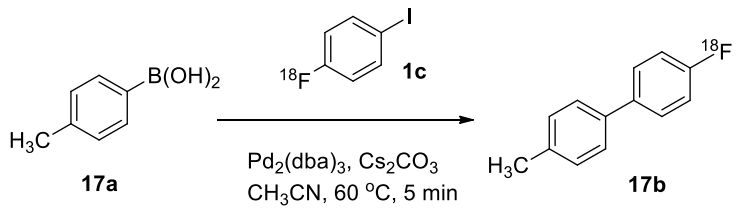

Figure 2.18. Suzuki cross coupling reaction to synthesize biphenyl derivatives.

Optimized reaction conditions were applied to the cross coupling of a wide variety of different aryl boronic acid derivatives with 4-[^{18}F]fluoroiodobenzene (**1c**) to afford the corresponding ^{18}F-labelled biphenyl. It was shown that the Suzuki reaction is tolerable to many functional groups while providing high radiochemical yields, except for bromo- and carboxylic acid-containing aryl boronic acid compounds[46].

2.3.3. Sonogashira reaction with [^{18}F]fluorohalobenzenes

Further extension of C-C bond formations in ^{18}F chemistry was achieved through application of the Sonogashira reaction. The Sonogashira reaction with 4-

[^{18}F]fluoroiodobenzene (**1c**) results in the formation of 4-[^{18}F]fluorophenyl-ethynyl-substituted compounds.

Product	Radiochemical yield (%)
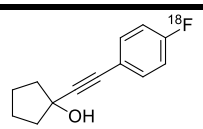	85
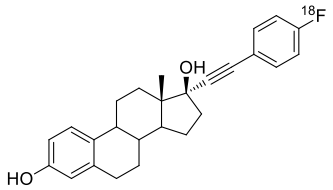	65-88
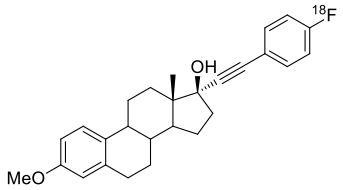	34-64

Table 2.5. Sonogashira reaction with 4-[^{18}F]fluoroiodobenzene.

The Sonogashira reaction was used by Wuest *et al.* to react ethynylcyclopentyl carbinol (**32a**), 17α-ethynyl-3,17β-estadiol (**33a**), and 17α-ethynyl-3,17β-estradiol-3-methylether (**34a**), with 4-[^{18}F]fluoroiodobenzene[47]. This reaction was performed at 100 °C for 20 min using THF as the solvent in the presence of triethylamine as the base, $Pd(PPh_3)_4$ as palladium source, and CuI as additive. The radiochemical yields of resulting cross-coupled compounds are summarized in *Table 2.5.*

2.3.4. Buchwald *N*-arylation reactions with 4-[^{18}F]fluorohalobenzenes

Besides C-C bond forming reactions according to the Stille, Suzuki, and Sonogashira reactions, 4-[^{18}F]fluorohalobenzenes can also be used in cross-

coupling reactions with heteroatoms. One of the most prominent class of reaction is the Buchwald *N*-arylation which results in the formation of C-N bonds. Application of *N*-arylation reactions in ^{18}F chemistry was first demonstrated through the synthesis of 5-HT_{2A} ligand [^{18}F]RP 62203 (**35b**) by Marriere *et al.*[48].

Optimized reaction conditions used toluene as the solvent, $Pd_2(dba)_3$ as the palladium source, P(o-tolyl)$_3$ as co-ligand, and NaOtBu as base. The reaction was completed within 15 min at elevated temperatures of 110 °C providing cross-coupled product (**35b**) in 60% radiochemical yield (*Figure 2.19.*).

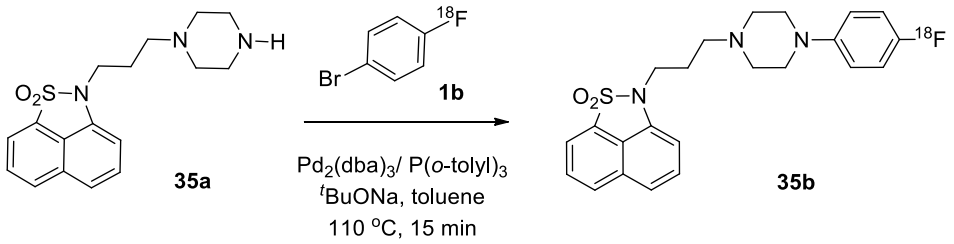

Figure 2.19. Buchwald N-arylation to yield a serotonin HT_{2A} receptor antagonist.

Another application of *N*-arylation reactions with 4-[^{18}F]fluorohalobenzenes as coupling partner was reported by Wuest *et al.*[49]. In a first set of reactions the authors studied the cross coupling reaction of 4-[^{18}F]fluoroiodobenzene (**1c**) with indole as model compound while screening different reaction conditions.

Optimized reaction conditions were applied to the synthesis of 4-[^{18}F]fluoro-phenyl-substituted indole derivatives. The use of $Pd_2(dba)_3$/(2-(dicyclohexyl-phosphino)-2'-(N,N-dimethylamino)-biphenyl as the catalyst system, toluene as the solvent and NaOtBu as the base afforded desired cross-coupling products in high radiochemical yields of 84 and 91% after a reaction time of 20 min at 100 °C (*Table 2.6.*).

Product	Radiochemical yield (%)
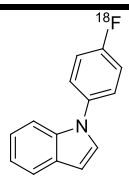	70
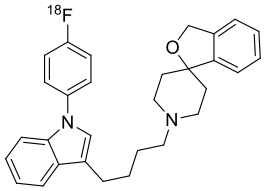	91
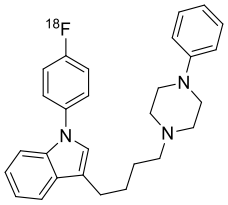	84

Table 2.6. Buchwald N-arylation with 4-[^{18}F]fluorohalobenzenes.

2.4. Novel developments

2.4.1. Palladium-mediated nucleophilic radiofluorinations

Recently, various Pd-complexes [LPd(II)Ar(F)], where L is a biaryl monophosphine ligand and Ar is an aryl group, have been described and conditions were identified under which reductive elimination occurs to form Ar-F bonds[50]. These studies revealed the importance of the biaryl monophosphine ligand used for successful reductive elimination. The ligands enable correct structural conformation for the reductive elimination reaction. Examples of biaryl monophosphine ligands L and the principle reaction sequence are given in *Figure 2.20.* and *Figure 2.21.*, respectively.

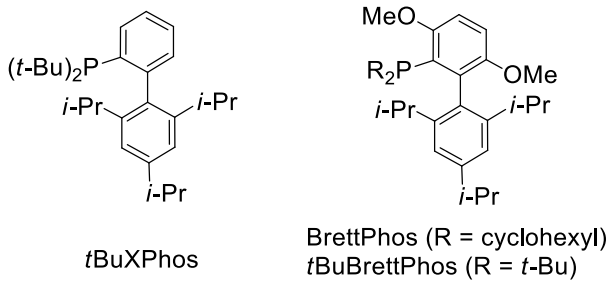

Figure 2.20. Examples of biaryl monophosphine ligands used in PMNR.

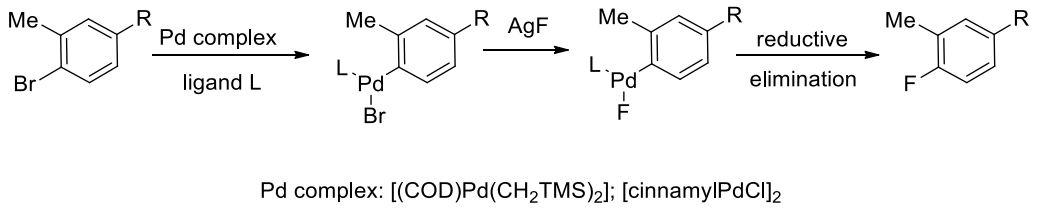

Figure 2.21. Palladium mediated nucleophilic radiofluorination reaction scheme.

Using biaryl monophosphine ligands BrettPhos and tBuBrettPhos, Selivanova *et al.* tested several arenes (**36**) containing activating, non-activating, and deactivating functional groups (R = H, OMe, nitro, phenyl) for Pd-mediated nucleophilic radiofluorinations (PMNR) with n.c.a. [^{18}F]fluoride (*Figure 2.22.*)[51].

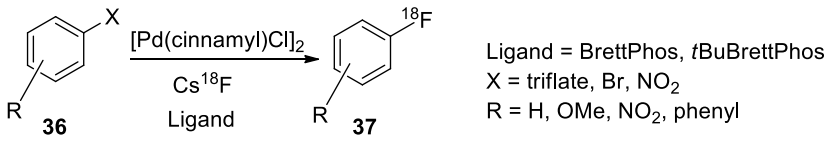

Figure 2.22. Palladium mediated nucleophilic radiofluorination of aromatic compounds.

The authors tested several reaction conditions and found that the reaction proceeded best with an activated aromatic ring at lower temperatures in dimethyl sulfoxide (DMSO). When using a non-activated aromatic system the reaction preceded best with toluene as the solvent. Radiofluorination reactions afforded better yields when carrier fluoride (CsF) was added. However, overall

radiochemical yields for [^{18}F]fluoroarenes **37** remained low (>5%) under these conditions. The authors noted that solubility of fluoride in toluene is not optimal. A comparable approach using BrettPhos as ligand was reported by Cardinale *et al.* (*Figure 2.23.*)[52].

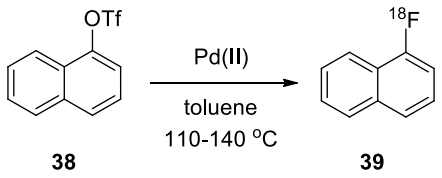

Figure 2.23. Palldium catalyzed nucleophilic fluorination of aryl triflates.

The authors also used toluene as solvent and elevated temperatures between 110 °C to 140 °C. All reactions were performed at a 25 μmole scale (naphthyl triflate **38**) with 4 mol% of palladium complex, 6 mol% of ligand (BrettPhos), and reacted for 45 minutes. Several catalysts were tested as well as c.a. and n.c.a. [^{18}F]fluoride. The best reaction conditions were found in the presence of 10 μmol of CsCl, with an overall radiochemical yield of 5%.

2.4.2. Electrophilic late-stage radiofluorinations

Late-stage electrophilic radiofluorination reactions were performed by Lee *et al.* which involved a Pd complex 41 as an electrophilic fluorination reagent[53]. Palladium complex 40 carries three formal positive charges, allowing for the nucleophilic capture of negatively charged n.c.a. [^{18}F]fluoride. This is specifically important in radiochemistry in which the concentration of [^{18}F]fluoride in solution is non-quantifiable.

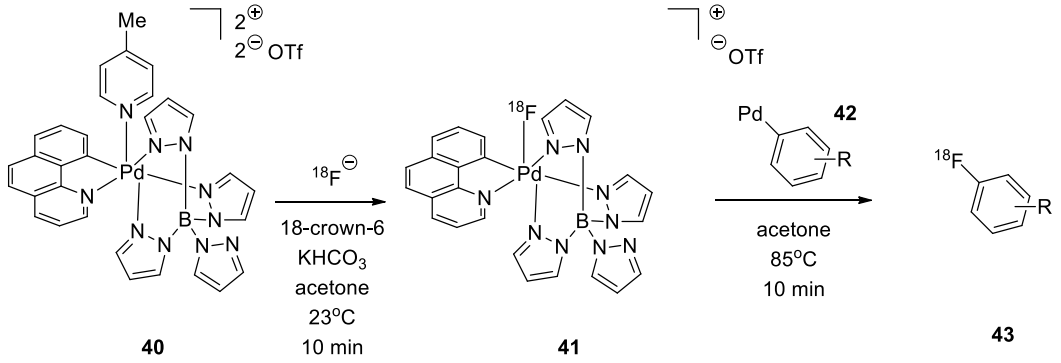

Figure 2.24. Electrophilic late stage radiofluorination reaction scheme.

Product	Radiochemical yield (%)
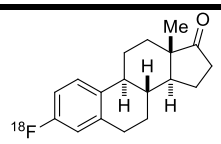	33 ± 7
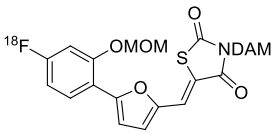	10 ± 2
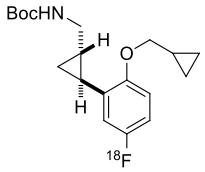	18 ± 5

*Table 2.7. Radiofluorination of Pd-aryl complexes **42** with electrophilic fluorination reagent **41.***

Resulting complex **41** contains Pd at the +IV oxidation state, thus acting as an oxidant and facilitating the transfer of a ligand to an electrophilic ^{18}F (*Figure 2.24.*). Best reaction conditions for the formation of [^{18}F] fluoride-palladium complex **41** were found to be 23 °C in acetone for 10 minutes. Reaction of Pd complex **41** with various Pd-aryl complexes **42** afforded aryl fluorides **43**. *Table 2.7.* summarizes the reported radiochemical yields.

2.5. Conclusions

Palladium-mediated cross-coupling reactions have proven to be an exceptionally valuable synthesis approach to further expand the arsenal of ^{18}F-labelled compounds. The compatibility towards a wide range of functional groups, the versatility to form distinct C-C and C-heteroatom bonds, and the favourable reaction conditions of palladium-mediated cross-coupling reactions with 4-[^{18}F]fluorohalobenzenes have made this class of reactions a popular novel labelling strategy in ^{18}F chemistry.

Novel developments like Pd-mediated late stage nucleophilic and electrophilic radiofluorination have the potential to revolutionize organic PET chemistry with ^{18}F. This highly innovative approach would allow late stage incorporation of n.c.a. [^{18}F]fluoride into aromatic systems.

Recent advancements towards the development of highly efficient catalyst systems as well as the implementation of novel labelling technology like micro-reactor and microfluidic technology will open novel opportunities for a broader application of palladium-mediated cross-couplings in ^{18}F chemistry. A current major challenge is the need to increase the radioactivity amount of the cross-coupled products and to implement aspects of radiopharmacy like good manufacturing practice (GMP) into the radiosynthesis to make the radiotracers available for potential clinical applications.

This will provide further stimulation to advance positron emission tomography (PET) as a powerful imaging technique in clinical and preclinical research, as well as in drug research and development.

2.6. Acknowledgements

The authors thank the Natural Sciences and Engineering Council of Canada (NSERC) and the Dianne and Irving Kipnes Foundation for supporting this work.

2.7. References

1 Qaim, S. M. Cyclotron production of medical radionuclides. In: Vertes, A.; Nagy, S.; Klencsar, Z. Handbook of Nuclear Chemistry, Volume 4, *Radiochemistry and Radiopharmaceutical Chemistry in Life Science.* Kluwer Academic Publishers, **2003**, 47-79.

2 Krasikova, R. Synthesis modules and automation in F-18 labelling. *Ernst Schering Res. Found Workshop*, **2007**, *62*, 289-316.

3 Lu, S. Y.; Pike, V. W. Micro-reactors for PET tracer labelling. *Ernst Schering Res. Found Workshop*, **2007**, *62*, 271-287.

4 Blodgett, T. M.; Meltzer, C. C.; Townsend, D. W. PET/CT: form and function. *Radiology*, **2007**, *242*, 360-385.

5 Surti, S,; Kuhn, A.; Werner, M. E.; Perkins, A. E.; Kolthammer, J.; Karp, J. S. Performance of philips gemini TF PET/CT scanner with special consideration for its time-of-flight imaging capabilities. *J. Nucl. Med.*, **2007**, *48,* 471-480.

6 Surti, S.; Karp, J. S.; Popescu, L. M.; Daube-Witherspoon, M. E.; Werner, M. Investigation of time-of-flight benefit for fully 3-D PET. *IEEE Trans Med Imaging,* **2006**, *25*, 529-538.

7 Zaidi, H. Recent developments and future trends in nuclear medicine instrumentation. *Z. Med. Phys*., **2006**, *16*, 5-17.

8 Sossi, V.; Ruth, T. J. Micropet imaging: *in vivo* biochemistry in small animals. *J. Neural Transm*., **2005**, *112*, 319-330.

9 Park, B. K.; Kitteringham, N. R.; O'Neill, P. M. Metabolism of fluorine-containing drugs. *Annu. Rev. Pharmacol. Toxicol.,* **2001**, *41*, 443.

10 Brinkman, G. A. Reactions of radioactive recoil atoms with arenes. *Chem. Rev.* **1981**, *81,* 270.

11 DiRaddo, P.; Diksic, M.; Jolly, D. The ^{18}F radiofluorination of arylsilanes. *J. Chem. Soc. Chem. Commun*., **1984**, 159-160.

12 Speranza, M.; Shiue, C.-Y.; Wolf, A. P.; Wilbur, D. S.; Angelini, G. Electrophilic radiofluorination of aryltrimethylsilanes as a general route to ^{18}F-labelled aryl fluorides. *J. Fluor. Chem.,* **1985**, *30*, 97-107.

14 Coenen, H. H.; Moerlein, S. M. Regiospecific aromatic fluorodemetallation of group IVb metalloarenes using elemental fluorine and acetyl hypofluorite. *J. Fluor. Chem.*, **1987**, *36*, 63-75.

15 Knochel, A.; Zwernemann, O. Aromatic n.c.a. labelling with ^{18}F by modified Balz-Schiemann decomposition. *Appl. Radiat. Isot*., **1991,** *42*, 1077-1080.

16 Kilbourn, M. R.; Welch, M. J.; Dence, C. S.; Tewson, T. J.; Saji, H. and Maeda M. Carrier-added and no-carrier-added syntheses of [^{18}F]spiroperidol and [^{18}F]haloperidol. *Int. J. Appl. Radiat. Isot*., **1984**, *35,* 591-598.

17 Ermert J.; Hocke, C.; Ludwig T.; Gail, R. and Coenen R. R. Comparison of pathways to the versatile synthon of no-carrier-added 1-bromo-4-[^{18}F]fluorobenzene. *J. Labelled Compd. Radiopharm.,* **2004**, *47*, 429-441.

18 Berridge, M.; Crouzel, C. and Comar, D. No-carrier-added ^{18}F-fluoride in organic solvents production and labelling results. *J. Labelled Compd. Radiopharm.*, **1982**, *19*, 1639-1640.

19 Lazarova, N.; Siméon, F. G.; Musachio, J. L.; Lu, S. Y.; Pike, V. W. Integration of a microwave reactor with Synthia to provide a fully automated radiofluorination module. *J. Labelled Compd. Radiopharm,.* **2007**, *50*, 463–465.

20 Satyamurthy, N.; Barrio, J. R. Nucleophilic fluorination of aromatic compounds. *Patent: WO 2010/008522* A2 **2010**

21 Gail, R.; Coenen, H. H. A one step preparation of the n.c.a. fluorine-18 labelled synthons: 4-fluorobromobenzene and 4-fluoroiodobenzene. *Appl. Radiat. Isot.,* **1994**, *45*, 105-111.

22 Allain-Barbier, L.; Lasne, M-C.; Perrio-Huard C.; Mureau, B. and Barre, L. Synthesis of 4-[^{18}F]fluorophenyl -alkenes and -arenes via palladium-catalyzed coupling of 4-[^{18}F]fluoroiodobenzene with vinyl and aryl tin reagents. *Acta Chem. Scand.*, **1998**, *52*, 480-489.

23 Shiue, C-Y.; Watanabe, M.; Wolf, A. P.; Fowler, J. S.; Salvadori P. Application of the nucleophilic substitution reaction to the synthesis of no-carrier-added [^{18}F]fluorobenzene and other ^{18}F-labelled aryl fluorides. *J. Labelled Compd. Radiopharm.*, **1984**, *21*, 533-547.

24 Forngren, T.; Anderson, Y.; Lamm, B.; Langstrom, B. Synthesis of [4-^{18}F]-1-bromo-4-fluorobenzene and its use in palladium-promoted cross-coupling reactions with organostannanes. *Acta Chem. Scand.,* **1998**, *52*, 475-479.

25 Gail, R.; Hocke, C.; Coenen, H. H. Direct n.c.a. ^{18}F-fluorination of halo- and alkylarenes via corresponding diphenyliodonium salts. *J. Labelled Compd. Radiopharm.*, **1995**, *40*, 50-53.

26 Shah, A.; Widdowson, D. A. and Pike V. W.; Synthesis of substituted diaryliodonium salts and investigation of their reactions with no-carrier added [^{18}F]fluoride. *J. Labelled Compd. Radiopharm.,* **1995**, *40*, 65-67.

27 Grushin V. V.; Carboranylhalonium ions: from striking reactivity to a unified mechanistic analysis of polar reactions of diarylhalonium compounds. *Acc. Chem. Res.,* **1992**, *25*, 529–536.

28 Carroll, M. A.; Martín-Santamaría, S.; Pike, V. W.; Rzepa, H. S.; Widdowson, D. A.; An ab initio and MNDO-d SCF-MO computational study of stereoelectronic control in extrusion reactions of R_2I–F iodine(III) intermediates. *J. Chem. Soc. Perkin Trans. 2*, **1999**, 2707–2714.

29 Martín-Santamaría, S.; Carroll, M. A.; Pike, V. W.; Rzepa, H. S.; Widdowson, D. A.; An ab initio and MNDO-d SCF–MO computational study of the extrusion reactions of R_2I–F iodine(III) via dimeric, trimeric and tetrameric transition states. *J. Chem. Soc. Perkin Trans. 2*, **2000**, 2158– 2161.

30 Ross, T. L.; Ermert, J.; Hocke, C.; Coenen, H. H.; Nucleophilic ^{18}F-fluorination of heteroaromatic iodonium salts with no-carrier-added [^{18}F]fluoride. *J. Am. Chem. Soc.*, **2007**, *129*, 8018–8025.

31 Caroll, M. A.; Nairne, J.; Smith, G.; Widdowson, D. A. Radical scavengers: apractical solution to the reproducibilty issue in the fluoridation of diaryliodonium salts. *J. Fluor. Chem.,* **2007**, *128*, 127-132.

32 Ross, T. L.; Ermert, J.; Coenen, H. H. Nucleophilic ^{18}F-fluorination of heteroaromatic iodonium salts with no-carrier-added [^{18}F]fluoride. *J. Am. Chem. Soc.*, **2007**, *129*, 8018-8025.

33 Basuli, F.; Wu, H.; Griffiths, G. Synthesis of meta-[^{18}F]fluorobenzadehyde and meta-[^{18}F]fluobenzylbromide from phenyl(3-Formylphenyl)iodonium salt precursors. *J. Labelled Compd. Radiopharm.,* **2011**, *54*, 224-228.

34 Zhang, M. R.; Kumata, K.; Suzuki, K. A practical route for synthesizing a PET ligand containing [^{18}F]fluorobenzene using reaction of phenyliodonium salt with [^{18}F]F^{-}. *Tetrahedron Lett.,* **2007**, *48*, 8632-8635.

35 Martín-Santamaría, S.; Carroll, M. A.; Carroll, C. M.; Carter, C. D.; Pike, V. W.; Rzepa, H. S.; Widdowson, D. A. Fluoridation of heteroaromatic iodonium salts—experimental evidence supporting theoretical prediction of the selectivity of the process. *Chem. Commun.,* **2000**, 649–650.

36 Fischer, C. R.; Mu, L.; Becaud, J.; Schubiger, P. A.; Schibli, R.; Ametamey, S. M.; Graham, K. Stellfeld, T.; Dinkelborg, L. M.; Lehmann, L. ^{18}F-labelling of unactivated aromatic compounds using triarylsulfonium salts. *J. Labelled Compd. Radiopharm.*, **2011**, *54*, S71.

37 Mu, L.; Fischer, C. R.; Holland, J. P.; Becaud, J.; Schubiger, P. A.; Schibli, R.; Ametamey, S. M.; Graham, K. Stellfeld, T.; Dinkelborg, L. M.; Lehmann, L. ^{18}F-Radiolabelling of aromatic compounds using triarylsulfonium salts. *Eur. J. Org. Chem.*, **2012**, *In Press*.

38 Wust, F. R.; Kniess, T. Synthesis of 4-[^{18}F]fluoroiodobenzene and its application in Sonogashira cross-coupling reactions. *J. Labelled Compd. Radiopharm*., **2003**, *46*, 699-713.

39 Chun, J. H.; Lu, S.; Pike, V. W. Rapid and efficient radiosynthesis of *meta*-substituted [^{18}F]fluoroarenes from [^{18}F]fluoride ion and diaryliodonium tosylates within a microreactor. *Eur. J. Org. Chem*., **2011**, 4439-4447.

40 Chun, J. H.; Lu. S.; Lee, Y. S.; Pike, V. W. Fast and high yield microreactor syntheses of *ortho*-substituted [^{18}F]fluoroarenes from reactions of [^{18}F]fluoride ion with diaryliodonium salts. *J. Org. Chem.,* **2010**, *75*, 3332-3338.

41 Milstein, D.; Stille, J. K. Palladium-catalyzed coupling of tetraorganotin compounds with aryl and benzyl halides. Synthetic utility and mechanism. *J. Am. Chem. Soc*., **1979**, *17*, 4994-4998.

42 Marriere, E.; Rouden, J.; Tadino, V.; Lasne, M. C. Synthesis of analogues of ()-cystine for *in vivo* studies of nicotinic receptors using positron emission tomography. *Organic Letters*, **2000**, *8*, 1121-1124.

43 Wust, F. R.; Kniess, T. No-carrier added synthesis of ^{18}F-labelled nucleosides using Stille cross-coupling reactions with 4-

[^{18}F]fluoroiodobenzene. *J. Labelled Compd. Radiopharm.*, **2004**, *47*, 457-468.

44 Wust, F. R.; Hohne, A.; Metz, P. Synthesis of ^{18}F-labelled cyclooxygenase-2 (COX-2) inhibitors via Stille reaction with 4-[^{18}F]fluoroiodobenzene as radiotracers for positron emission tomography (PET). *Org. Biomol. Chem.*, **2005**, *3*, 503-507.

45 Suzuki, A. Cross-coupling reaction via organoboranes. *Journal of Organometallic Chemistry*, **2002**, *653*, 83-90.

46 Steiniger, B.; Wuest, F. R. Synthesis of ^{18}F-labelled biphenyls via Suzuki cross-coupling with 4-[^{18}F]fluoroiodobenzene. *J. Labelled Compd. Radiopharm.*, **2006**, *49*, 817-827.

47 Sonogashira, K.; Tohda, Y.; Hagihara, N. A convient synthesis of acetylenes: catalytic substitutions of acetylenic hydrogen with bromoalkenes, iodoarenes, and bromopyridines. *Tetrahedron Letters*, **1975**, *50*, 4467-4470.

48 Marriere, E.; Chazalviel, L.; Dhilly, M.; Toutain, J.; Perrio, C.; Dauphin, F.; Lasne, M. C. Synthesis of [^{18}F]RP 62203, a potent and selective serotonin 5-HT_{2A} receptor antagonist and biological evaluations with *ex-vivo* autoradiography. *J. Labelled Compd. Radiopharm.,* **1999**, *42*, S69-S71.

49 Wust, F. R.; Kniess, T. *N*-Arylation of indoles with 4-[^{18}F]fluoroiodobenzene: synthesis of ^{18}F-labelled s_2 receptors ligands for

positron emission tomography (PET). *J. Labelled Compd. Radiopharm.,* **2005**, *48*, 31-43.

50 Watson, D. A.; Su, M.; Teverovskiy, G.; Zhang, Y.; Garcia-Fortanet, J.; Kinzel, T.; Buchwald, S. L. Formation of ArF from LPdAr(F): catalytic conversion of aryl triflates to aryl fluorides. *Science*, **2009**, *325*, 1661-1664.

51 Selivanova, S. V.; Combe, F.; Schubiger, A. P.; Ametamey, S. M. P-423 palladium catalyzed nucleophilic radiofluorination of aromatic compounds. *J. Labelled Compd. Radiopharm*., **2011**, *54*, S512.

52 Cardinale, J.; Ermert, J.; Kuegler, F.; Fabian, H.; Andreas, C.; Heinz, H. P-390 studies on Pd-catalysed nucleophilic ^{18}F-fluorination of aryl triflates. *J. Labelled Compd. Radiopharm.*, **2011**, *54*, S479.

53 Lee, E.; Kamlet, A. S.; Powers, D. C.; Neumann, C. N.; Boursalian, G. B.; Furuya, T.; Choi, D. C.; Hooker, J. M.; Ritter, T. A fluoride-derived electrophilic late-stage fluorination reagent for PET imaging. *Science,* **2001**, *334*, 639-642.

Chapter 3

*Automated radiosynthesis of no-carrier added 4-[^{18}F]fluoroiodo-benzene: a versatile building block in ^{18}F radiochemistry.**

Jenilee Way, Frank Wuest

3.1. Introduction

The success of positron emission tomography (PET) for functional molecular imaging depends largely on the availability of suitable radiotracers. Recent advancements in radionuclide production[1], automation of radiotracer synthesis[2,3], and significant improvement of PET scanner instrumentation[4-7], including small animal PET-scanners[8], have further stimulated clinical and preclinical research activities focused on the visualization and assessment of biochemical processes in living organisms. However, design and synthesis of innovative PET radiotracers remains a special challenge, and PET chemistry has evolved into a complex chemical science. Special attention is attributed to radiochemistry with the short-lived positron emitter fluorine-18 (^{18}F, $t_{1/2}$ = 109.8 min). The relatively long half-life, the low maximal positron energy (0.635 MeV), and the ease of large scale cyclotron production make ^{18}F an ideal radionuclide for the design and synthesis of PET radiotracers.

PET chemistry of ^{18}F and the applications of ^{18}F-labelled radiotracers have been reviewed frequently over the last decades. Within the plethora of ^{18}F-labelled radiotracers, only a few have been prepared by the use of transition-metal mediated cross coupling reactions. These transition metal-mediated cross coupling

* *J. Labelled Compds. Radiopharm.*, **2014**; *57:* 104-109.

reactions mainly exploited palladium complexes and 4-[^{18}F]fluorohalobenzenes as electrophilic coupling partners for the preparation of PET radiotracers containing a 4-[^{18}F]fluorophenyl group.

Over the last two decades, numerous methods have been reported for the preparation of 4-[^{18}F]fluorohalobenzenes. Methods include hot atom recoil chemistry, direct electrophilic and nucleophilic aromatic radiofluorination chemistry. Significant improvements were achieved by using iodonium and sulfonium salts as labelling precursors. Moreover, novel technologies like microwave activation and microfluidic devices have also been applied to prepare 4-[^{18}F]fluorohalobenzenes. A comprehensive summary of methods and technologies for the preparation of 4-[^{18}F]fluorohalobenzenes has recently been published. Based on the reported radiochemical yields and the availability of starting materials, nucleophilic aromatic radiofluorination reactions using sulfonium salts as labelling precursors seem to be the most promising synthesis route for the preparation of 4-[^{18}F]fluorohalobenzenes. Therefore, we decided to adapt sulfonium salt-based chemistry to an automated synthesis procedure enabling the preparation of large amounts of n.c.a. 4-[^{18}F]fluorohalobenzenes with special focus on 4-[^{18}F]fluoroiodobenzene.

Herein, we describe fully automated synthesis of n.c.a. 4-[^{18}F]fluoroiodobenzene on a GE TRACERlab™ FX automated synthesis unit (ASU) starting from commercially available (4-iodo-phenyl)diphenylsulfonium triflate as the labelling precursor.

3.2. Experimental

3.2.1. General

All chemicals used were obtained from Sigma-Aldrich® and used as received without further purification. Water was obtained from a Barnstead Nanopure water filtration system (Barnstead Diamond Nanopure pack organic free RO/DIS).

High performance liquid chromatography (HPLC) purification and analysis of ^{18}F-radiolabelled products were performed using a Phenomenex LUNA® C18(2) column (100 Å, 250 x 10 mm, 10 μm) using gradient elution specific to the given compound (Gilson 321 pump, 171 diode array detector, Berthold Technologies Herm LC). Radio-TLC were performed using either EMD Merck F254 silica gel 60 aluminum backed thin layer chromatography (TLC) plates or Analtech RP18 with UV254 aluminum backed TLC plates (Bioscan AR-2000). Quantification of radioactive samples during chemistry was achieved using a Biodex ATOMLAB™ 400 dose calibrator. Reaction parameters were screened using an IKAMAG® Ret-G Stir plate with an oil bath.

3.2.2. Preparation of kryptofix 2.2.2. solution

Into a 50 mL volumetric flask, K_2CO_3 (92.3 mg, 668 μmol) in water (7.0 mL) is added. Next, kryptofix 2.2.2. (500 mg, 1.38 mmol) is added with CH_3CN (43.0 mL) to the mark of the flask. The solution is then sealed in an amber vial and stored at 4 °C.

3.2.3. Manual synthesis of 4-[^{18}F]fluoroiodobenzene ([^{18}F]FIB)

N.c.a. [^{18}F]fluoride was produced via the ^{18}O(p,n)^{18}F nuclear reaction from [^{18}O]H_2O (Rotem Industries Ltd, Hyox oxygen-18 enriched water, min. 98%) on an ACSI TR19/9 Cyclotron (Advanced Cyclotron Systems Inc., Richmond, Canada). Cyclotron-produced [^{18}F]fluoride was then trapped on a Waters SepPak® light QMA anion exchange cartridge and eluted off with 86% K2.2.2./K_2CO_3 (1.5 mL) into a long screw top test tube. This solution was then dried azeotropically with additional CH_3CN (6 mL) under nitrogen at 95 °C in an oil bath. Once fully dried the reaction vessel was allowed to cool for 5 minutes and labelling precursor (4-iodophenyl)diphenylsulfonium triflate (7 mg) was added in CH_3CN (1 mL), and the reactor was sealed. The reaction proceeded for 15 minutes at 85 °C. Upon completion the reaction mixture was diluted with water (20 mL) and trapped on a Waters Sep-Pak® tC18 plus light cartridge. The solid phase extraction (SPE) cartridge was then washed with 10mL of additional water and the final product of [^{18}F]FIB was eluted off in CH_3CN (3 mL).

3.2.4. Fully automated synthesis of 4-[^{18}F]fluoroiodobenzene ([^{18}F]FIB)

Radiosynthesis of 4-[^{18}F]fluoroiodobenzene was performed on a GE TRACERlab™ FX (General Electric Company, Fairfield, Connecticut, United States.) This ASU was modified in terms of program and hardware (*Figure 3.1.*).

The synthetic procedure started with the elution of resin-bound cyclotron-produced [^{18}F]fluoride from the Waters Sep-Pak®light QMA anion exchange column into reactor 1 (**R1**) of the GE TRACERlab™ FX using a solution of 86% K2.2.2./K_2CO_3 (1.5 mL). [^{18}F]Fluoride was dried azeotropically under vacuum

under a steady stream of nitrogen at 50 °C and 95 °C. To dried [^{18}F]fluoride, (4-iodophenyl)diphenylsulfonium triflate (**V3**, 10 mg) in CH_3CN (1 mL) was added and reacted for 15 min at 90 °C.

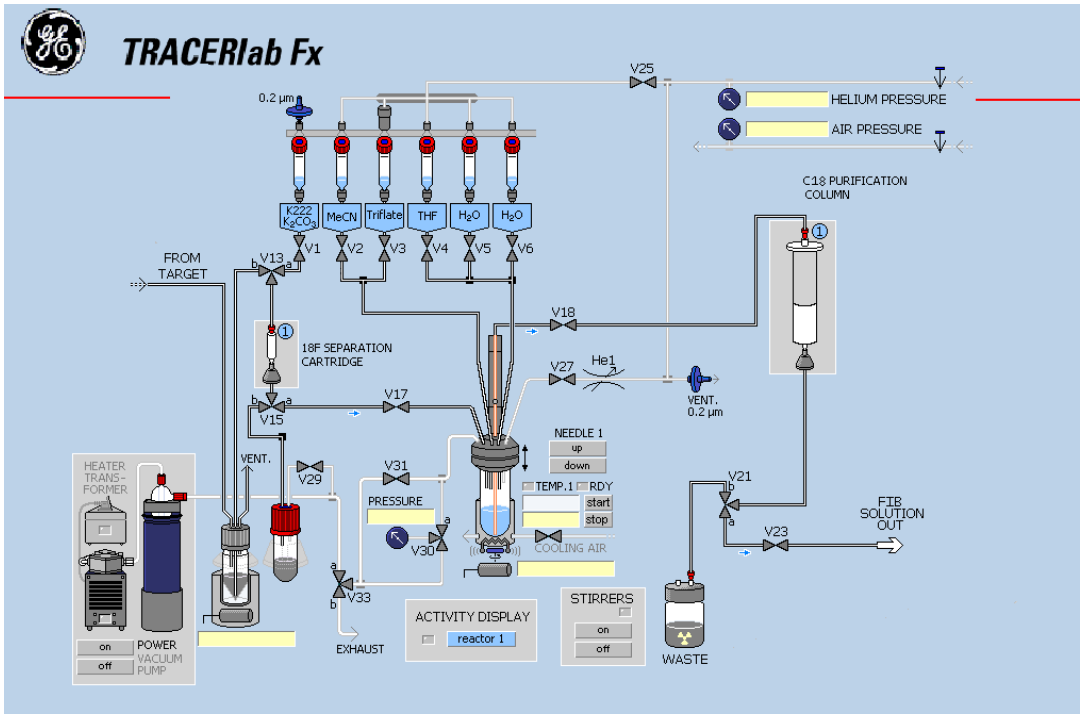

Figure 3.1. Scheme of the automated synthesis unit for the synthesis of 4-[^{18}F]fluoroiodobenzene.

Once the reaction was completed, the mixture was diluted with water (**V5**, 12 mL) and passed through a Waters Sep-Pak*tC18 plus light cartridge (300 mg). The cartridge was washed with additional water (**V6**, 10 mL) and 4-[^{18}F]fluoroiodobenzene ([^{18}F]FIB) was eluted off in CH_3CN (**V4**, 3.0 mL) into a 20 mL sealed collection vial with a vent needle.

3.2.5. HLPC purification of 4-[^{18}F]fluoroiodobenzene ([^{18}F]FIB)

HPLC purification of the crude SPE purified [^{18}F]FIB was performed using a graditent elution as follows: (A: water; B: CH_3CN; 0 min 50% B, 8 min 50% B,

21 min 80% B, 33 min 100% B). The flow rate of the system was 3 mL/min , which gave a retention time of ~22 minutes for the [^{18}F]FIB product as confirmed with the use of a commercially available reference compound. The radiochemical purity was determined by the area under the peak of interest compared to the rest of the radio-chromatogram; as well the specific activity of [^{18}F]FIB was calculated against a standard curve.

3.3. Results and discussion

3.3.1. Optimization of reaction parameters for manual synthesis of 4-[^{18}F]fluoroiodobenzene

Radiosynthesis of 4-[^{18}F]fluoroiodobenzene ([^{18}F]FIB) **3** starting from (4-iodophenyl)diphenylsulfonium triflate **1** is depicted in *Figure 3.2*. The manual syntheses were performed to optimize reaction conditions by screening various reaction parameters (solvent, temperature, synthesis time, precursor concentration) and solid-phase extraction (SPE) methods aimed at increasing the radiochemical yield and radiochemical purity of [^{18}F]FIB **3**, and decreasing the amount of inevitably formed by-product [^{18}F]fluorobenzene **2**.

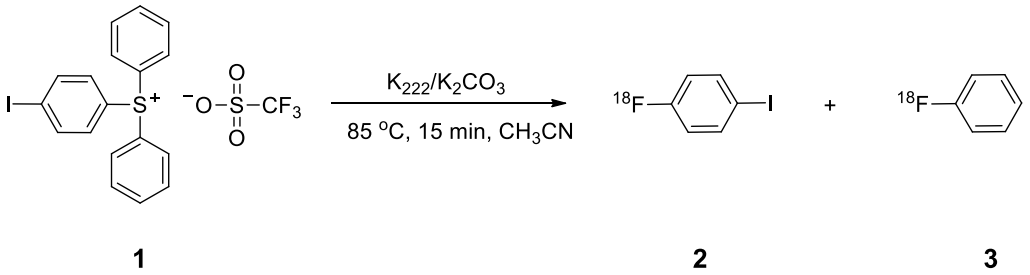

*Figure 3.2. Synthetic procedure for the radiosynthesis of 4-[^{18}F]fluoroiodobenzene **3.***

3.3.1.1. Influence of solvent on radiosynthesis of [^{18}F]FIB

Based on the publication of Linjing *et al.*[19] as a general guide, the following solvents were tested for the synthesis of 4-[^{18}F]fluoroiodobenzene: acetonitrile (CH_3CN), toluene, dioxane, *N,N*-dimethylformamide (DMF), and tetrahydrofuran (THF).

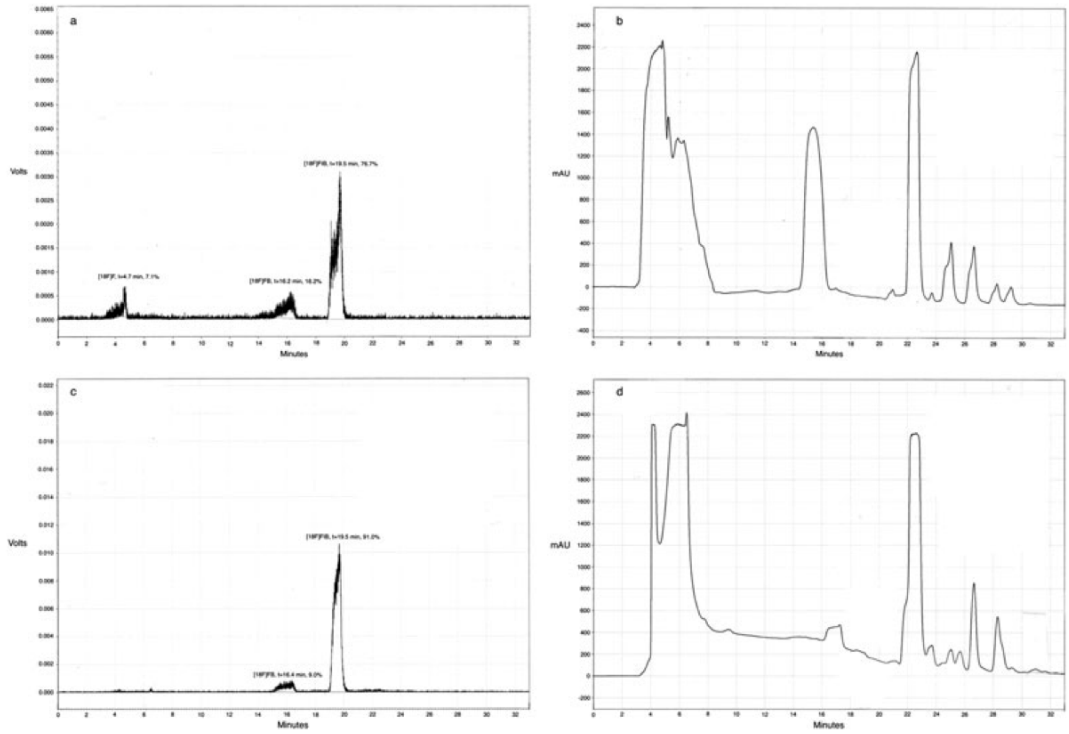

Figure 3.3. Comparison of DMF and CH_3CN as solvents for the ^{18}F-radiolabelling of (4-iodophenyl)diphenylsulfonium triflate

Labelling precursor (4-iodophenyl)diphenylsulfonium triflate **1** was poorly soluble in toluene, THF and dioxane. Only CH_3CN and DMF proved to be suitable solvents for (4-iodophenyl)diphenylsulfonium triflate **1**. Results of using DMF (*Figure 3.3.a/3.3.b*) and CH_3CN (*Figure 3.3.c/3.3.d*) as solvents for the

synthesis of 4-[^{18}F]fluoroiodobenzene are depicted as respective radio-HPLC and UV traces of the reaction mixture (*Figure 3.3.*).

Reaction in both solvents proceeded with a comparable 40 % radiochemical yield. However, radiochemical purity of 4-[^{18}F]fluoroiodobenzene in the reaction mixture was higher in CH_3CN (91%) compared to that of using DMF as the solvent (70 %).

Also the UV-traces as determined by HPLC (displayed in the bottom panels) clearly demonstrate that there are more possible contaminants pushed near the retention time of the peak of interest in DMF as the solvent vs. CH_3CN. Overall, CH_3CN was chosen to be the solvent of choice and it was used in all further experiments.

3.3.1.2. Influence of temperature on radiosynthesis of [^{18}F]FIB

Reaction between (4-iodophenyl)diphenylsulfonium triflate **1** and n.c.a. [^{18}F]fluoride required elevated temperatures. However, at elevated temperature significant amounts of non-radioactive by-products were present in the reaction mixture. Therefore, careful testing of reaction temperature on the radiochemical yield and formation of non-radioactive by-products was necessary. Various reaction temperatures were tested to determine their influence on radiochemical yield and the formation of non-radioactive by-products as represented by their respective HPLC profiles. The results are summarized in *Figure 3.4.a*.

Reaction temperature of 70 °C resulted in only low radiochemical yields of 1-2 %. Radiochemical yields increased significantly at elevated temperatures of 85 °C (61 %) to 120 °C (44 %). However, only reaction temperature of 85 °C gave

sufficient radiochemical yields while showing low amount of non-radioactive by-products in the UV trace of the HPLC trace. Therefore, a reaction temperature of 85 °C was used for further optimization of reaction conditions.

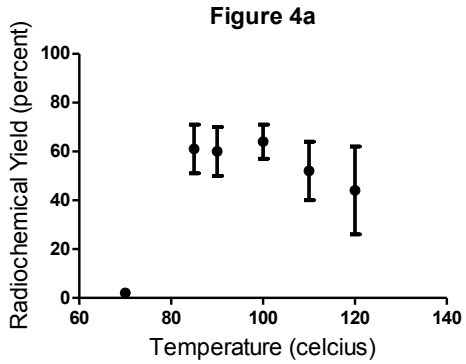

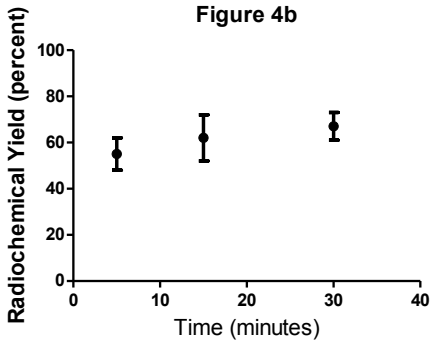

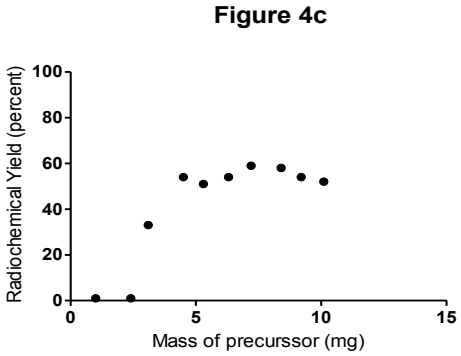

[a]Radiochemical yield determined by radio-TLC representing the percentage of 4-[^{18}F]fluoroiodobenzene present in the reaction mixture.

Figure 3.4.a-3.4.c: Influence of reaction temperature (n=3), reaction time (n=3) and concentration of labelling precursor 1 (n=1) on radiochemical yield[a] of 4-[^{18}F]fluoroiodobenzene.

3.3.1.3. Influence of reaction time on radiosynthesis of 4-[^{18}F]FIB

All reactions were performed at 85 °C using different reaction times varying from 5 min to 30 min. At each time point, aliquots of the reaction mixture were taken and analyzed via radio-TLC with 50 % EtOAc/hexane as the solvent to develop TLC plates (see *Figure 7.9*). As shown in *Figure 3.4.b*, no significant

improvement of radiochemical yield was observed at reaction times longer than 15 min.

3.3.1.4. Influence of labelling precursor amount on radiosynthesis of 4-[^{18}F]FIB

After optimization of reaction temperature, solvent and reaction time, the amount of labelling precursor **1** needed was tested using the reaction conditions of 85 °C in CH_3CN for of 15 min. Progress of the reaction was monitored using radio-TLC. Results are summarized in *Figure 3.4.c*. Results in *Figure 3.4.c* indicate that 5 to 7 mg of labelling precursor **1** provided sufficient radiochemical yields of [^{18}F]FIB (50-59 %). Further increases in the mass of sulfonium salt **1** did not result in significantly higher radiochemical yields. To reduce the amount of potential cold contaminations in the reaction mixture, a labelling precursor amount of 5-7 mg seems to be optimal.

3.3.1.5. Influence of solid phase extraction (SPE) cartridges on radio-synthesis of [^{18}F]FIB

Four different SPE cartridges were tested for their ability to retain and purify [^{18}F]FIB. SPE cartridges tested included Mackerey-Nagel Chromafix® HR-P (M), Phenomenex Strata® C18-U (500 mg), Waters Sep-Pak® tC18 plus light, and Waters Sep-Pak® C18 plus light.

All cartridges gave comparable results, and we decided to use Waters Sep-Pak® tC18 plus light cartridges for further experiments. Also since they are no significant by products in this reaction, the SPE cartridge may not be fully required

3.3.1.6. Summary of optimized reaction parameters for the manual synthesis of [^{18}F]FIB

Optimal reaction conditions resulted in the following manual radiosynthesis of [^{18}F]FIB: Radiosynthesis of [^{18}F]FIB was performed using (4-iodophenyl)diphenylsulfonium triflate as the labelling precursor (7 mg) in CH_3CN (1 mL) at a temperature of 85 °C for 15 min. Application of these reaction conditions afforded [^{18}F]FIB in 41 ± 9 % decay-corrected radiochemical yields after SPE and HPLC purification within a total synthesis time of over a 64 ± 4 min. (n=17). Radiochemical purity was greater than 99 %. In a typical experiment, 235 MBq of [^{18}F]FIB were prepared starting from 850 MBq of n.c.a. [^{18}F]fluoride. These optimized reaction parameters are very similar to that of Linjing *et al.* [19] and provide confirmation that [^{18}F]FIB can be produced selectively and sufficiently over [^{18}F]fluorobenzene as by-product. Moreover, application of HPLC purification afforded [^{18}F]FIB in high radiochemical and chemical purity suitable for subsequent reactions like transition metal-mediated cross-coupling reactions.

3.3.2. Automated synthesis of [^{18}F]FIB

Reaction conditions from optimized manual synthesis were directly transferred to the GE TRACERlab FX fully automated synthesis unit (ASU). Radiosynthesis of [^{18}F]FIB in the ASU gave comparable results as found for the manual synthesis. The reaction temperature was slightly increased to 90 °C since larger amounts of non-reacted [^{18}F]fluoride were found in the reaction mixture when a reaction temperature of 85 °C was used. In summary, ASU synthesis provided [^{18}F]FIB in

decay-corrected radiochemical yields of 89 ± 10 % (n=7) within a reaction time of 59 ± 2 min including HPLC purification. Radiochemical purity was 97 ± 3 %. Specific activity of [^{18}F]FIB was greater than 40 GBq/µmol (see *Figure 7.10/Table 7.1*). In a typical ASU synthesis, 6.4 GBq of [^{18}F]FIB could be prepared from 10.4 GBq of n.c.a. [^{18}F]fluoride.

3.3.3. HLPC purification of 4-[^{18}F]fluoroiodobenzene ([^{18}F]FIB)

Purification was completed as described in experimental section, eluting [^{18}F]FIB after 22 minutes as shown in *Figure 3.5*.

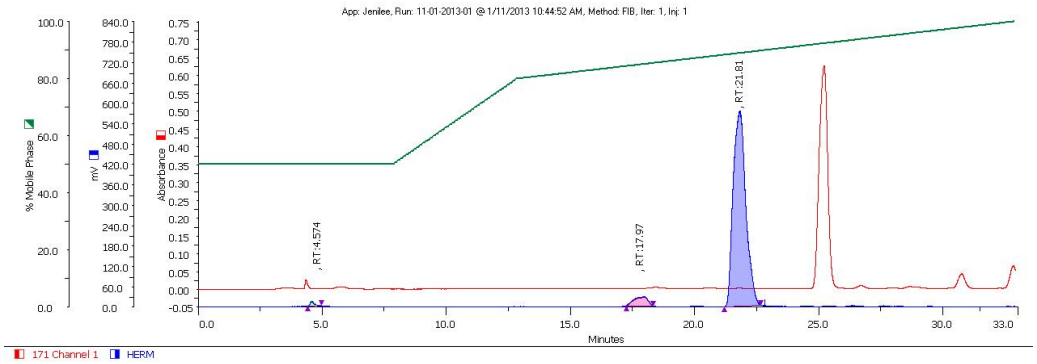

Figure 3.5. HPLC trace of 4-[^{18}F]fluoroiodobenzene as produced from the ASU.

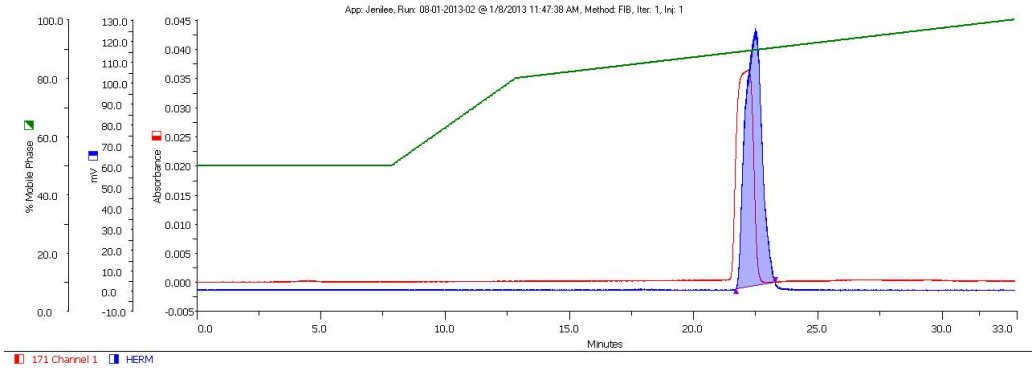

Figure 3.6. HPLC purified [^{18}F]FIB along with [^{19}F]FIB.

A co-injection with a commercially available cold reference compound is demonstrated in *Figure 3.6*. The slight difference in retention time is due to the tubing time delay between the two detectors with the UV detector being reached first in the system followed by the gamma detector.

3.4. Conclusions

A fully automated synthesis for the production of 4-[^{18}F]fluoroiodobenzene has been developed from a readily / commercially available precursor material. Allowing for a near quantitative radiochemical yield and radiochemical purity over 60 minutes including HPLC purification. Also the HPLC purification of [^{18}F]FIB had been fully optimized to allow for a chemically pure radiotracer to be collected for use in further cross coupling reactions. By employing this automated methodology, we have opened the availability of a commonly used prosthetic group, which has been otherwise more difficult to synthesize in large quantities previously.

3.5. Acknowledgements

The authors would like to thank John Wilson, David Clendening and Blake Lazurko from the Edmonton PET Center for radionuclide production and excellent technical support. We also gratefully acknowledge the Dianne and Irving Kipnes Foundation and the National Science and Engineering Research Council of Canada (NSERC) for supporting this work.

3.6. Conflict of Interest

The authors did not report any conflict of interest.

3.7. References

1 S. M. Qaim. Cyclotron production of medical radionuclides. In Handbook of Nuclear Chemistry, Vol. 4, (Eds: A. Vertes, S. Nagy, Z. Klencsar), *Radiochemistry and Radiopharmaceutical Chemistry in Life Science*. Kluwer Academic Publishers, **2003**, pp. 47–79, *Q10.*

2 R. Krasikova, *Ernst Schering Res. Found. Workshop* **2007**, *62*, 289–316.

3 S. Y. Lu, V. W. Pike, *Ernst Schering Res. Found. Workshop* **2007**, *62*, 271–287.

4 T. M. Blodgett, C. C. Meltzer, D. W. Townsend, *Radiology* **2007**, *242*, 360–385.

5 S. Surti, A. Kuhn, M. E. Werner, A. E. Perkins, J. Kolthammer, J. S. Karp, *J. Nucl. Med.* **2007**, *48*, 471–480.

6 S. Surti, J. S. Karp, L. M. Popescu, M. E. Daube-Witherspoon, M. Werner, *IEEE Trans. Med. Imaging* **2006**, *25*, 529–538.

7 H. Zaidi, *Z. Med. Phys.* **2006**, *16*, 5–17.

8 V. Sossi, T. J. Ruth, *J. Neural Transm.* **2005**, *112,* 319–330.

9 P. A. Schubiger, L. Lehmann, M. Friebe (Eds). (**2007**). *Ernst Schering Research Foundation Workshop 6:* PET Chemistry (1st edn.). Springer, Berlin, Germany.

10 R. Littich, P. J. H. Scott, *Angew. Chem. Int. Ed.* **2012**, *51*, 1106–1109.

11 M. M. Alauddin, Am. *J. Nucl. Med. Mol. Imaging* **2012**, *2*, 55–76

12 J. Ermert, C. Hocke, T. Ludwig, R. Gail, R. R. Coenen, *J. Labelled Compd. Radiopharm.* **2004**, *47,* 429–441.

13 N. Lazarova, F. G. Siméon, J. L. Musachio, S. Y. Lu, V. W. Pike, *J. Labelled Compd. Radiopharm* **2007**, *50*, 463–465.

14 R. Gail, H. H. Coenen, *Appl. Radiat. Isot.* **1994**, *45*, 105–111.

15 L. Allain-Barbier, M. C. Lasne, C. Perrio-Huard, B. Mureau, L. Barre, *Acta Chem. Scand.* **1998**, *52*, 480–489.

16 C. Y. Shiue, M. Watanabe, A. P. Wolf, J. S. Fowler, P. Salvadori, *J. Labelled Compd. Radiopharm.* **1984**, *21*, 533–547.

17 M. A. Caroll, J. Nairne, G. Smith, D. A. Widdowson, *J. Fluor. Chem.* **2007**, *128*, 127–132.

18 F. Basuli, H. Wu, G. Griffiths, *J. Labelled Compd. Radiopharm*. **2011**, *54*, 224–228.

19 M. Linjing, C. R. Fischer, J. P. Holland, J. Becaud, P. A. Schubiger, R. Schibli, S. M. Ametamey, K. Graham, T. Stellfeld, L. M. Dinkelborg, L. Lehnmann, *Eur. J. Org. Chem*. **2012**, *5*, 889–892.

20 J. Way, V. Bouvet, F. Wuest. Synthesis of 4-[18F]fluorohalobenzenes and palladium-mediated cross-coupling reactions for the synthesis of 18F-labelled radiotracers, *Curr. Org. Chem*. In press.

Chapter 4

*Synthesis and evaluation of 2-amino-5-(4-[^{18}F]fluorophenyl)pent-4-ynoic acid ([^{18}F]FPhPA): A novel ^{18}F-labelled amino acid for oncologic PET imaging.**

Jenilee Way, Monica Wang, Ingrit Hamann, Melinda Wuest, Frank Wuest

4.1. Introduction

Radiolabelled amino acids are useful radiotracers for functional imaging of up-regulated amino acid metabolism, as typically found in many cancer cells[1-3]. Amino acid metabolism is increased in proliferating tumors and radiolabelled amino acids show more specific uptake compared to 2-deoxy-2-[^{18}F]fluoro-D-glucose ([^{18}F]FDG) as the most commonly used metabolic radiotracer for positron emission tomography (PET). Although some radiolabelled amino acids are incorporated into proteins, most radiolabelled amino acids primarily reflect increased rate of amino acid transport in malignant cells[4-6]. Passage of amino acids across cell membranes is mediated by membrane-associated carrier proteins. More than 20 distinct amino acid transporters have been identified in mammalian cells. Several amino acid transporters are up-regulated in cancer cells such as Na^+-independent system L amino acids transporter LAT1 and Na^+-dependent glutamine transporter ASCT2[7,8]. Beyond their role to supply amino acids for protein synthesis in cancer cells, both amino acid transporters are also involved in cell signaling through the mTOR pathway that regulates cell growth, cell division, and extracellular nutrient sensing[9-11]. Among radiolabelled amino acids, particularly ^{18}F-labelled amino acids have gained much attention for their use in

* *Nucl. Med. Biol.*, **2014**; *41:* 660-669.

preclinical and clinical cancer imaging due to the favorable physical and chemical properties of fluorine-18 (^{18}F, $t_{1/2}$ = 109.8 min). ^{18}F-labelled amino acids have been used for clinical oncologic imaging of brain tumors and some peripheral cancers like prostate cancer, lung cancer, head and neck cancer, as well as neuroendocrine tumors[7].

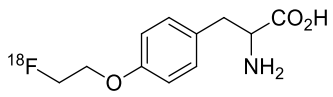

[^{18}F]FET
Nucleophilic aliphatic substitution

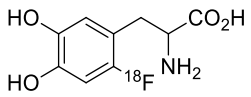

[^{18}F]FDopa
Electrophilic and nucleophilic aromatic substitution

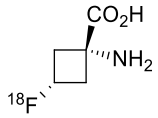

anti-3-[^{18}F]FACBC
Nucleophilic aliphatic substitution

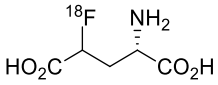

(2S)-4-[^{18}F]fluoroglutamate
Nucleophilic aliphatic substitution

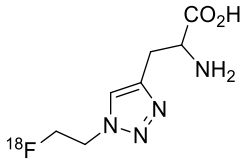

(S)-AFETP
Nucleophilic aliphatic substitution

Figure 4.1. Selection of ^{18}F-labelled amino acids.

All radiofluorinated amino acids are non-natural, and they span a broad variety of structures ranging from ^{18}F-labelled analogues of natural amino acids to alicyclic and α,α-dialkyl amino acids. Synthesis of ^{18}F-labelled amino acids exploits two basic strategies based on (1) direct radiofluorination of an amino acid labelling precursor or (2) indirect labelling using ^{18}F-labelled intermediates. Synthesis methods include electrophilic and nucleophilic substitution of aromatic systems, nucleophilic substitution of aliphatic systems, and more recently click chemistry. Examples of various ^{18}F-labelled amino acids demonstrating their structural variety in combination with applied synthesis method are summarized in *Figure 4.1*. Recent developments in ^{18}F-radiochemistry have further advanced application

of Pd-mediated C-C bond forming reactions for radiotracer synthesis. Prominent examples include the Stille, Suzuki, and Sonogashira cross-coupling reactions with 4-[^{18}F]fluorohalobenzenes as the coupling partner[12-14]. However, to the best of our knowledge, Pd-mediated cross-coupling reactions have not been used for the synthesis of ^{18}F-labelled amino acids.

In the present work, we describe synthesis of 2-amino-5-(4-[^{18}F]fluorophenyl)pent-4-ynoic acid ([^{18}F]FPhPA) as novel ^{18}F-labelled amino acid based on the Sonogashira cross-coupling reactions between commercially available propargylglycine and 4-[^{18}F]fluoroiodobenzene. Radiosynthesis of [^{18}F]FPhPA was optimized through screening different Pd-complexes, solvents, reaction temperatures and reaction times. Influence of used amounts of propargylglycine and triethylamine was also tested. The radiopharmacological profile of [^{18}F]FPhPA was evaluated in comparison with *O*-(2-[^{18}F]fluoroethyl)-L-tyrosine ([^{18}F]FET) using murine breast cancer cell line EMT6. Radiopharmacological evaluation involved cell uptake studies, radiotracer uptake competitive inhibition experiments, and small animal PET imaging.

4.2. Materials and methods

4.2.1. General

D-Propargylglycine, L-propargylglycine, and 2-amino-2-norbornanecarboxylic acid (BCH) were obtained from Santa Cruz Biotechnology (USA). 4, 7, 13, 16, 21, 24-hexaoxa-1, 10-diazabicycle [8.8.8] hexacosane (Krypofix 2.2.2), L-serine, and 2-(methylamino)isobutyric acid (MeAIB) were obtained from TCI America (USA). All other chemicals were obtained from Sigma-Aldrich® and used without

further purification. Water was obtained from a Barnstead Nanopure water filtration system (Barnstead Diamond Nanopure pack organic free RO/DIS).

High performance liquid chromatography (HPLC) purification and analysis of the ^{18}F-labelled products were performed using a Phenomenex LUNA® C18(2) column (100 Å, 250 x 10 mm, 10 μm) using gradient elutions specific to the given compound (Gilson 321 pump, 171 diode array detector, Berthold Technologies Herm LC). Chiral separations were performed on a Phenomenex Chirex® 3126 (D) – penicillamine column (110 Å, 150 x 4.60 mm, 5 μm) (Shimadzu DGU-20A, LC-20AT, SPD-M20A, CBM-20A, SIL-20A HT, Raytest RamonaStar) at a flow rate of 1 mL/min. Radio-TLC was performed using either EMD Merck F254 silica gel 60 aluminum backed thin layer chromatography (TLC) plates or Analtech RP18 with UV254 aluminum backed TLC plates (Bioscan AR-2000). Quantification of radioactive samples during chemistry was achieved using a Biodex ATOMLAB™ 400 dose calibrator. A PerklinElmer 2480 Auto-matic Gamma Counter WIZARD$^{2®}$ was used for the cellular uptake studies. Centrifugation of non-radioactive samples was achieved with a Hettich Zentrifugen Rotina 35R, whereas ^{18}F-labelled samples were centrifuged on a Fisher Scientific Mini Centrifuge. Protein content quantification was achieved using a Molecular Devices Spectramax 340PC. Reactions parameters were screened using an Eppendorf Thermomixer R and an IKAMAG® Ret-G Stir plate with an oil bath. Formulation of ^{18}F-radiolabelled products for animal injection were done using glassware kept in an Isotemp Vacuum Oven Model 285A and a rotary evaporator of a Buchi HB 140 Rotavpor-M with a Fisher Maxima C Plus

Model M8C pump. Nuclear Magnetic Resonance (NMR) data was collected using a Bruker Ascend™ 600 MHz. High resolution Mass Spectroscopy was recorded using an Agilent Technologies 6220 oaTOF.

In-house preparations of buffers were as follows: Krebs (Krebs-Ringer) buffer (120 mM sodium chloride, 25 mM sodium bicarbonate, 4 mM potassium chloride, 1.2 mM potassium phosphate monobasic, 2.5 mM magnesium sulfate, 70 μM calcium chloride, pH 7.4), PBS (Phosphate Buffered Saline) buffer (140 mM sodium chloride, 2.7 mM potassium chloride, 5.4 mM sodium phosphate dibasic, 570 μM potassium phosphate monobasic, pH 7.4), and RIPA (Radio-Immunoprecipitation Assay) buffer (50 mM tris(hydroxymethyl)aminomethane, 150 mM sodium chloride, 3.5 mM sodium dodecyl sulfate, 12 mM sodium deoxycholate, 8.5 mM Triton X 100).

4.2.2. Chemistry

4.2.2.1. General procedure for the synthesis of D/L-FPhPA, L-FPhPA, and L-FPhPA

Propargylglycine (D-, L-, and D/L-isomer, 10 mg), CuI (4 mg), triethlyamine (50 μL), $PdCl_2(PPh_3)_2$ (2 mg), and 4-fluoroiodobenzene (10 μL) were reacted in water (750 μL) and DMF (750 μL) in thermoshaker for 30 min at 85 °C. Upon reaction completion, 2N HCl (2 mL) was added and the reaction mixture was passed through a Millipore Millex-FG (0.2 μm) filter into a 10 mL clear glass vial containing PBS buffer (4.0 mL). Product was purified by HPLC and the collected

product fractions are evaporated to dryness by rotary evaporation to the desired compound.

4.2.2.2. D/L-(2-amino-5-(4-[^{19}F]fluorophenyl)pent-4-ynoic acid) (D/L-FPhPA)

Yield: 3 mg (30 %) as a fine white powder. ^{1}H-NMR (600 MHz, D_2O): δ 2.66 (dd, ^{2}J= 21.2 Hz, ^{3}J= 5.6 Hz, 2H), δ 3.38 (t, ^{3}J= 5.6 Hz, ^{3}J= 5.6 Hz, 1H), δ 7.02 (m, 2H), δ 7.40 (m, 2H) (see *Figure 7.1.*). ^{19}F-NMR (564 MHz, D_2O): δ-112.15 (m, 1F) (see *Figure 7.3.*). ^{13}C-NMR (150 MHz, D_2O): δ 25.4, δ 54.6, δ 81.8, δ 86.1, δ 115.5, δ 118.9, δ 133.5, δ 162.7, δ 181.2. (see *Figure 7.2.*). LR-MS m/z (ESI): 206.1 $[M-H]^-$, 242.0 $[M+Cl]^-$ (see *Figure 7.4.*). HR-MS m/z (ESI): $C_{11}H_9FNO_2$ ($[M-H]^-$) calcd. 206.0623, found 206.0625; $C_{11}H_9FClNO_2$ ($[M+Cl]^-$) calcd. 242.0390, found 242.0389 (see *Figure 7.5.*).

4.2.2.3. Synthesis of L-(2-amino-5-(4-[^{19}F]fluorophenyl)pent-4-ynoic acid) (L-FPhPA)

Yield: 5.2 mg (29 %) as a fluffy white powder. LR-MS m/z (ESI): 206.1 $[M-H]^-$, 242.0 $[M+Cl]^-$. HR-MS m/z (ESI): $C_{11}H_9FNO_2$ ($[M-H]^-$) calcd. 206.0623, found 206.0625. HPLC-analysis (Phenomenex Chirex® 3126 (D) - penicillamine column (110 Å, 150 x 4.60 mm, 5 μm), isocratic elution with 2 mM copper(II)sulfate in 2-propanol/water (5/95), 1 mL/min): t_R = 38 min.

4.2.2.4. Synthesis of D-(2-amino-5-(4-[^{19}F]fluorophenyl)pent-4-ynoic acid) (D-FPhPA)

Yield: 10.0 mg (56 %) as a white powder LR-MS m/z (ESI): 206.1 $[M-H]^-$, 242.0 $[M+Cl]^-$. HR-MS m/z (ESI): $C_{11}H_9FNO_2$ ($[M-H]^-$) calcd. 206.0623, found

206.0625; $C_{11}H_9FClNO_2$ ([M+Cl]$^-$) calcd. 242.0390, found 242.0389. HPLC-analysis (Phenomenex Chirex® 3126 (D) - penicillamine column (110 Å, 150 x 4.60 mm, 5 μm), a isocratic elution with 2 mM copper(II)sulfate in 2-propanol/water (5/95), 1 mL/min): t_R = 42 min.

4.2.3. Radiochemistry

4.2.3.1. Syntheses of 4-[^{18}F]fluoroiodobenzene ([^{18}F]FIB) and *O*-(2-[^{18}F]fluoroethyl-L-tyrosine ([^{18}F]FET)

4-[^{18}F]Fluoroiodobenzene ([^{18}F]FIB) and *O*-(2-[^{18}F]fluoroethyl)-L-tyrosine ([^{18}F]FET) were prepared according to literature procedures[15,16].

4.2.3.2. Formulation of 4-[^{18}F]fluoroiodobenzene ([^{18}F]FIB) for use in cross-coupling reactions

The collected product of [^{18}F]FIB from the HPLC (6 mL) was diluted into water (50 mL) and trapped onto a Waters Sep-Pak®tC18 plus light cartridge (300 mg). Elution from the cartridge took place in the solvent of interest, such as DMF (1.5 mL), CH_3CN (3.0 mL), toluene (3.0 mL), acetone (3.0 mL), and tetrahydrofuran (THF, 3.0 mL). Purified [^{18}F]FIB was used accordingly in the different cross-coupling reactions.

4.2.3.3. Manual synthesis of 2-amino-5-(4-[^{18}F]fluorophenyl)pent-4-ynoic acid ([^{18}F]FPhPA)

To an Eppendorf Lobind 1.5 mL eppendorf tube, D/L-propargylglycine (1 mg) was added along with CuI (1 mg), triethlyamine (25 μL) and a palladium catalyst ($PdCl_2(PPh_3)_2$, 1 mg). Next, water (500 μL) was added along with HPLC purified

[^{18}F]FIB (500 μL) in the respective solvent. The mixture was then allowed to react in a thermoshaker for 30 min at 85 °C. Upon completion, 2 N HCl (1 mL) was added and the reaction mixture was passed through a Millipore Millex-FG (0.2 μm) filter into a 10 mL clear glass vial containing PBS buffer (2.0 mL). This product mixture containing 4 mL of solution is purified fully by HPLC. This manual procedure was used for all *in vitro* and *in vivo* sample preparations. [^{18}]FPhPA was analyzed by a dual plate system, using two normal phase silica TLC plates (EtOAc:n-hexane (1:1) (see *Figure 7.11.*), R_f=0.0; CH_3CN:water (85:15), R_f=0.83 (see *Figure 7.12.*)).

4.2.3.4. HLPC purification of [^{18}F]FPhPA

HPLC purification of the crude [^{18}F]FPhPA was performed using a graditent elution as follows: (A: water; B: CH_3CN; 0 min 15% B, 19.9 min 15% B, 20 min 100% B, 35 min 100% B). The flow rate of the system was 3 mL/min, which gave a retention time of 19 min for the [^{18}F]FPhPA product as confirmed with the retention time of corresponding reference compound (see *Figure 7.13*). Specific activity of [^{18}F]FPhPA was calculated against a standard curve.

4.2.3.5. Formulation of [^{18}F]FPhPA solutions for use in cell and small animal PET studies

The collected product of [^{18}F]FPhPA from the HPLC (6 mL) was collected into a pear shaped flask and evaporated using a mini-rotary evaporator to complete dryness. The fully dried product was then resolubilized using Kreb's buffer (300

μL) and the reformulated [^{18}F]FPhPA was used accordingly in the differenct cell uptake and small animal PET imaging studies.

4.2.4. Pharmacology and Radiopharmacology

4.2.4.1 Cell cultures

EMT6 cells (Gift from Dr. David Murray, Cross Cancer Institute, University of Alberta, Edmonton, Canada) a murine mammary epithelial cell line were grown in DMEM/F12 medium (in-house preparation) supplemented with 10% fetal bovine serum (FBS) (Gbico®), 2mM l-glutamine (Invitrogen) and 1% antibiotic/antimycotic (Invitrogen). EMT6 cells were incubated at 37 °C in a humidified incubator with a 5% (v/v) CO_2 atmosphere (ThermoForma Series II Water Jacketed CO_2 Incubator). Cells were kept for a maximum of 20 passages, with the cell growth medium being changed every other day and routinely reseeded once 90% confluency was achieved. Protein content was determined by taking the quality control EMT6 cells (2 wells) on the 12 well plate and removing the Krebs buffer. Next, cells were lysed with CelLytic™ M (300 μL) and the cell solution mixture (300 μL) was transferred into Eppendorf tube. The cell suspensions were subsequently spun down on a centrifuge at 4 °C and 10000 rpm for 10 min. Total protein was determined according to the instruction of bicinchoninic acid (BCA) BCA™ Protein Assay Kit (Pierce). Briefly, the unknown protein sample dilutions (1:1) were prepared by dilution of 30 mL of the cell suspension with 30 mL of PBS. Next, standards containing diluted albumin (BSA) were prepared at concentrations of 0, 50, 100, 200, 300, 400, 600, and 800

mg/mL. 25 μL of each standard was pipetted into a 96-well microplate (Corning) in descending concentration, along with 25 μL of the unknown protein content sample and 25 μL of the 1:1 unknown protein sample dilution. Beside the microplate a multipipette basin was used to combine 5 μL of BCA Reagent A (Pierce) with 100 μL of BCA reagent B (Pierce), this was mixed thoroughly to achieve a green color. From this basin 200 μL of this solution is dispensed using a multichannel pipetter into the wells of the 96 well microplate that contain the protein content samples. Finally the microplate was allowed to incubate for 25 min at 37 °C and then the protein content was determined using an absorbance microplate reader.

4.2.4.2. Western blot for detection of amino acid transporter expression

EMT6 cells were grown in 6-well plates to about 80% confluence. Cells were harvested using 100 μL CelLytic™ M with added protease inhibitor cocktail (both Sigma-Aldrich, Oakville, ON, Canada) per well, and collected in pre-chilled tubes. After cell lysis for 30 min on ice, whole cell extracts were centrifuged at 13,500 g for 5 min at 4 °C to remove cell debris. Protein determination was conducted using a BCA-based protein assay (Pierce/Thermo Scientific, Rockford, USA). Aliquots of the supernatants were mixed with 1/4 volume of 4 x Laemmli buffer (250 mM Tris/HCl, 8 % (w/v) SDS, 40 % glycerol, 200 mM dithiothreitol and 0.04 % (w/v) bromophenol blue, pH 6.8) and heated for 10 min at 70 °C. EMT6 whole cell extract (41 μg for LAT1 and ASCT1, 50 μg for ASCT2) were applied to SDS-polyacrylamide gels, followed by electrophoresis and blotting

onto PVDF membranes. Immunodetection was performed using the following antibodies: rabbit anti-LAT1, rabbit anti-ASCT1, rabbit anti-ASCT2 and mouse anti-α-tubulin (Santa Cruz Biotechnology, Dallas, TX, USA). Horseradish peroxidase (HRP)-conjugated anti-rabbit IgG and anti-mouse IgG secondary antibodies were obtained from Sigma-Aldrich and Santa Cruz, respectively. Incubation with the primary and secondary antibody was performed in 5 % (w/v) non-fat dry milk in Tris-buffered saline containing 0.1 % (v/v) of Tween-20 (TBST).

4.2.4.3. Cellular uptake studies

EMT6 cells were seeded into 12-well plates (Corning) approximately 24 hr prior to the cell uptake studies and grown to greater than 85% confluency. On the day of experiment, the growth media was removed and the cells were washed twice with Krebs buffer. EMT6 cells were then immediately incubated with the radiotracer (300 μL, 0.4 MBq/mL) that was diluted in Krebs buffer supplemented with 5 mM glucose. Incubation with the radiotracer solution occurred at 37 °C for 1 to 120 minutes (Fisher Scientific Isotemp Incubator Model 546), with time points being collected at 1, 5, 10, 15, 30, 45, 60, 90, and 120 min. Uptake was stopped by removal of the radiotracer followed by washing of the EMT6 cells with ice-cold PBS buffer twice. Cells were then lysed with RIPA buffer (400 μL) at 37 °C for 5 min and then transferred to a scintillation vial (300 μL) to be counted by a gamma counter. Calculated uptake values were expressed as percentage of total activity normalized to mg of the cellular protein content.

4.2.4.4. Cellular uptake inhibition studies

EMT6 cells were treated similarly as for the cellular uptake studies with the exception that cells were pre-incubated in Krebs buffer containing the inhibitor of interest for 1 h prior to the addition of the radiotracer. Inhibitors used in this study included L-serine (1.5, 3.0, and 10.0 mmol), α-(methylamino)-isobutyric acid ((MeAIB), 1.5, 3.0, and 10.0 mmol), 2-aminobicyclo-(2,2,1)-heptane-2-carboxylic acid ((BCH), 1.5, 3.0, and 10.0 mmol), and L-Glutamine (1.5, 3.0, and 10.0 mmol). Radiotracer [^{18}F]FPhPA was also diluted in Krebs buffer supplemented with 5 mM glucose that contained identical concentration of inhibitor as used for the pre-incubation. Radiotracer uptake was calculated and expressed as percentage of total activity normalized to mg of cellular protein content.

4.2.4.5. Determination of lipophilicity (logP)

Lipophilicity (log*P*) of [^{18}F]FPhPA was determined at pH 7.4 according to the method reported by Wilson et al. (2001)[17] (see *Figure 7.29.*).

4.2.4.6. Small animal PET imaging studies

Positron emission tomography (PET) experiments were performed using EMT-6 tumor-bearing BALB/c mice. All animal experiments were carried out in accordance to guidelines of the Canadian Council on Animal Care (CCAC) and approved by the local animal care committee (Cross Cancer Institute, University of Alberta). Murine EMT-6 cells ($5x10^6$ cells in 100 μL PBS) were injected into the upper left flank of female Balb/C mice (20-24 g, Charles River, Saint-Constant, Quebec, Canada). The EMT-6 tumor-bearing mice were imaged after allowing 7 to 10 days for tumors reaching sizes of about 300 - 500 mg.

The animals were anesthetized with isoflurane in 40% oxygen / 60% nitrogen (gas flow, 1 l/min) and body temperature was kept constant at 37°C for the entire experiment. Mice were positioned and immobilized in the prone position in the centre of the field of view of the microPET® R4 scanner (Siemens Preclinical Solutions, Knoxville, TN, USA). A transmission scan for attenuation correction was not acquired. The radioactivity of the injection solution in a 0.5 mL syringe was determined with a dose activimeter (Atomlab™ 300, Biodex Medical Systems, New York, U.S.A.). The emission scan of 60 min PET acquisition was started and with a delay of approximately 15 s 4-5 MBq of L-[^{18}F]FPhPA or [^{18}F]FET in 80 -120 μL of saline was injected through a needle catheter into a tail vein. Data acquisition continued for 60 min in 3D list mode. The dynamic list mode data were sorted into sinograms with 53 time frames (10x2, 8x5, 6x10, 6x20, 8x60, 10x120, 5x300 s). The frames were reconstructed using maximum a posteriori (MAP) reconstruction modes. The pixel size was 0.085x0.085x0.12 cm, and the resolution in the center field of view was 1.8 mm. Correction for partial volume effects was not performed. The image files were further processed using the ROVER v2.0.51 software (ABX GmbH, Radeberg, Germany). Masks defining 3D regions of interest (ROI) were set and the ROIs were defined by thresholding. Mean standardized uptake values [SUV_{mean} = (activity/mL tissue)/(injected activity/body weight), mL/g] were calculated for each ROI. Time-activity curves (TAC) were generated from dynamic scans. All semi-quantified PET data are presented as means ± SEM.

4.2.4.7. Data analysis

All data are expressed as means ± S.E.M. from n investigated animals. All TACs were constructed using GraphPad Prism 4.0 (GraphPad Software, San Diego, CA, USA). Where applicable, statistical differences were tested using unpaired Student's t test and were considered significant for $P < 0.05$.

4.3. Results

4.3.1. Chemistry

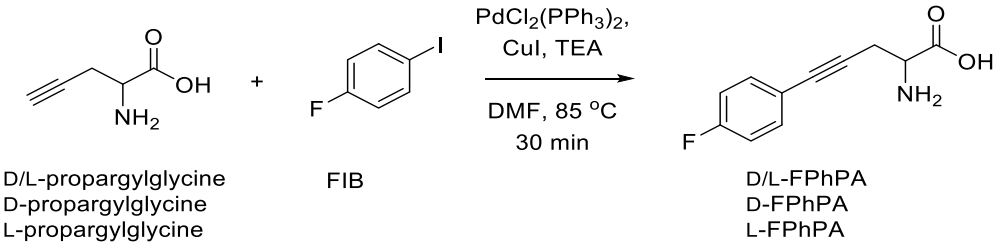

Figure 4.2. Synthesis of D/L-FPhPA, D-FPhPA, and L-FPhPA.

Reference compounds D/L-FPhPA, D-FPhPA, and L-FPhPA were prepared from respective commercially available propargylglycine and 4-fluoroiodobenzene in the presence of CuI, TEA as the base and $PdCl_2(PPh_3)_2$ as the Pd-source for the cross-coupling reaction. D/L-FPhPA, D-FPhPA, and L-FPhPA could be obtained in chemical yields of 30%, 56%, and 29%, respectively, after HPLC purification. Synthesis scheme is shown in *Figure 4.2*.

4.3.2. Radiochemistry

General outline of the radiosynthesis of D/L-[^{18}F]FPhPA, D-[^{18}F]FPhPA, and L-[^{18}F]FPhPA according to a Sonogashira cross-coupling reaction between propargylglycine and 4-[^{18}F]fluoroiodobenzene is depicted in *Figure 4.3*.

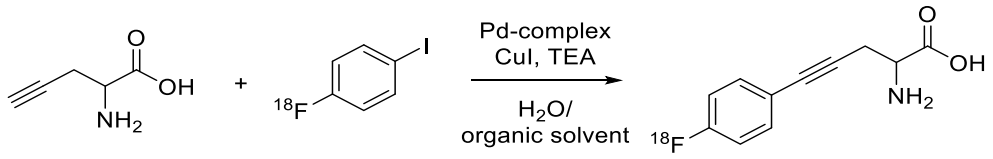

Figure 4.3. General reaction scheme for the preparation of [^{18}F]FPhPA.

4-[^{18}F]Fluoroiodobenzene was prepared starting from sulfonium salt precursor according to an automated synthesis procedure recently published by our group[15]. Reaction conditions for the Sonogashira cross-coupling reaction between 4-[^{18}F]fluoroiodobenzene and propargylglycine for the radiosynthesis of D/L-[^{18}F]FPhPA were optimized by screening several Pd-complexes (see *Figure 7.19.*), solvents (see *Figure 7.21.*), reaction temperatures (see *Figure 7.25.*), reaction times (see *Figure 7.26.*), and concentration of D/L-propargylglycine (see *Figure 7.20.*). Radiochemical purity was determined by radio-TLC of aliquots taken from the reaction mixture representing the percentage of cross-coupled product D/L-[^{18}F]FPhPA present in the reaction mixture. The results are summarized in *Table 4.1*.

The first set of reactions (entries 1 to 4) tested the influence of various Pd-complexes on the radiochemical purity. All reactions were carried out at 85 °C for 30 min using a 1:1 mixture of H_2O/DMF as the solvent. All of the used Pd-complexes gave high radiochemical purity of greater 80%. The results indicate that the reaction is not sensitive toward the utilization of Pd(II)-complexes like $Pd(OAc)_2$ and $PdCl_2(PPh_3)_2$ (entries 1 and 2) or Pd(0)-complexes like $Pd(PPh_3)_4$ and $Pd_2(dba)_3$ (entries 3 and 4). However, highest radiochemical purity of greater

90% were achieved with $Pd(OAc)_2$, and thus $Pd(OAc)_2$ was utilized as the Pd-complex for all further optimization experiments.

Entry	Palladium complex	Concentration of D/L-PPG	Reaction time	Reaction temperature	Solvent	Radiochemical purity[a,b,c] (n=3)
1	$Pd(OAc)_2$	1 mg/mL	30 min	85 ºC	H_2O/DMF	92 ± 7
2	$PdCl_2(PPh_3)_2$	1 mg/mL	30 min	85 ºC	H_2O/DMF	81 ± 13
3	$Pd(PPh_3)_4$	1 mg/mL	30 min	85 ºC	H_2O/DMF	84 ± 4
4	$Pd_2(dba)_3$	1 mg/mL	30 min	85 ºC	H_2O/DMF	81 ± 2
5	$Pd(OAc)_2$	0.1 mg/mL	30 min	85 ºC	H_2O/DMF	40 ± 24
6	$Pd(OAc)_2$	1 mg/mL	30 min	85 ºC	H_2O/DMF	66 ± 2
7	$Pd(OAc)_2$	10 mg/mL	30 min	85 ºC	H_2O/DMF	71 ± 9
8	$Pd(OAc)_2$	100 mg/mL	30 min	85 ºC	H_2O/DMF	68 ± 10
9	$Pd(OAc)_2$	2 mg/mL	30 min	85 ºC	H_2O/DMF	97 ± 0.1
10	$Pd(OAc)_2$	5 mg/mL	30 min	85 ºC	H_2O/DMF	98 ± 0.7
11	$Pd(OAc)_2$	1 mg/mL	30 min	85 ºC	H_2O/DMF	92 ± 3
12	$Pd(OAc)_2$	1 mg/mL	30 min	85 ºC	H_2O/CH_3CN	94 ± 5
13	$Pd(OAc)_2$	1 mg/mL	30 min	85 ºC	H_2O/THF	95 ± 2
14	$Pd(OAc)_2$	1 mg/mL	30 min	85 ºC	H_2O/acetone	96 ± 1
15	$Pd(OAc)_2$	1 mg/mL	30 min	85 ºC	H_2O/toluene	92 ± 2
16	$Pd(OAc)_2$	1 mg/mL	30 min	25 ºC	H_2O/DMF	59 ± 33
17	$Pd(OAc)_2$	1 mg/mL	30 min	55 ºC	H_2O/DMF	91 ± 2
18	$Pd(OAc)_2$	1 mg/mL	30 min	65 ºC	H_2O/DMF	93 ± 2
19	$Pd(OAc)_2$	1 mg/mL	5 min	55 ºC	H_2O/DMF	86 ± 8
20	$Pd(OAc)_2$	1 mg/mL	15 min	55 ºC	H_2O/DMF	93 ± 2
21	$Pd(OAc)_2$	1 mg/mL	60 min	55 ºC	H_2O/DMF	94 ± 0.1

[a] Radiochemical purity were determined by radio-TLC representing percentage of product present in the reaction mixture.
[b] 1 mg of CuI was used
[c] 25 mL of TEA was used

Table 4.1. Influence of reaction conditions and parameters on the synthesis of D/L-[^{18}F]FPhPA.

The next series of experiments (entries 5 to 10) studied the influence of the amount of propargylglycine as the coupling partner within the catalytic cycle of the Sonogashira reaction on the radiochemical yield. High radiochemical purity greater than 90% was obtained using D/L-propargylglycine concentrations of about 1 mg/mL (entry 1). Application of lower concentrations of D/L-propargylglycine (entries 5 to 8) resulted in a reduction of radiochemical purity, whereas increase of D/L-propargylglycine concentration to up to 5 mg/mL (entries 9 and 10) did not significantly increase radiochemical yield.

Use of very low concentration of D/L-propargylglycine as little as 0.1 mg/mL (entry 5) still afforded 40% of compound D/L-[^{18}F]FPhPA. Based on these observations and findings, an apparent optimal concentration of 1 mg/mL was used for further optimization attempts.

The influence of different solvents as 1:1 mixtures with water on the radiochemical purity for the Sonogashira cross-coupling reaction between D/L-propargylglycine and 4-[^{18}F]fluoroiodobenzene was studied in the next series of optimization experiments.

The used solvents DMF, acetonitrile, THF, acetone, and toluene gave comparable high radiochemical purity greater than 90% as shown in entries 11 to 15. The found wide compatibility of the Sonogashira reaction involving 4-[^{18}F]fluoroiodobenzene towards various solvents allows application of the cross-coupling reaction in mixtures of organic and aqueous solutions. Acetonitrile was used as the solvent of choice for additional optimization reactions since acetonitrile is also the solvent of final product solution containing 4-[^{18}F]fluoroiodobenzene as collected from the HPLC purification.

The last reaction parameters tested within the optimization process were the influence of reaction time and reaction temperature on the radiochemical purity (entries 16 to 21).

Reactions proceeded in high radiochemical purity of greater than 90% using a reaction temperatures at than 55 °C and higher (entries 1, 17 and 18) and a reaction time longer than 10 min (entries 1, 20 and 21). Results given in *Table 4.1.* confirm the robustness of the Sonogashira reaction on reaction temperature

and reaction time. The reaction proceeds rapidly, and high radiochemical purity of 86 ± 8% (n = 3) can already be achieved after 5 min (entry 19). The reaction tends to be more sensitive at lower temperatures as demonstrated by the lower radiochemical purity obtained at room temperature (entry 16).

Based on these experiments, the following optimized reaction conditions were determined for the preparation of D/L-[^{18}F]FPhPA according to a Sonogashira cross-coupling reaction between D/L-propargylglycine and 4-[^{18}F]fluoroiodobenzene: 1 mg of $Pd(OAc)_2$, CuI, D/L-propargylglycine, and 25 μL of TEA in 1 mL of acetonitrile:water (50:50) at 55 °C for 30 min. Use of optimized reaction conditions to large scale preparation of D/L-[^{18}F]FPhPA including HPLC purification gave decay-corrected radiochemical yields of 42 ± 10% (n=11) within 56 ± 5 min based on 4-[^{18}F]fluoroiodobenzene. This refers to a decay-corrected radiochemical yield of 29 ± 14 % based on [^{18}F]fluoride. In a typical experiment, 480 MBq of D/L-[^{18}F]FPhPA could be isolated in high radiochemical purity of greater 95% starting from 1200 MBq of 4-[^{18}F]fluoroiodobenzene. The specific activity of D/L-[^{18}F]FPhPA at the end-of-synthesis was determined from the quality control sample to be greater than 200 GBq/μmol (see *Figure 7.28./Table 7.2.*). Optimized reaction conditions were also used for the radiosynthesis of D-[^{18}F]FPhPA and L-[^{18}F]FPhPA, which could be prepared in comparable radiochemical yields. Noticeable, no racemization of the α-carbon atom in enantiomeric pure propargylglycine as the starting material was detected during the synthesis of corresponding D-[^{18}F]FPhPA and L-[^{18}F]FPhPA as confirmed by chiral radio-HPLC analysis (see *Figure 7.14. to*

Figure 7.18.). This important finding confirms the suitability of the Sonogashira cross-coupling reaction for the synthesis of enantiomerically pure compounds such as amino acids.

4.3.3. Determination of logP

The logP of [^{18}F]FPhPA was determined using the shake flask method by adding 1 mL of purified D/L-[^{18}F]FPhPA into a 2.0 mL Eppendorf vial containing mixtures of n-octanol (0.5 mL) and PBS buffer (0.5 mL, pH 7.4). The log*P* value was determined to be -0.27 (n=9) confirming the hydrophilic nature of this amino acid [^{18}F]FPhPA at physiological pH of 7.4.

4.3.4. Cell uptake studies

Radiotracer uptake of D/L-[^{18}F]FPhPA, D-[^{18}F]FPhPA, and L-[^{18}F]FPhPA was studied in the murine breast cancer cell line EMT6 (*Figure 4.4.*).

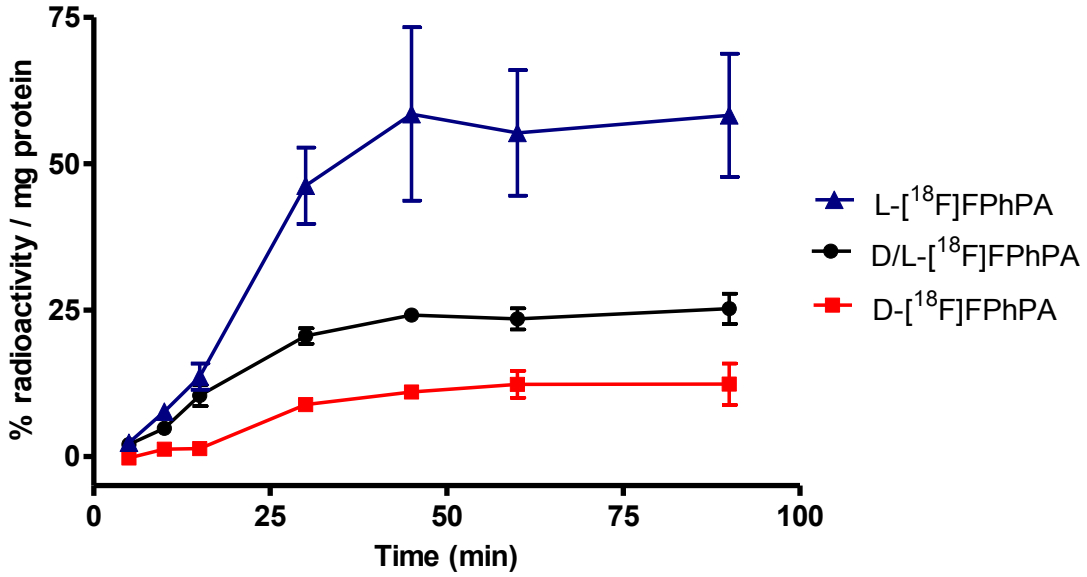

Figure 4.4. Cell uptake of D/L-[^{18}F]FPhPA, D-[^{18}F]FPhPA, and L-[^{18}F]FPhPA in EMT6 cells.

As expected, highest uptake was found with L-[^{18}F]FPhPA reaching a maximum of 58.3 ± 14 % radioactivity/mg protein (n=3) at 90 min. Uptake of the radiotracer did not increase for the remaining time of the study. A lower uptake was observed with racemic [^{18}F]FPhPA with a maximum uptake of 25 ± 3 % radioactivity/mg protein (n=3) at 90 min. The lowest uptake in EMT6 cells was found for D-[^{18}F]FPhPA. Maximum uptake of D-[^{18}F]FPhPA was 12.3 ± 4 ID/mg protein (n=3) at 90 min, representing 20% of that of the L-isomer.

The data confirmed that the L-configuration of [^{18}F]FPhPA is an important requirement for sufficient uptake in tumor cells.

4.3.5. Radiotracer uptake competitive inhibition experiments

Competitive uptake inhibition experiments in EMT6 cells were performed to study the uptake mechanism of L-[^{18}F]FPhPA.

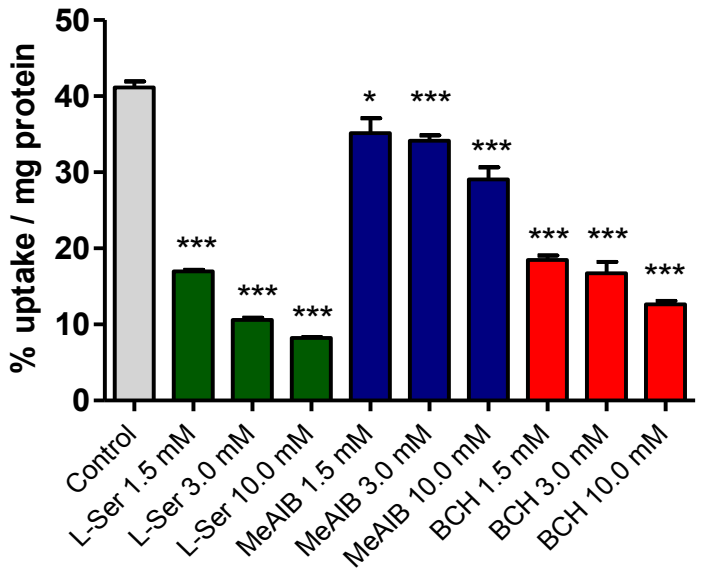

*Figure 4.5. Competitive inhibition studies of L-[^{18}F]FPhPA with MeAIB, BCH and L-Ser. Each bar represents the mean±SEM (n=6). * P<.05; *** P<.001.*

The inhibitors specific for Na^+-dependent amino acid transport systems A and ASC, and Na^+-independent amino acid transport system L were used. Cellular uptake of L-[^{18}F]FPhPA was determined in the presence and absence of system A inhibitor [*N*-methyl]-α-methylaminoisobutyric acid (MeAIB), system L inhibitor 2-aminobicyclo[2.2.1]heptane-2-carboxylate (BCH), and system ASC inhibitors L-Ser. Results of competitive uptake studies are summarized in *Figure 4.5*.

Results shown in *Figure 4.5.* indicates that system A inhibitor MeAIB had only little effects on L-[^{18}F]FPhPA uptake into EMT6 cells. Inhibitory effect of MeAIB was most noticeable when high inhibitor concentrations (10.0 mM) were used. Smaller inhibitory effects were observed at lower inhibitor concentrations of 1.5 mM and 3.0 mM, respectively. This finding suggests only a minor contribution of amino acid transport system A to the cellular uptake of the radiotracer into EMT6 cells. However, system L inhibitor BCH and system ASC inhibitor L-Ser showed more distinct inhibitory effects upon L-[^{18}F]FPhPA uptake in a concentration dependent manner. System L inhibitor BCH could reduce 50% of L-[^{18}F]FPhPA uptake at a 1.5 mM concentration. Uptake was further reduced to 43% and 30% of that of the control at 3 mM and 10 mM, respectively. System ASC inhibitor L-Ser showed strong inhibitory effects upon L-[^{18}F]FPhPA uptake at 1.5 mM (reduction to 46%), 3.0 mM (reduction to 24%), and 10.0 mM (reduction to 17%) indicating a strong contribution of system ASC to the transport of L-[^{18}F]FPhPA across the membrane of EMT6 cells. Results of this study suggests that transport of L-[^{18}F]FPhPA in EMT6 cells involves both Na^+-independent system L and Na^+-dependent system ASC with an apparent

preference for system ASC. However, BCH also inhibits amino acid transport system B^0, and observed inhibition of L-[^{18}F]FPhPA uptake in EMT6 cells by BCH also suggest a possible involvement of system B^0 in radiotracer uptake.

The next series of experiment studied the selectivity of L-[^{18}F]FPhPA uptake towards the system ASC subtypes ASCT1 and ASCT2. Results of competitive inhibition studies of L-[^{18}F]FPhPA in EMT6 cells in the presence of different concentrations of L-Ser as inhibitor for both system ASC subtypes ASCT1 and ASCT2, and L-Gln as specific system ASC subtype ASCT2 inhibitor are depicted in *Figure 4.6*. Results of competitive uptake studies are represented as percentage of radiotracer uptake normalized to mg protein.

Both inhibitors showed comparable inhibitory profiles towards L-[^{18}F]FPhPA uptake in EMT6 cells in a concentration dependent manner. Uptake of L-[^{18}F]FPhPA could be reduced to almost 40% of that of the control at a concentration of 1.5 mM for both inhibitors. Further inhibition of L-[^{18}F]FPhPA uptake was observed at higher concentrations of 3.0 mM and 10.0 mM, respectively.

The comparable inhibitory profiles of L-Ser as inhibitor for ASCT1 and ASCT2, and L-Gln as specific ASCT2 inhibitor suggest that system ASC subtype ASCT2 is preferentially involved in the transport of L-[^{18}F]FPhPA into EMT6 cells. However, based on our results using L-Ser as a dual inhibitor for ASCT1 and ASCT2, participation of ASCT1 for the transport of L-[^{18}F]FPhPA in EMT6 can not be excluded. Moreover, L-Gln also inhibits Na^+-dependent amino acid transport system N, which preferentially transports glutamine, histidine,

asparagine, and serine[18]. However, possible involvement of system N in radiotracer uptake into EMT6 cells was not further elucidated in this study.

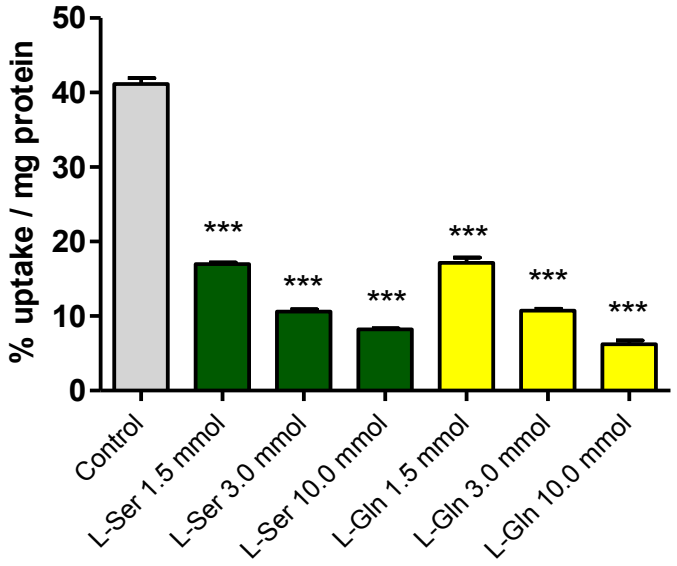

*Figure 4.6. Competitive inhibition studies of L-[^{18}F]FPhPA with system ASC inhibitors L-Ser and L-Gln. Each bar represents the mean±SEM (n=6). *** P<.001.*

4.3.6. Characterization of LAT1, ASCT1 and ASCT2 expression in EMT6 cells

All three amino acid transporter (LAT1, ASCT1 and ASCT2) could be detected in EMT6 cells. Results are displayed in *Figure 4.7*.

The immuno-reactive band for LAT1 appeared at 45 kDa, which is consistent with reported molecular weight of LAT1[19]. The molecular weight of immuno-reactive ASCT1 was 70 kDa, which corresponds with posttranslational modification of the protein as described in the literature[20]. Glycosylated ASCT2 was found at 55 kDa and 70-80 kDa, respectively, which is consistent with

literature reports[21]. For all experiments, a-tubulin (55 kDa) was used as loading control.

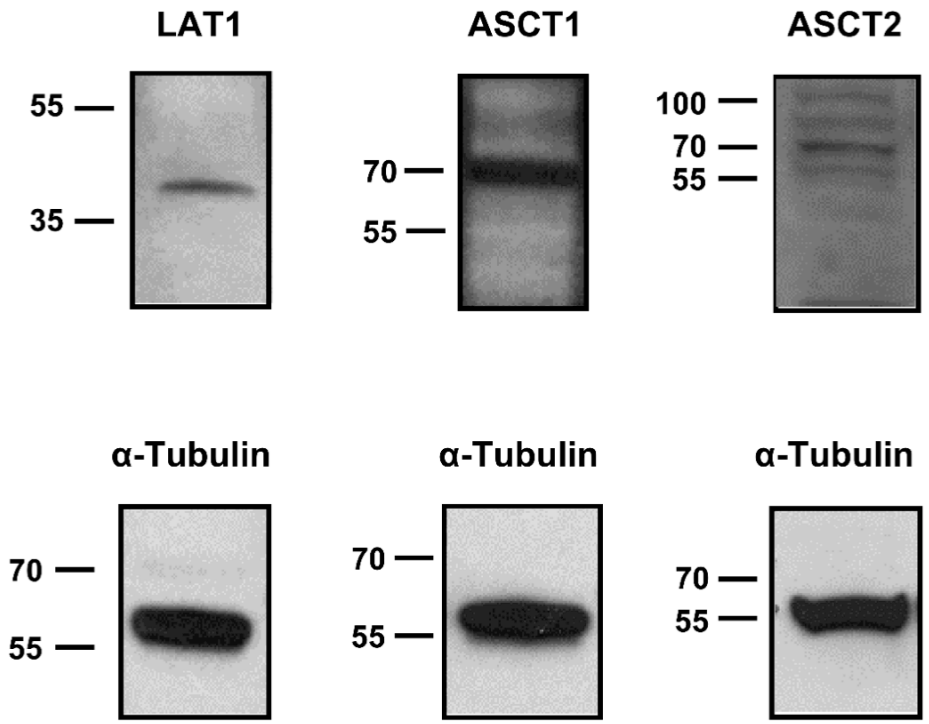

Figure 4.7. Qualitative detection of LAT1, ASCT1 and ASCT2 in murine EMT6 cells. EMT6murine cells were grown to near confluence, washed with PBS and lysed in CelLytic™ M. LAT1, ASCT1 and ASCT2 were detected by Western blotting and immuno-detection using specific antibodies. α-Tubulin staining was used as loading control.

4.3.7. Small animal PET studies

Dynamic small-animal PET imaging was performed in BALB/c mice bearing subcutaneous EMT6 tumors to evaluate the distribution and clearance pattern of novel amino acid L-[^{18}F]FPhPA in comparison with L-[^{18}F]FET.

Selected PET images of novel amino acid L-[^{18}F]FPhPA and radiofluorinated amino acid L-[^{18}F]FET as reference compound at different time points (10 min, 30 min, and 60 min) are given in *Figure 4.8*. PET images of L-[^{18}F]FET were

taken from our recent publication[16]. Time-activity curves derived from defined ROIs over the tumor, muscle, heart (blood pool), kidney, and brain were generated from three individual animals as shown in *Figure 4.9*.

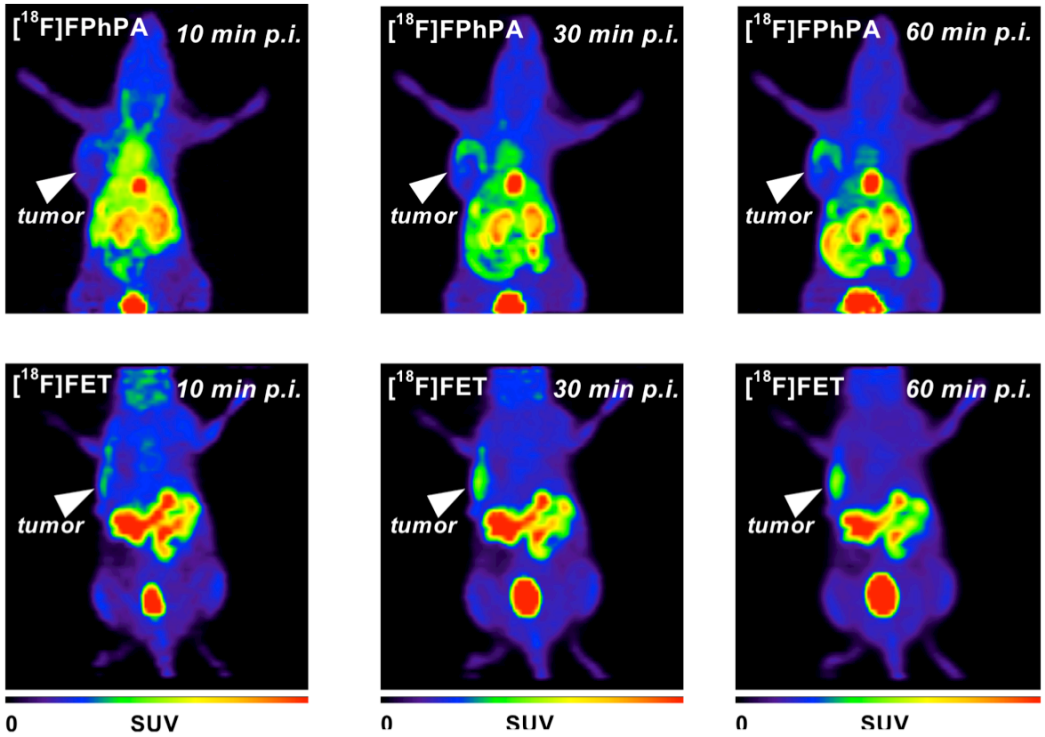

Figure 4.8. Representative PET images displayed as maximum-intensity projections (MIPs) of EMT6 tumor bearing mice at 10 min, 30 min and 60 min after injection (4-5 MBq in 100-120 mL of saline) of L-[^{18}F]FPhPA (top) and L-[^{18}F]FET (bottom, taken from literature 16). Isoflurane was used for anesthesia of the mice.

Both radiolabelled amino acids were rapidly distributed into different organs and tissues after i.v. injection of L-[^{18}F]FPhPA or L-[^{18}F]FET. Radiotracer uptake kinetics in EMT6 tumors were comparable for both radiolabelled amino acids within the first 30 min p.i. of the PET study. At later time points L-[^{18}F]FET showed some tendency for a washout of radioactivity, whereas L-[^{18}F]FPhPA

exhibited no washout pattern during the entire time course of the study. Amino acid L-[^{18}F]FPhPA gave a maximum standardized uptake value (SUV) of 1.35 after 60 min p.i. which was higher compared to L-[^{18}F]FET (SUV_{60min} 1.22). Tumors became clearly visible after 10 min p.i. reaching SUV values of 1.01 for L-[^{18}F]FPhPA and 1.05 for L-[^{18}F]FET, respectively.

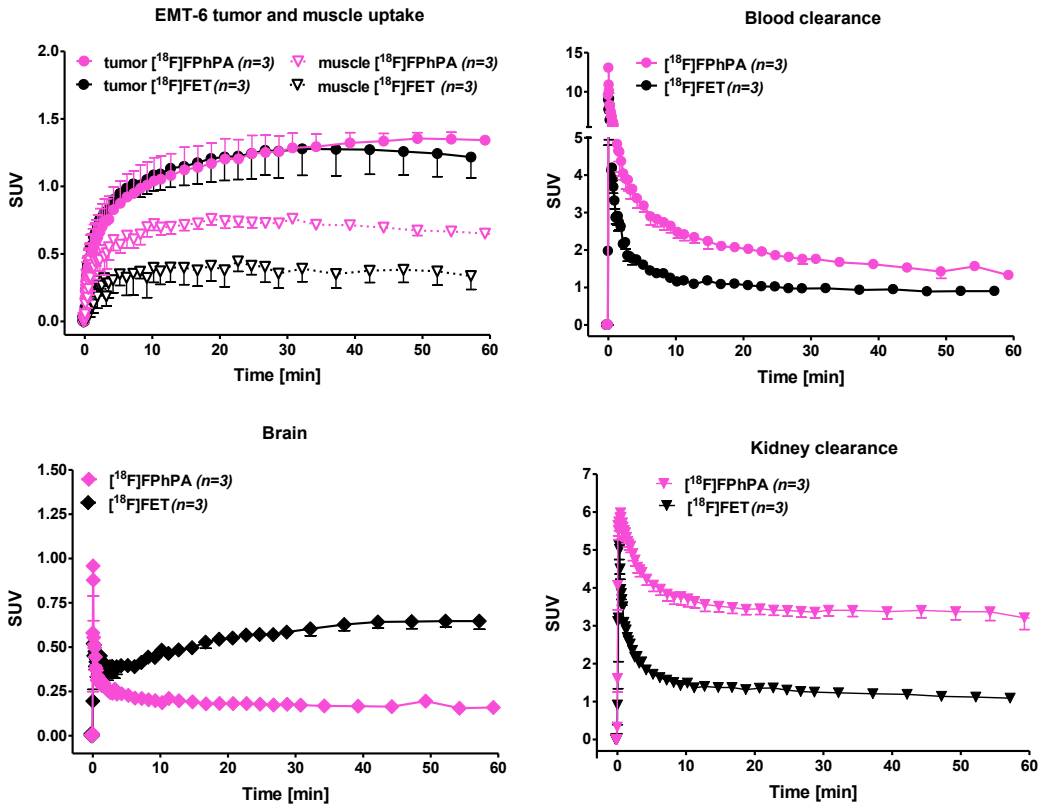

Figure 4.9. Time-activity curves (TACs) reflecting the kinetics of L-[^{18}F]FPhPA (purple) and L-[^{18}F]FET (black) in tumor and muscle (A), heart (B), brain (C) and kidneys (D). Data are given as SUV from three different experiments with each radiolabelled amino acid.

Further increasing accumulation of radioactivity in the tumors over time resulted in clear delineation of the tumor in the PET images after 30 min and 60 min p.i.. A major difference in the distribution pattern between L-[^{18}F]FPhPA and L-

[^{18}F]FET was the slower clearance of L-[^{18}F]FPhPA from the blood. Radioactivity levels of L-[^{18}F]FPhPA in the blood were always higher compared to blood radioactivity levels of L-[^{18}F]FET. Moreover, L-[^{18}F]FPhPA showed also higher radioactivity levels in muscle compared to L-[^{18}F]FET with no clearance for both radiolabelled amino acids during the time course of the PET study. The higher uptake and retention of radioactivity in the muscle in the case of L-[^{18}F]FPhPA led to a lower tumor-to-muscle ratio of 1.45 at 10 min, 1.73 at 30 min, and 2.08 at 60 min p.i. when compared with reference amino acid L-[^{18}F]FET (3.26 at 10 min, 3.56 at 30 min, and 3.62 at 60 min p.i.). The higher retention of radioactivity levels in blood, and the higher muscle uptake of L-[^{18}F]FPhPA may be attributed to the higher lipophilicity of amino acid L-[^{18}F]FPhPA as determined as log$P$ = -0.27 compared to a reported log$P$ value of -1.51 for L-[^{18}F]FET[22]. However, different expression levels of amino acid transporters as relevant for the transport of L-[^{18}F]FET (LAT1) and L-[^{18}F]FPhPA (LAT1 and ASC system) should also contribute to the found differences in biodistribution pattern. Novel amino acid L-[^{18}F]FPhPA also showed significantly higher retention of radioactivity in the kidney compared to L-[^{18}F]FET. Both radiotracers exhibited comparable clearance pattern of radioactivity from kidney with an overall more than two-fold higher radioactivity retention in the kidneys for L-[^{18}F]FPhPA after the initial clearance period. An interesting observation was the significant different brain uptake and retention pattern of L-[^{18}F]FPhPA and L-[^{18}F]FET. Both radiotracers showed rapid brain uptake. However, L-[^{18}F]FPhPA was rapidly cleared from the brain whereas L-[^{18}F]FET showed increasing accumulation of radioactivity in the

brain over time as typical for reference amino acid L-[^{18}F]FET. The favorable clearance pattern of L-[^{18}F]FPhPA from the brain resulted in a low baseline radioactivity level compared to L-[^{18}F]FET. The rapid washout of L-[^{18}F]FPhPA from normal brain tissue suggests potential applications of L-[^{18}F]FPhPA as radiotracer for PET imaging of brain tumors.

4.4. Discussion

In the present study, we described the synthesis and radiopharmacological evaluation of ^{18}F-labelled amino acid 2-amino-5-(4-[^{18}F]fluorophenyl)pent-4-ynoic acid ([^{18}F]FPhPA) as a novel radiotracer for oncologic PET imaging. We used SONOGASHIRA cross-coupling reaction between 4-[^{18}F]fluoroiodobenzene ([^{18}F]FIB) and propargylglycine as a novel radiochemistry tool for the synthesis of ^{18}F-labelled amino acids. Radiopharmacological evaluation of L-[^{18}F]FPhPA involved radiotracer uptake studies into EMT6 cells, competitive inhibition experiments in EMT6 cells, and small animal PET imaging studies in comparison with L-[^{18}F]FET as reference amino acid tracer in EMT6 tumor bearing mice.

This study revealed the following important results: (1) The Pd-mediated Sonogashira cross-coupling reaction is an efficient and versatile synthesis methodology for the robust and high yield preparation of ^{18}F-labelled radiotracers as demonstrated for L-[^{18}F]FPhPA; (2) Cellular uptake studies of [^{18}F]FPhPA into EMT6 cells confirmed that L-configuration of [^{18}F]FPhPA is important for high uptake into EMT6 cells; (3) Amino acid L-[^{18}F]FPhPA is transported via Na^+-dependent amino acid transport system ASC and Na^+-independent amino acid transport system L into EMT6 cells; (4) ASC subtype ASCT2 seems to be mainly

involved in the ASC-mediated transport of L-[^{18}F]FPhPA into EMT6 cells; (5) Dynamic small animal PET studies showed accumulation of L-[^{18}F]FPhPA into EMT6 tumors; (6) L-[^{18}F]FPhPA exhibited higher uptake and retention of radioactivity in muscle and blood compared with L-[^{18}F]FET; (7) L-[^{18}F]FPhPA showed rapid washout of radioactivity from brain tissue.

The first part of the present study was focused on the development of a novel radiochemistry platform for the synthesis of ^{18}F-labelled amino acids based on the Pd-mediated Sonogashira cross-coupling reactions.

To date, synthesis of ^{18}F-labelled amino acids is mainly accomplished using standard ^{18}F-radiochemistry protocols allowing their convenient and safe preparation in remotely-controlled synthesis apparatus in high radioactivity amounts according to GMP guidelines as demonstrated with [^{18}F]FET and [^{18}F]FDopa[3,7]. The site of radiofluorine incorporation into amino acids is an important consideration for the design of ^{18}F-labelled amino acids. Radiolabelling should result in retention of biological activity and favorable radiopharmacological profile of the prepared radiolabelled amino acid. Various Pd-mediated cross-coupling reactions with [^{18}F]FIB as the coupling partner have proven as valuable synthesis tools for site-specific incorporation of 4-[^{18}F]fluorophenyl groups into a variety of structurally divers compounds. However, to the best of our knowledge, Pd-mediated cross-coupling reactions with [^{18}F]FIB have not been used for the radiosynthesis of ^{18}F-labelled amino acids. Among Pd-mediated cross-coupling reactions, the Sonogashira reaction between [^{18}F]FIB and terminal alkynes has provided an excellent synthesis

platform for the preparation of various lipophilic ^{18}F-labelled compounds like steroids employing organic solvents[23]. However, application of the Sonogashira reaction to the synthesis of ^{18}F-labelled amino acids preferentially should include the use of aqueous reaction conditions. Results described in *Table 4.1.* of this study confirmed the robustness of the Sonogashira reaction as a versatile synthetic tool for amino acids in aqueous solvents, and the applied reaction conditions are compatible for the radiosynthesis of [^{18}F]FPhPA. Synthesis of [^{18}F]FPhPA according a Sonogashira reaction greatly benefited from our recently reported improved automated synthesis of [^{18}F]FIB[15]. Based on our new [^{18}F]FIB synthesis method, we were able to prepare [^{18}F]FPhPA in radioactivity amounts suitable for potential clinical studies. Besides the site-specific incorporation of the radiolabel, retention of stereochemistry at the α-carbon atom centre is another important requirement essential for biological activity of ^{18}F-labelled amino acids like L-[^{18}F]FPhPA. Cross-coupling reaction between [^{18}F]FIB and L-propargylglycine or D-propargylglycine to form corresponding L-[^{18}F]FPhPA and D-[^{18}F]FPhPA, respectively, according to a Sonogashira reaction resulted in no noticeable racemization of the a-carbon atom centre. This important finding further confirms suitability of the Sonogashira reaction as a versatile synthesis tool to prepare optically active ^{18}F-labelled compounds like amino acid [^{18}F]FPhPA while employing mild reaction conditions.

The second part of this study dealt with the radiopharmacological evaluation of L-[^{18}F]FPhPA as novel ^{18}F-labelled amino acid for oncologic PET imaging. Cellular uptake studies of L-[^{18}F]FPhPA, D-[^{18}F]FPhPA, and racemic D/L-[^{18}F]FPhPA

into murine breast cancer cell line EMT6 demonstrated importance of L-configuration for sufficient cell uptake. This observation is in line with the general consideration that L-amino acids are preferably transported into mammalian cells compared with their D-isomers[3,4,7]. Uptake of L-[^{18}F]FPhPA into EMT6 cells was about 5-times higher at 90 min compared to the uptake of D-[^{18}F]FPhPA (*Figure 4.4.*). First insights into the cellular uptake mechanism of L-[^{18}F]FPhPA were elucidated by competitive inhibition studies. [^{18}F]FPhPA is a neutral ^{18}F-labelled aromatic amino acid, prominent examples for other neutral ^{18}F-labelled aromatic amino acid include [^{18}F]FET and [^{18}F]FDopa. Both amino acids are preferentially transported via Na^+-independent system L amino acid transporter. In addition to system L, we also included Na^+-dependent system A and system ASC into our competitive inhibition study. Inhibition studies using different concentrations of system A inhibitor MeAIB, system ASC inhibitor L-Ser, and system L inhibitor BCH suggested transport of L-[^{18}F]FPhPA to a large extend via system L and system ASC. System A amino acid transporter seems not to contribute significantly to the cellular uptake of L-[^{18}F]FPhPA into EMT6 cells. This observation is not surprising since system A preferentially transports glycine and amino acids with small, neutral side chains like alanine and glutamine[4,9]. However, the observed small inhibitory effects are statistically significant, and involvement of system A upon L-[^{18}F]FPhPA uptake in EMT6 can not be excluded. On the other hand, the found involvement of a system L amino acid transporter within the cellular uptake of L-[^{18}F]FPhPA is in line with expected transport properties as typically found for neutral aromatic amino acids[7].

However, amino acid transport system B^0 is also sensitive towards inhibition with BCH. System B^0 prefers large aliphatic neutral amino acids like leucine, isoleucine, valine, methionine, and threonine. Despite the significant structural differences between L-[^{18}F]FPhPA and above mentioned aliphatic amino acids, our performed competitive inhibition experiments with BCH can not exclude the involvement of system B^0 in the uptake of L-[^{18}F]FPhPA into EMT6 cells.

Results of competitive inhibition studies using inhibitors L-Ser and L-Gln imply a significant contribution of Na^+-dependent ASC system, and especially involvement of subtype ASCT2, for the uptake of L-[^{18}F]FPhPA into EMT6 cells (*Figure 4.5.* and *Figure 4.6.*). This is an interesting observation since primary substrates for system ASC amino acid transporter are non-aromatic amino acids like L-alanine, L-cysteine, L-serine. Additionally, L-glutamine is a key substrate of ASCT2 with important roles in tumor metabolism. Recently, system ASC and in particular its subtype ASCT2, was reported to be associated with tumor growth and proliferation[9,25]. Upregulation of ASCT2 has been shown in several human cancers including breast, prostate, and colon cancer. Therefore, development of amino acid radiotracers targeting the ASC system in cancer has attracted considerable attention. Recent examples of ^{18}F-labelled amino acids targeting ASC system in cancer are 3-(1-[^{18}F]fluoromethyl)-L-alanine (L-[^{18}F]FMA) and 3-[^{18}F]fluoro-cyclobutyl-1-carboxylic acid ([^{18}F]FACBC)[25-27]. However, inhibitors L-Ser and L-Gln are not specific for the ASC system. L-Ser and L-Gln also inhibit amino acid transport system A, and L-Gln is also an inhibitor for system N, which transports amino acids such as glutamine, histidine, asparagine and serine[18].

Based on our competitive inhibition experiments and the structural characteristics of L-[^{18}F]FPhPA, we conclude that L-[^{18}F]FPhPA seems to be transported mainly via systems L and system ASCT2. However, involvement of other amino acid transport systems such as Na^+-dependent systems A, N, and B^0 can not be excluded. This interesting finding warrants further investigations of amino acid L-[^{18}F]FPhPA as potential novel radiotracer for targeting amino acid transport systems in cancer. The found expression of LAT1, ASCT1, and ASCT2 in EMT6 cells (*Figure 4.7.*) and the results of our competitive inhibition studies (*Figure 4.5.* and *Figure 4.6.*) suggest a significant contribution of LAT1 and ASCT2 upon the uptake of L-[^{18}F]FPhPA into EMT6 cells.

Radiopharmacological evaluation was further concluded with dynamic small animal PET studies of L-[^{18}F]FPhPA in comparison with L-[^{18}F]FET in EMT6 tumor bearing mice. Both radiotracers showed appreciable uptake in EMT6 tumors reaching maximum SUV values of greater than 1.2 after 60 min p.i. (*Figure 4.8.*).

Amino acid L-[^{18}F]FPhPA showed significantly higher uptake and retention in muscle and blood compared to L-[^{18}F]FET resulting in a less favorable tumor-to-non target ratio for this novel ^{18}F-labelled amino acid. The higher radioactivity levels of L-[^{18}F]FPhPA in blood and muscle during the time course of the PET study make amino acid L-[^{18}F]FPhPA less favorable for imaging peripheral tumors in comparison with L-[^{18}F]FET. Moreover, L-[^{18}F]FPhPA displayed markedly different brain uptake and clearance pattern compared to that of L-[^{18}F]FET. However, it can not be excluded that the observed rapid brain uptake of

L-[^{18}F]FPhPA is mainly representing blood radioactivity since initial blood radioactivity level is also quite high. Amino acid L-[^{18}F]FPhPA exhibited an interesting distribution pattern in peripheral organs and brain notably different from that of L-[^{18}F]FET. The found differences in the biodistribution pattern can be attributed to significantly different lipophilicities between L-[^{18}F]FET (log*P* = -1.51) and L-[^{18}F]FPhPA (log*P* = -0.27). However, different expression levels of amino acid transporters as relevant for the transport of L-[^{18}F]FET (LAT1) and L-[^{18}F]FPhPA (LAT1 and ASC system) should also contribute to the found differences in biodistribution pattern. High expression levels of amino acid transport system ASCT2 has been reported in kidneys, large intestine, lung, heart and muscle[28]. This correlates with the observed high radioactivity levels in muscle, heart, gall bladder, and intestines during the small animal PET imaging studies with novel amino acid radiotracer L-[^{18}F]FPhPA.

4.5. Conclusion

We have synthesized the ^{18}F-labelled amino acid [^{18}F]FPhPA as a novel radiotracer for oncologic PET imaging. The Pd-mediated Sonogashira cross-coupling reaction was used for efficient radiosynthesis of [^{18}F]FPhPA under mild conditions compatible with delicate biologically active compounds like amino acids. [^{18}F]FPhPA is the first ^{18}F-labelled amino acid prepared through a Pd-mediated C-C bond forming reaction demonstrating the power and potential of this class of reactions for the synthesis of ^{18}F-labelled radiotracers. Applied mild reaction conditions including the use of aqueous reaction mixtures suggest extension of the Sonogashira cross-coupling reaction to the radiolabelling of other

classes of hydrophilic compounds like peptides with ^{18}F. [^{18}F]FPhPA displayed promising properties as novel amino acid radiotracer for molecular imaging of system ASC and system L amino acid transporters in cancer.

4.6. Acknowledgments

The authors would like to thank John Wilson, David Clendening and Blake Lazurko from the Edmonton PET Center for radionuclide production and excellent technical support. We also gratefully acknowledge the Dianne and Irving Kipnes Foundation and the National Science and Engineering Research Council of Canada (NSERC) for supporting this work.

4.7. References

1 Langen KJ, Hamacher K, Weckesser M, *et al.* *O*-(2-[^{18}F]fluoroethyl)-L-tyrosine: uptake mechanisms and clinical applications. *Nucl Med Biol.* **2006**; *33*: 287-94.

2 Kaira K, Oriuchi N, Shimizu K, *et al*. ^{18}F-FMT uptake seen within primary cancer on PET helps predict outcome of non-small cell lung cancer. *J Nucl Med.* **2009**; *50*: 1770-76.

3 McConathy J, Goodman Mark M. Non-natural amino acids for tumor imaging using positron emission tomography and single photon emission computed tomography. *Cancer Metastasis Rev.* **2008**; *27*: 555-73.

4 Langen KJ, Bröer S. Molecular transport mechanisms of radiolabelled amino acids for PET and SPECT. *J Nucl Med.* **2004**; *45*: 1435-36.

5 Jager PL, Vaalburg W, Pruim J, de Vries EG, Langen KJ, Piers DA. Radiolabelled amino acids: basic aspects and clinical applications in oncology. *J Nucl Med.* **2001**; *42*: 432-45.

6 Ishiwata K, Kubota K, Murakami M, Kubota R, Senda M. A comparative study on protein incorporation of L-[methyl-^{3}H]methionine, L-[1-^{14}C]leucine and L-2-[^{18}F]fluorotyrosine in tumor bearing mice. *Nucl Med Biol*. **1993**; *20*: 895-99.

7 Huang C, McConathy J. Fluorine-18 labelled amino acids for oncologic imaging with positron emission tomography. *Curr Top Med Chem.* **2013**; *13*: 871-91.

8 Hediger MA, Romero MF, Peng JB, Rolfs A, Takanaga H, Bruford EA. The ABCs of solute carriers: physiological, pathological and therapeutic implications of human membrane transport proteins. *Pflugers Arch* **2004**; *447*: 465-68.

9 Fuchs BC, Bode BP. Amino acid transporters ASCT2 and LAT1 in cancer: partners in crime? S*emin Cancer Biol.* **2005**; *15*: 254-66.

10 Fuchs BC, Finger RE, Onan MC, Bode BP. ASCT2 silencing regulates mammalian target-of-rapamycin growth and survival signaling in human hepatoma cells. *Am J Physiol Cell Physiol.* **2007**; *293*: C55-63.

11 Nicklin P, Bergman P, Zhang B, Triantafellow E, Wang H, Nyfeler B *et al*. Bidirectional transport of amino acids regulates mTOR and autophagy. *Cell.* **2009**; *136*: 521-34.

12 Wuest F. Fluorine-18 labelling of small molecules: the use of ^{18}F-labelled aryl fluorides derived from no-carrier-added [^{18}F]fluoride as labelling precursors. *Ernst Schering Res Found Workshop.* **2007**; *62*: 51-78

13 Wuest F, Berndt M, Kniess T. Palladium-mediated cross-coupling reactions with [^{11}C]methyl iodide and 4-[^{18}F]fluorohalobenzenes for the synthesis of positron emission tomography (PET) radiotracers. Research Signpost. *Recent Advances of Bioconjugation Chemistry in Molecular Imaging. X. Chen (Ed.).* **2008**; 155-73.

14 Way J, Bouvet V, Wuest F. Application of palladium-mediated cross-coupling reactions for the synthesis of ^{18}F-labelled compounds. *Curr Org Chem.* **2013**; *17*: 2138-52.

15 Way J D, Wuest F. Automated radiosynthesis of no-carrier added 4-[^{18}F]fluoroiodobenzene: A versatile building block in ^{18}F radiochemistry. *J Labelled Compds Radiopharm.* **2014**; *57*: 104-9.

16 Bouvet V, Wuest M, Tam PH, Wang M, Wuest F. Microfluidic technology: an economical and versatile approach for the synthesis of *O*-(2-[^{18}F]fluoroethyl)-L-tyrosine ([^{18}F]FET). *Bioorg Med Chem Lett.* **2012**; *22*: 2291-95.

17 Wilson AA, Jin L, Garcia A, DaSilva JN, Houle S. An admonition when measuring the lipophilicity of radiotracers using counting techniques. *Appl Radiat Isot.* **2001**; *54*: 203-08.

18 Mackenzie B, Erickson JD. Sodium-coupled neutral amino acid (System N/A) transporters of the SLC38 gene family. *Pflugers Arch*. **2004**; *447:* 784-95.

19 Duelli R, Enerson BE, Gerhart DZ, Drewes LR. Expression of large amino acid transporter LAT1 in rat brain endothelium. *J Cereb Blood Flow Metab.* **2000**; *20*: 1557-62.

20 Talukder JR, Kekuda R, Saha P, Sundaram U. Mechanism of leukotriene D4 inhibition of Na-alanine cotransport in intestinal epithelial cells. *Am J Physiol Gastrointest Liver Physiol.* **2008**; *295*: G1-G6.

21 Gliddon CM, Shao Z, LeMaistre JL, Anderson CM. Cellular distribution of the neutral amino acid transporter subtype ASCT2 in mouse brain. *J Neurochem.* **2009**; *108*: 372-83.

22 Wester HJ, Herz M, Weber W, Heiss P, Senekowitsch-Schmidtke R, Schwaiger M *et al.* Synthesis and radiopharmacology of *O*-(2-[^{18}F]fluoroethyl)-L-tyrosine for tumor imaging. *J Nucl Med.* **1999**; *40*: 205-12.

23 Wuest F, Kniess F. Synthesis of 4-[^{18}F]fluoroiodobenzene and its application in the Sonogashira cross-coupling reaction with terminal alkynes. *J Label Compd Radiopharm.* **2003**; *46*: 699-713.

24 Bröer S. The role of the neutral amino acid transporter B0AT1 (SLC6A19) in Hartnup disorder and protein nutrition. *IUBMB Life.* **2009**; *61*: 591-9.

25 Wang L, Zha Z, Qu W, Qiao H, Lieberman BP, Plössl K *et al*. Synthesis and evaluation of ^{18}F labelled alanine derivatives as potential tumor imaging agents. *Nucl Med Biol.* **2012**; *39*: 933-43.

26 Ono M, Oka S, Okudaira H, Schuster DM, Goodman MM, Kawai K et al. Comparative evaluation of transport mechanisms of trans-1-amino-3-[^{18}F]fluorocyclobutanecarboxylic acid and L-[methyl-^{11}C]methionine in human glioma cell lines. *Brain Res.* **2013**; *1535*: 24-37.

27 Oka S, Okudaira H, Yoshida Y, Schuster DM, Goodman MM, Shirakami Y. Transport mechanisms of trans-1-amino-3-fluoro[1-(^{14}C)]cyclobutane-carboxylic acid in prostate cancer cells. *Nucl Med Biol.* **2012**; *39*: 109-19.

28 Utsunomiya-Tate N, Endou H, Kanai Y. Cloning and functional characterization of a system ASC-like Na+-dependent neutral amino acid transporter. *J Biol Chem*. **1996**; *271*:14883-90.

Chapter 5

*Sonogashira reaction with 4-[^{18}F]fluoroiodobenzene for ^{18}F-labelling of peptides.**

Jenilee Way, Cody Bergman, Frank Wuest

5.1. Introduction

Radiolabelled peptides have been the subject of intense research efforts for targeted diagnostic imaging and radiotherapy over the last 20 years[1]. The high interest in radiolabelled peptides mainly stems from the over-expression of specific peptide-binding receptors in numerous cancers and inflammatory tissues[2]. For PET imaging, the majority of peptides were labelled with radiometals like copper-64, gallium-68, and yttrium-86[3]. Unlike radiometals, short-lived positron emitter fluorine-18 offers several advantages like high abundance of β^+-emission (97%), high yield production on small biomedical cyclotrons, high spatial resolution through low positron energy (0.635 MeV) and convenient half-life of 109.8 min for radiochemistry and molecular imaging studies[4].

However, radiofluorination of peptides is still a special challenge, and only a few ^{18}F-labelled peptides have been used in the clinic.

Currently used methods for the radiolabelling of peptides with fluorine-18 can be subdivided into three categories: (1) use of ^{18}F-labelled prosthetic groups which are activated as active esters or maleimides to undergo bioconjugation reaction with functional groups of the peptide backbone such as NH_2 and SH; (2) exploitation of fluoride-acceptor chemistry based on the strong affinity of

**As prepared for future publication.*

[^{18}F]fluoride to silicon (Si-^{18}F), boron (B-^{18}F), and aluminum (Al-^{18}F); and (3) application of various click chemistry concepts.

Scope and limitations of various methods for radiofluorination of peptides have been summarized in numerous excellent reviews. A selection of representative examples of currently used methods for peptide labelling with ^{18}F is given in *Table 5.1*.

Author	Peptide	Method	Synthesis time (min)	Radiochemical yield (%)
Richter *et al.*[5]	Bombesin	Prosthetic group (SFB)	30	27
Hackel *et al.*[6]	Cystine knot peptides	Prosthetic group (SFB)	45	7
Kapty *et al.*[7]	PS-binding peptides	Prosthetic group (FBAM)	60	97
Schirrmacher *et al.*[8]	RDG	Si-^{18}F acceptor chemistry	10	55
Li *et al.*[9]	dimeric cycloRGD	B-^{18}F acceptor chemistry	15	10
McBride *et al.*[10]	IMP467	Al-^{18}F acceptor chemistry	15	87
Ramenda *et al.*[11]	Neurotensin	Cu(I)-assisted click chemistry	20	66
Knight *et al.*[12]	Bombesin	Copper-free click chemistry	20	50
Campell-Verduyn *et al.*[13]	Bombesin	Copper-free click chemistry	15	37

Table 5.1. Selection of various methods for peptide labelling with ^{18}F.

Transition metal-mediated cross-coupling reactions have stimulated novel advances in PET radiochemistry, especially with the short-lived positron emitter carbon-11 and fluorine-18. Various palladium-mediated cross-coupling reactions have proven to be valuable and popular labelling strategies for the synthesis of ^{18}F-labelled compounds[14]. Palladium-mediated cross-coupling reactions were

successfully applied to the synthesis of small molecule PET tracers, like ^{18}F-labelled steroids[15], nucleosides[16], and amino acids[17]. However, the potential of palladium-mediated reactions has not yet been fully recognized for the ^{18}F-labelling of higher molecular weight compounds like peptides and proteins. An exception is the recently reported synthesis of ^{18}F-labelled polypeptides using Suzuki-Miyaura[18] cross-coupling reaction with 4-[^{18}F]fluorophenylboronic acid as the coupling partner.

On the other hand, various reports described the application of the Sonogashira cross-coupling reaction for peptide and protein functionalization in aqueous medium. In a first report, Dibowski *et al.*[19] described the Castro-Stephens-Sonogashira reaction for bioconjugation of peptides in water using a palladium-guanidinophosphane catalysts. The reaction was applied to cross-coupling reactions with 4-iodobenzoate with propargylglycine to form the desired cross-coupled product in good chemical yields of 75% after a reaction time of 3 h. Further proof-of-concept of this regioselective carbon-carbon bond formation was demonstrated by the reaction of biotinylglutamoyl-propargylamide with 4-iodophenyl-functionalized undecapeptide in buffer to yield the cross-coupled product in 91% after 3 h.

Additional reports further demonstrated the chemoselective Sonogashira cross-coupling reaction of peptides in water. It was shown that the reaction proceeded best at pH 5.5 to provide high yields yields[20]. The use of 4-[^{19}F]fluoroiodo-benzene in Sonogashira cross-coupling reactions with alkyne-encoded proteins in aqueous medium was reported by Li *et al.*[21]. These reports clearly demonstrate the

suitability of Sonogashira cross-coupling reactions in bioorthogonal chemistry for the introduction of fluorophenyl groups into peptides and proteins in aqueous solvents under mild conditions.

However, to the best of our knowledge the Sonogashira cross-coupling reaction with 4-[^{18}F]fluoroiodobenzene ([^{18}F]FIB) has not yet been used for peptide labelling in ^{18}F radiochemistry.

Here we describe the first application of the Sonogashira cross-coupling reaction of [^{18}F]FIB with alkyne-functionalized peptides in aqueous solution as a novel method for site-specific peptide labelling with the short-lived positron emitter ^{18}F. The reaction was optimized through screening of different Pd catalysts, solvents, reaction times and temperatures. We also tested the influence of peptide amount on radiochemical yield.

5.2. Results

5.2.1. Synthesis of labelling precursor pBBN and reference compound [^{19}F]FBpBBN

We have recently developed various metabolically stabilized ^{18}F-labelled bombesin derivatives for molecular targeting of gastrin-releasing peptide receptors (GRPRs) in prostate cancer. The radiolabel was introduced via acylation reaction using prosthetic group [^{18}F]SFB. Based on the favorable radiopharmacological profile of recently prepared ^{18}F-labelled bombesins, we decided to use a bombesin derivative to explore the Sonogashira cross-coupling reaction with [^{18}F]FIB. Application of the Sonogashira reaction with [^{18}F]FIB requires presence of a terminal alkyne group and introduction of this terminal

alkyne group was achieved through coupling bombesin derivative at the N-terminal end with L-propargylglycine. The synthesis of propargylglycine-containing bombesin derivative pBBN as labelling precursor was performed using solid-phase peptide synthesis. Peptide pBBN was isolated in 20% yield after HPLC purification and lyophilisation. Reference compound [^{19}F]FBpBBN was prepared using Sonogashira reaction conditions with [^{19}F]FIB in solution and on resin in 9% and 15% yield, respectively, after HPLC purification and lyophilization. Higher chemical yields of 15% favor on-resin Sonogashira cross-coupling compared with reaction in solution.

Structures of peptide pBBN as labelling precursor and [^{19}F]FBpBBN as reference compound are displayed in *Figure 5.1.*

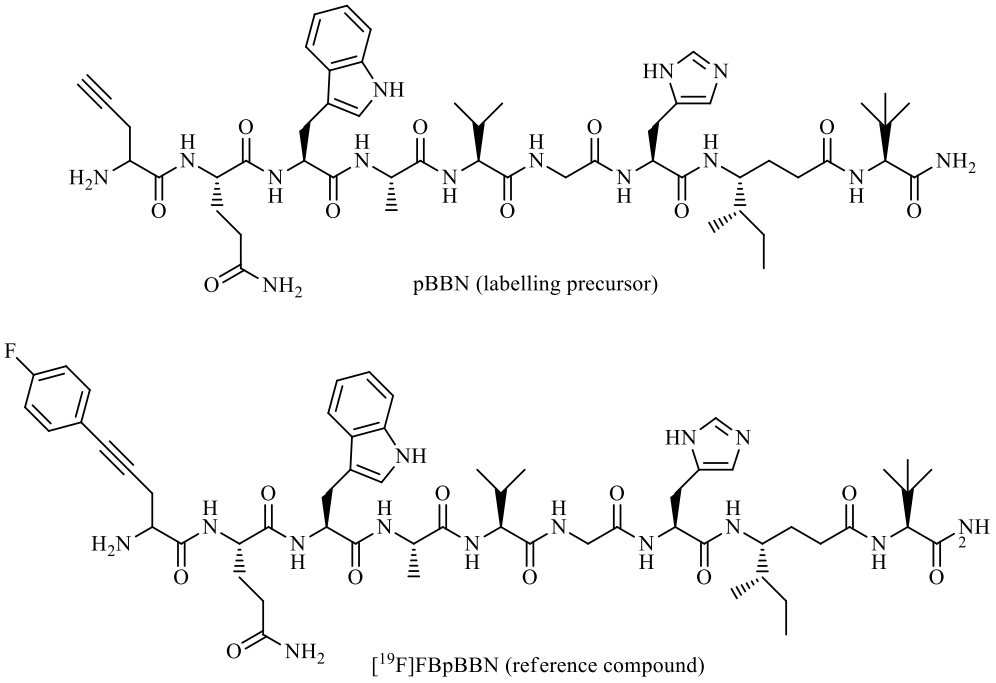

Figure 5.1. Structure of peptides pBBN and [^{19}F]FBpBBN.

5.2.2. Radiochemistry

Reaction conditions for the Sonogashira cross-coupling between [^{18}F]FIB and alkyne-functionalized bombesin derivative pBBN for the radiosynthesis of [^{18}F]FBpBBN were optimized by screening several Pd-complexes (see *Figure 7.33.*), solvents, reaction temperatures (see *Figure 7.35.*), reaction times (see *Figure 7.38.*), and peptide concentration (see *Figure 7.34.*). The general outline of the radiolabelling reaction is depicted in *Figure 5.2*.

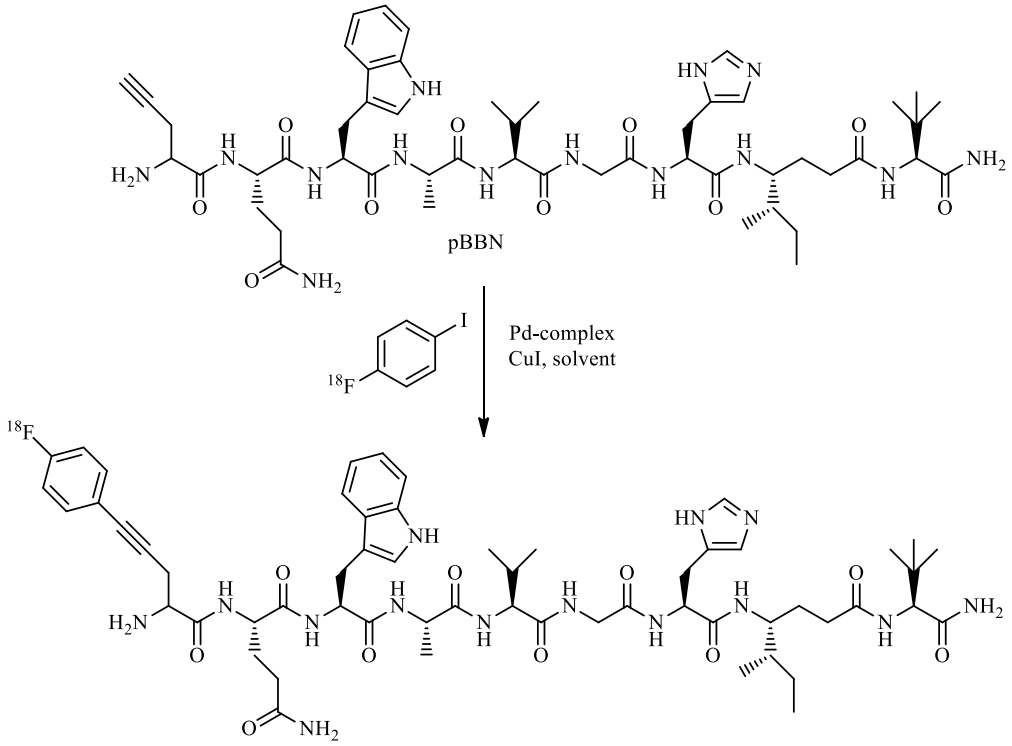

Figure 5.2. Radiolabelling of [^{18}F]FIB with pBBN to yield [^{18}F]FBpBBN.

All reactions were processed by acidification of the reaction mixture with 1N HCl (0.7 mL), followed by centrifugation for 5 min, and transfer of the reaction mixture from the Eppendorf tube into a glass vial. Both the Eppendorf tube and the glass vial were measured for radioactivity amount, and the reaction mixture

was analyzed using radio-TLC. Radiochemical yields represented show the percentage of product present in the reaction mixture. The results are summarized in *Table 5.2*.

Entry	Palladium complex	Peptide concentration	Reaction time	Reaction temperature	Solvent	Radiochemical yield[a,b,c] (n=3)
1	$PdCl_2(PPh_3)_2$	85 μg/mL	45 min	45 ºC	H_2O/CH_3CN	8 ± 1
2	$Pd(PPh_3)_4$	85 μg/mL	45 min	45 ºC	H_2O/CH_3CN	10 ± 5
3	$Pd(OAc)_2$	85 μg/mL	45 min	45 ºC	H_2O/CH_3CN	2 ± 0
4	$Pd_2(dba)_3$	85 μg/mL	45 min	45 ºC	H_2O/CH_3CN	2 ± 1
5	$PdCl_2(PPh_3)_2$	1.3 mg/mL	45 min	45 ºC	H_2O/CH_3CN	39 ± 11
6	$PdCl_2(PPh_3)_2$	130 μg/mL	45 min	45 ºC	H_2O/CH_3CN	18 ± 6
7	$PdCl_2(PPh_3)_2$	13 μg/mL	45 min	45 ºC	H_2O/CH_3CN	7 ± 3
8	$PdCl_2(PPh_3)_2$	1.3 μg/mL	45 min	45 ºC	H_2O/CH_3CN	0 ± 0
9	$PdCl_2(PPh_3)_2$	85 μg/mL	45 min	25 ºC	H_2O/DMF	11 ± 2
10	$PdCl_2(PPh_3)_2$	85 μg/mL	45 min	25 ºC	H_2O/CH_3CN	10 ± 2
11	$PdCl_2(PPh_3)_2$	85 μg/mL	45 min	45 ºC	H_2O/DMF	13 ± 7
12	$PdCl_2(PPh_3)_2$	85 μg/mL	45 min	45 ºC	H_2O/CH_3CN	24 ± 8
13	$PdCl_2(PPh_3)_2$	85 μg/mL	45 min	65 ºC	H_2O/DMF	19 ± 6
14	$PdCl_2(PPh_3)_2$	85 μg/mL	45 min	65 ºC	H_2O/CH_3CN	8 ± 3
15	$Pd(NO_3)_2$	250 μg/mL	45 min	45 ºC	H_2O/CH_3CN	3 ± 0
16	$Pd(tppts)_4$	250 μg/mL	45 min	45 ºC	H_2O/CH_3CN	25 ± 8
17	$Pd(tppts)_4$	85 μg/mL	1 min	25 ºC	H_2O/CH_3CN	60 ± 5
18	$Pd(tppts)_4$	85 μg/mL	5 min	25 ºC	H_2O/CH_3CN	51 ± 4
19	$Pd(tppts)_4$	85 μg/mL	10 min	25 ºC	H_2O/CH_3CN	71 ± 4
20	$Pd(tppts)_4$	85 μg/mL	15 min	25 ºC	H_2O/CH_3CN	73 ± 2
21	$Pd(tppts)_4$	85 μg/mL	10 min	25 ºC	H_2O/CH_3CN	37 ± 5[d]
22	$Pd(tppts)_4$	85 μg/mL	10 min	25 ºC	H_2O/CH_3CN	32 ± 6[e]
23	$Pd(tppts)_4$	85 μg/mL	10 min	25 ºC	H_2O/CH_3CN	40 ± 5[f]
24	$Pd(tppts)_4$	85 μg/mL	10 min	25 ºC	H_2O/CH_3CN	33 ± 2[g]
25	$Pd(tppts)_4$	85 μg/mL	10 min	25 ºC	H_2O/CH_3CN	35 ± 13[h]

[a] Radiochemical yields were determined by radio-TLC representing percentage of product present in the reaction mixture.
[b] 1 mg of CuI was used
[c] 50 μL of TEA was used
[d] 5 mg of NaOH was used instead of 50 μL of TEA
[e] 50 μL of DIPEA was used instead of 50 μL of TEA
[f] 10 mg of K_3PO_4 was used instead of 50 μL of TEA
[g] 10 mg of K_2CO_3 was used instead of 50 μL of TEA
[f] 10 mg of $NaHCO_3$ was used instead of 50 μL of TEA

Table 5.2. Summary of results for the Sonogashira reaction of [^{18}F]FIB with pBBN.

In the first set of reactions (entries 1 to 4), the influence of different palladium catalysts was tested. Two Pd(II) catalysts ($PdCl_2(PPh_3)_2$ and $Pd(OAc)_2$), and two Pd(0) catalysts ($Pd(PPh_3)_4$ and $Pd_2(dba)_3$) were used. The rest of the reaction mixture contained CuI (1 mg), TEA (50 μL), and pBBN (85 μg/mL) in PBS (0.5 mL) with [^{18}F]FIB in CH_3CN (100 μL). Pd-complexes containing a triphenylphosphine ligand (entry 1 and 2) seemed to be more sufficient regardless the oxidation state of the metal center, and comparable radiochemical yields of about 10% were obtained with $PdCl_2(PPh_3)_2$ and $Pd(PPh_3)_4$ (entry 1 and 2). Further optimization studies were carried out with $PdCl_2(PPh_3)_2$ as the Pd-complex. In the next series of experiments, the amount of peptide on the radiochemical yield was studied (entries 5 to 8). The amount of peptide in solution varied from 1.3 mg/mL down to 1.3 μg/mL. Results clearly demonstrated the importance of peptide amount on the radiochemical yield. High peptide concentration of 1.3 mg/mL provided highest radiochemical yield of 39%, whereas no product was formed when very low peptide concentration of 1.3 μg/mL was used (entry 5 vs. entry 8). We decided to continue optimization experiments with a peptide concentration of 85 μg/mL. In the next series of experiments, temperature and solvent were varied using DMF and CH_3CH, using a reaction temperature of 25 °C, 45 °C, and 65 °C, respectively (entries 9 to 14). Experiments displayed in entries 9 to 14 suggest that reactions using DMF as the co-solvent proceeded in higher radiochemical yield at higher reaction temperature (entries 9, 11, and 13). In the case of CH_3CN as the co-solvent, best radiochemical yields of 24% were achieved at 45 °C (entry 12), whereas lower radiochemical

yields were observed when lower temperature (25 °C, entry 10) or higher temperature (65 °C, entry 14) were applied.

In course of all experiments described in entries 1 to 14, we realized that a major limitation of the Sonogashira cross-coupling reaction with peptides in aqueous solutions is the solubility of the Pd-complex. As a consequence, we tested various water soluble Pd-complexes in the next set of reactions, and water soluble complexes $Pd(tppts)_4$ and $Pd(NO_3)_2$ were used. $Pd(tppts)_4$ was prepared starting from $Pd(OAc)_2$ (1.0 mg) by ligand exchange with 3,3′,3″-phosphanetriyltris trisodium salt (tppts) (10.5 mg) within 30 min through gentle vortexing[22]. Ligand exchange from $Pd(OAc)_2$ to $Pd(tppts)_4$ was easily visible by color change.

Color of the reaction changed from yellow ($Pd(OAc)_2$, **A**), to light orange (1 ligand substitution, **B**), to green (2 ligand substitution, **C**), to dark orange (3 ligand substitution, **D**), to ruby red (4 ligand substitution, **E** and **F**). Colorimetric ligand exchange of $Pd(OAc)_2$ with tppts is given in *Figure 5.3*.

Upon completion of ligand exchange reaction, complexes $Pd(tppts)_4$ and $Pd(NO_3)_2$ were used for the cross-coupling reactions with the pBBN peptide (entries 15 and 16) (see *Figure 7.37.*). Higher peptide concentration of 250 μg/mL was used. Pd-complex $Pd(NO_3)_2$ showed very poor cross-coupling potential compared to $Pd(tppts)_4$ as reflected by the very low radiochemical yield of 3% (entry 15) compared to 25% obtained with $Pd(tppts)_4$ (entry 16).

Therefore, further optimization experiments were done using $Pd(tppts)_4$ as a water soluble Pd-complex. Influence of the reaction time upon the radiochemical yield was studies in the following series of experiments (entries 17 to 20). Best

radiochemical yields of about 70% were obtained after a reaction time of 10 min at 25 °C (entry 19). The last set of experiments studied the influence of different bases upon the radiochemical yield of Sonogashira cross-coupling reaction with [^{18}F]FIB and peptide pBBN.

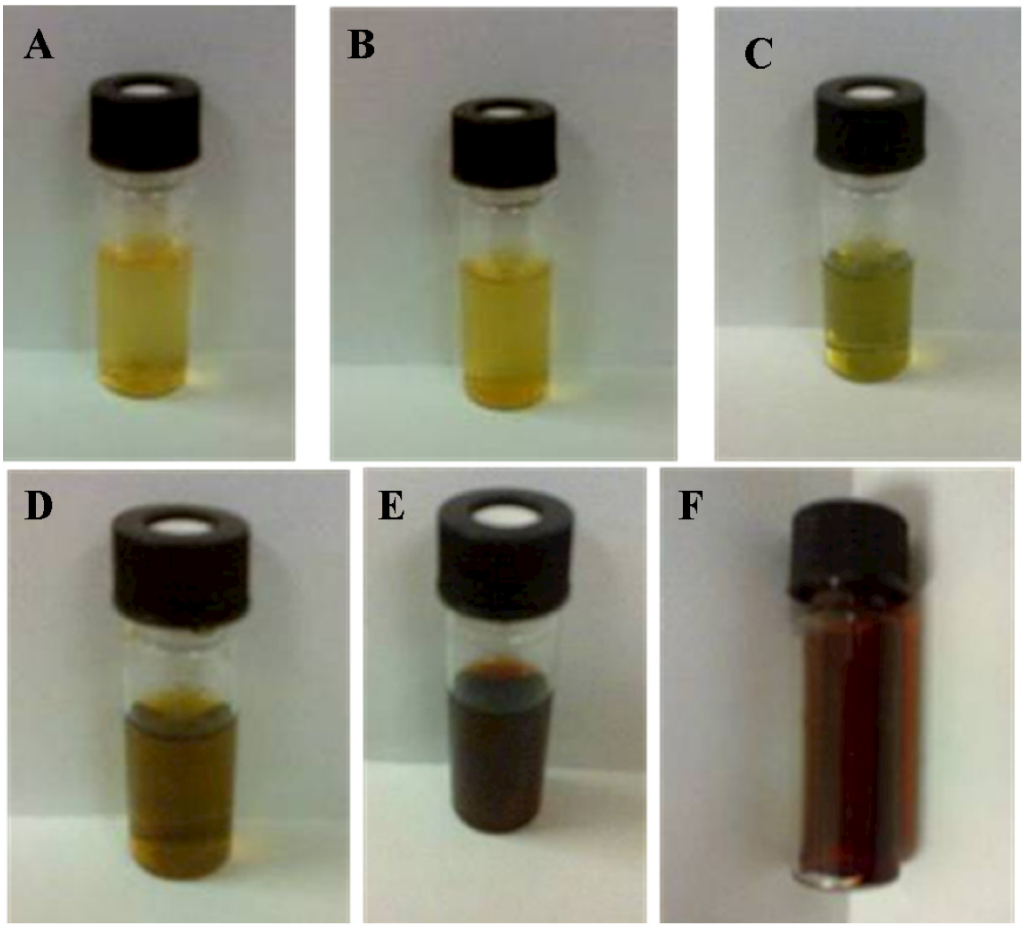

Figure 5.3. Colorimetric ligand substitution of $Pd(OAc)_2$ with tppts.

All reactions in entries 21 to 25 provided comparable radiochemical yields between 32 to 40% regardless the base used. Alternative bases NaOH (entry 21), DIPEA (entry 22), K_3PO_4 (entry 23), K_2CO_3 (entry 24), and $NaHCO_3$ (entry 25) gave lower radiochemical yields compared to reaction with TEA under comparable conditions (entry 19) (See *Figure 7.39.*).

Based on optimization experiments summarized in *Table 5.2.*, the following reaction conditions were selected for radiosynthesis of [^{18}F]FBpBBN according to a Sonogashira cross-coupling reaction between pBBN and [^{18}F]FIB: 0.1 mg of $Pd(tppts)_4$, 1.0 mg of CuI, 85 μg of pBBN, and 50 μL of TEA in 1 mL of CH_3CN:PBS (1:9) at 25°C for 10 min. Application of optimized reaction conditions, radiolabelled peptide [^{18}F]FBpBBN was obtained in 71 ± 4% radiochemical yield after a reaction time of 35 min, including HPLC purification. Specific activity of [^{18}F]FBpBBN was calculated to be 625 ± 334 GBq/μmol (n=3) (See *Figure 7.41./Table 7.3.*). The HPLC trace of purified [^{18}F]FBpBBN is given in *Figure 5.4*.

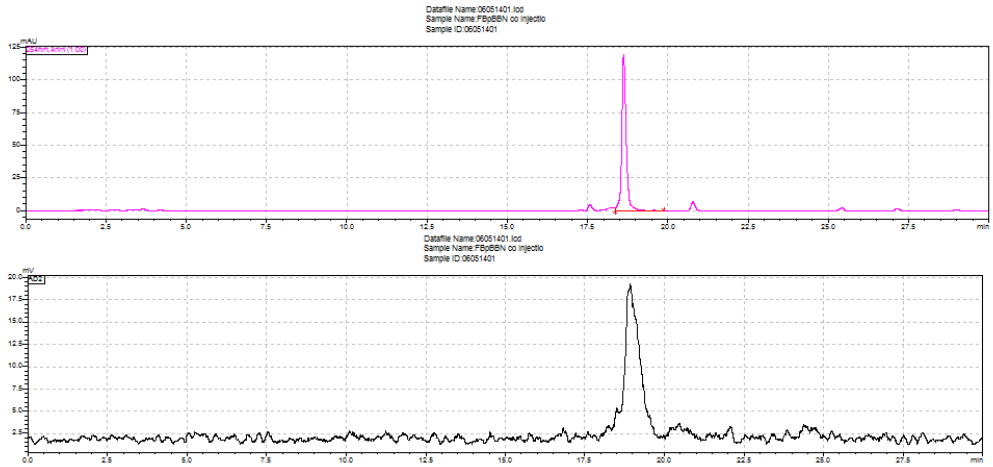

Figure 5.4. HPLC of purified [^{18}F]FBpBBN (bottom) and co-injected cold reference (top).

5.2.3. Determination of IC_{50} of [^{18}F]FBpBBN

IC_{50} value of [^{19}F]FBpBBN was determined as described by Richter et al.[5] using ^{125}I-labelled bombesin based assay with PC-3 cells. The IC_{50} value for peptide [^{19}F]FBpBBN was determined to be 48 ± 7 (n=3).

5.2.4. Determination of logP of [^{18}F]FBpBBN

The *logP* of [^{18}F]FBpBBN was determined using the shake flask method by adding the tracer into a 2.0 mL Eppendorf vial containing mixtures of n-octanol (0.5 mL) and PBS buffer (0.5 mL, pH 7.4). The log*P* value was determined to be 0.27 (n=3) (see *Figure 7.42.*) confirming the slightly hydrophobic nature of bombesin derivative [^{18}F]FBpBBN.

5.3. Discussion

In the present study, we describe the synthesis of ^{18}F-labelled bombesin derivative [^{18}F]FBpBBN according to a Sonogashira cross-coupling reaction with 4-[^{18}F]fluoroiodo-benzene. Reaction conditions were carefully optimized by screening different Pd-complexes, peptide mass, temperature, reaction time, solvents and bases. To date, as summarized in *Table 5.1.*, synthesis of ^{18}F-labelled peptides is most commonly accomplished through the use of prosthetic groups. Only one report describes the use of a Pd-mediated cross-coupling reaction for peptide labelling with fluorine-18[18].

Optimization of reaction conditions for Sonogashira cross-coupling for the synthesis of [^{18}F]FBpBBN first started with screening of different palladium complexes. Palladium complexes that contained triphenylphosphine ligands seemed to provide highest radiochemical yields. This observation was also made with water soluble Pd-complex containing phosphine ligand tppts. This trend is also mirrored in various non-radioactive Sonogashira reactions, in which aromatic-substituted palladium complexes were used in aqueous media for the synthesis of peptides and proteins[19-21].

The amount of peptide as labelling precursor was found to be another important reaction parameter, and peptide amounts of at least 85 μg/mL afforded good radiochemical yields. This fairly low peptide amount was also beneficial to obtain reasonably high specific activities. Moreover, the use of only small amount of peptide is extremely promising if the peptide in question is (1) very costly or (2) difficult to synthesize. Comparatively, most of the previously reported peptide syntheses with fluorine-18 typically required between 0.1 to 2 mg of peptide to provide reasonable radiochemical yields[5-13].

Using non-water soluble Pd-complexes, the reaction was optimally performed at 45 °C in CH_3CN over 45 min. In the case of water soluble complexes, the reaction proceeded more favorably, and good results were obtained when the reaction was performed at 25 °C in CH_3CN:PBS within a short reaction time of 10 min. This ability for the reaction to proceed at room temperature in mostly PBS buffer is very beneficial to future biological molecules that maybe either more sensitive to higher temperature reactions or to organic solvents, and leads to an overall very promising synthetic radiolabelling procedure for biological molecules.

Moreover, only very little copper is required for the reaction to proceed, thus decreasing any toxicity concerns that may result from residual CuI. Another interesting aspect is the possibility to incorporate alkyne-containing amino acids like homopropargylglycine in a directed way into the structure of proteins[23].

This would allow for a site-specific radiolabelling reaction exploiting the Sonogashira cross-couplings with [^{18}F]FIB compared to the random incorporation using prosthetic groups like [^{18}F]SFB into the peptide or protein backbone. This

site-directed radiolabelling provides radiolabelled compounds without the potential loss of biological activity resulting from non-specific bioconjugation reactions.

5.4. Conclusion

We were able to synthesize the peptide [^{18}F]FBpBBN in good radiochemical yields from readily available [^{18}F]FIB as starting material. The Sonogashira cross-coupling reaction was found to be applicable for peptide labelling with ^{18}F under aqueous conditions. The best results were obtained with water soluble Pd-complexes, and the reaction could be completed under mild reaction conditions within a short reaction time of 10 min. In relation to the Sonogashira cross-coupling reactions using ^{19}F compounds[15-17], experiments with fluorine-18 provided comparable results with high radiochemical yields of over 70 % applying low reaction temperature and aqueous media. This confirms that Sonagashira cross-coupling reaction for peptide labelling is applicable for both, conventional organic chemistry and radiochemistry.

Overall, we have developed a novel radiolabelling method for site-specific incorporation of fluorine-18 into peptides under mild and physiological conditions. The Sonogashira cross-coupling reaction with [^{18}F]FIB has the potential to be extended to other bio-macromolecules such as proteins and oligonucleotides. This will further expand the arsenal of useful ^{18}F-labelled radiotracers for molecular imaging with PET.

5.5. Materials and Methods

5.5.1. General

All chemicals used, with the exception of water were obtained from Sigma-Aldrich®, with the quality of some reagents as follows: copper(I) iodide of trace metal grade and the acetonitrile (CH_3CN) over molecular sieves (H_2O ≤0.01%), ≥99.8% (GC). Water was obtained from a Barnstead Nanopure water filtration system (Barnstead Diamond Nanopure pack organic free RO/DIS).High performance liquid chromatography (HPLC) purification and analysis of the ^{18}F-radiolabelled products were performed using a Phenomenex LUNA®C18(2) column (100 Å, 250 x 10 mm, 10 μm) using gradient elutions specific to the given compound (Gilson 321 pump, 171 diode array detector, Berthold Technologies Herm LC). Quality control analysis were performed on a PhenomenexLuna®10u C18(2) column (100 Å, 250 x 4.60 mm) (Shimadzu DGU-20A, LC-20AT, SPD-M20A, CBM-20A, SIL-20A HT, RaytestRamonaStar). Radio-TLC were performed using either EMD Merck F254 silica gel 60 aluminum backed thin layer chromatography (TLC) plates or Analtech RP18 with UV254 aluminum backed TLC plates (Bioscan AR-2000). Quantification of radioactive samples during chemistry was achieved using a Biodex ATOMLAB™ 400 dose calibrator. Centrifugation of non-radioactive samples was achieved with a HettichZentrifugenRotina 35R, whereas ^{18}F-radiolabelled samples were centrifuged on a Fisher Scientific Mini Centrifuge. Reactions parameters were screened using an EppendorfThermomixer R and an IKAMAG® Ret-G Stir plate with an oil bath. Final formulation of the final ^{18}F-radiolabelled products for

animal injection were done using glassware kept in an Isotemp Vacuum Oven Model 285A and a rotary evaporator of a Buchi HB 140 Rotavpor-M with a Fisher Maxima C Plus Model M8C pump. High resolution Mass Spectroscopy was achieved with an Agilent Technologies 6220 oaTOF.

5.5.2. Chemistry

5.5.2.1. Resin synthesis of propargylglycine-bombesin derivative (pBBN)

Peptide BBN1 was prepared as per Richter *et al.*[3], with the N-terminus of the peptide containing the L-propargylglycine moiety. This peptide coupling was performed using solid-phase peptide synthesis (SPPS) on a Syro I (MultiSynTech/Biotage).

5.5.2.2. General manual procedure for the synthesis of [^{19}F]FBpBBN

To an Eppendorf Lobind 2.0 mL eppendorf tube, propargylglycine modified bombesin derivative (pBBN) (3 mg) was added along with copper (I) iodide (3mg), triethlyamine (300μL) and $PdCl_2(PPH_3)_2$ (3 mg). Next, water (400 μL) and DMF (300 μL) were added along with a commerically available [^{19}F]FIB (10 μL). The mixture was then allowed to react in a thermoshaker for 60 minutes at 55 °C. Upon reaction completion, 2N hydrochloric acid (HCl, 1 mL) was added and the reaction mixture was centrifuged to remove all precipitates. The product was purified by Beckmann HPLC and the collected product fractions are evaporated to dryness by rotary evaporation to yield the desired compound. Yield: 0.5 mg (9 %) as a fluffy white powder. HR-MS m/z (ESI): $C_{57}H_{80}FN_{14}O_{10}$ ($[M+H]^+$) calcd. 1139.616, found 1139.6151, ($[M+Na]^+$) calcd. 1161.598, found 1161.5971 (see

Figure 7.6.). HPLC-analysis (Luna 10u C18(2)) (100 Å, 250 x 10 mm, 10μm), gradient elution with (A: water; B: CH_3CN; 0 min 15 % B, 1.20 min 15 % B, 58.20 min 100 % B, 60.20 min 100% B, 3 mL/min): t_R = 19.5 min.

5.5.2.3. On-resin synthesis of [^{19}F]FBpBBN

To pBBN, synthesized on resin according to an amino acid loading of 0.6 mmol/g of starting resin (125 mg). The cross coupling reaction was carried out manually on resin through the addition of the following reagents to the peptide synthesis tube: [^{19}F]FIB (43.3 μL), CuI (5.7 mg), $PdCl_2(PPh_3)_2$ (10.5 mg), triethylamine (2 mL), and 1,4-dioxane (4 mL). The resin reaction was allowed to react for 72 hours at room temperature and once completed the peptide was cleaved off the resin. A cocktail (4 mL) solution containting 88% trifluoroacetic acid, 5% thioanisole, 5% water, and 2% ethane dithiol, was half (2 mL) used for the cleavage reaction of 3 hours at room temperature, followed by a subsequent wash with the remaining (2 mL) of solution made. Once cleaved the solution was dried under a stream of nitrogen and diethyl ether was used to precipitate the compound of interest. The [^{19}F]FBpBBN was isolated by filtration and purified using Gilson HPLC and the collected fractions lyophillizated to yield 13.2 mg (15 %) purified peptide as a white powder. LR-MS m/z (ESI): $C_{57}H_{80}FN_{14}O_{10}$ ($[M+H]^+$) calcd. 1139.6, found 1139.6, ($[M+Na]^+$) calcd. 1161.6, found 1161.6 (see *Figure 7.7.*). HPLC-analysis (Jupiter 10u Proteo) (90 Å, 250 x 10 mm, 10μm), gradient elution with (A: water; B: CH_3CN; 0 min 20 % B, 10 min 35 % B, 30 min 75 % B, 40 min 75 B, 3 mL/min): t_R = 18.1 min (see *Figure 7.8.*).

5.5.3. Radiochemistry

5.5.3.1. Syntheses of 4-[^{18}F]fluoroiodobenzene ([^{18}F]FIB)

4-[^{18}F]Fluoroiodobenzene ([^{18}F]FIB) were prepared according to literature procedure[18].

5.5.3.2. Formulation of 4-[^{18}F]fluoroiodobenzene ([^{18}F]FIB) for use in cross-coupling reactions

The collected product of [^{18}F]FIB from the HPLC (6 mL) was diluted into water (50 mL) and trapped onto a Waters Sep-Pak®tC18 plus light cartridge (300 mg). Elution from the cartridge took place in the solvent of interest, such as DMF (1.5 mL), CH_3CN (3.0 mL), toluene (3.0 mL), acetone (3.0 mL), and tetrahydrofuran (THF, 3.0 mL). Purified [^{18}F]FIB was used accordingly in the different cross-coupling reactions.

5.5.3.3. Manual synthesis of [^{18}F]FBpBBN

To an Eppendorf Lobind 1.5 mL eppendorf tube, pBBN (0.1 mg) was added along with CuI (1 mg), triethylamine (25 μL) and a palladium catalyst ($Pd(OAc)_2$0.1 mg, TPPTS 1 mg). Next, PBS Buffer (900 μL) was added along with HPLC purified [^{18}F]FIB (100 μL) in the respective solvent. The mixture was then allowed to react in a thermoshaker for 10 min at 25 °C. Upon completion, 2 N HCl (0.7 mL) was added and the reaction mixture was centrifuged. This product mixture was removed from the eppendorf with a syringe, avoiding the pelleted solids. [^{18}]FBpBBN was analyzed by a dual plate system.

5.5.3.4. TLC analysis of [^{18}F]FBpBBN

Another EMD Merck F254 silica gel 60 aluminum backed TLC plates, was spotted on the baseline and the plate was developed (63:37, CH_3CN: 0.2 % TFA in H_2O) (see *Figure 7.30.*). There was three possible spots, one of the any degradation and possible [^{18}F]FBpBBN compound which appeared on the baseline (R_f=0.0), any Pd-bound [^{18}F]FIB which appeared in the middle of the TLC plate (R_f=0.54)., and the starting material of [^{18}F]FIB which appeared at the solvent front (R_f=0.81). Next to show that this product peak was not fully degredation, another TLC plate was run to demonstrate movement of the product of interest. Using Analtech RP18 with UV254 aluminum backed TLC plates, a radioactive sample was spotted on the baseline and the plate was developed (7:3, CH_3CN:TEA) (see *Figure 7.31.*). There only two possible spots, one of the degradation products which appeared on the baseline (R_f=0.0) and the product of [^{18}F]FBpBBN plus any unreacted [^{18}F]FIB and palladium bound [^{18}F]FIB (R_f=0.65).

5.5.3.5. HLPC purification of [^{18}F]FBpBBN

Gilson HPLC purification of the crude [^{18}F]FhPA was performed using a graditent elution as follows: (Luna 10u C18(2)) (100 Å, 250 x 10 mm, 10μm), (A: water; B: CH_3CN; 0 min 15% B, 58 min 100% B, 60 min 100% B). The flow rate of the system was 3 mL/min, which gave a retention time of 23.2 minutes for the [^{18}F]FBpBBN product as confirmed with the use of a reference compound (see *Figure 7.32.*). The radiochemical purity was determined by the area under the

peak of interest compared to the rest of the radio-chromatogram; as well the specific activity of [^{18}F]FBpBBN was calculated against a standard curve.

5.6. References

1 Fani, M., Maecke, H. R. (2012) Radiopharmaceutical development of radiolabelled peptides. *Eur. J. Nucl. Med. Mol. Imaging. 39,* S11–S30.

2 Lozza, C., Navarro-Teulon, I., Pelegrin, A., Pouget, J. P., Vives, E. (2013) Peptides in receptor-mediated readiotherapy: from design to the clinical aplication in cancer. *FONC. 247,* 1-13.

3 Correia, J. D. G., Paulo, A., Santos, R., Santos, I. (2011) Radiometallated peptides for molecular imaging and targeted therapy. *Dalton Trans. 40,* 6144-6167.

4 Alauddin, M. M. (2012) Positron emission tomography (PET) imaging with ^{18}F-based radiotracers. *Am. J. Nucl. Med. Mol. Imaging. 2,* 55-76.

5 Richter, S., Wuest, M., Krieger, S. S., Rogers, B. E., Friebe, M., Bergmann, R., Wuest, F. (2013) Synthesis and radiopharmacological evaluation of a high-affinity and metabolically stabilized ^{18}F-labelled bombesin analoque for molecular imaging of gastrin-releasing peptide receptor-expressing prostate cancer. *Nucl. Med. Biol. 40,* 1025-1034.

6 Hackel, B. J., Kimura, R. H., Miao, Z., Liu, H., Sathirachinda, A., Cheng, Z., Chin, F. T., Gambhir, S. S. (2013) ^{18}F-Fluorobenzoate-Labelled Cystine Knot Peptides for PET Imaging of Integrin $\alpha_v\beta_6$. *J. Nucl. Med. 54,* 1101-1105.

7 Kapty, J., Kniess, T., Wuest, F., Mercer, J. R. (2011) Radiolabelling of phosphatidylserine-binding peptides with prosthetic groups N-[6-(4-[^{18}F]fluorobenzylidene)aminoxyhexyl]maleimide ([^{18}F]FBAM) and N-succinimidyl-4-[^{18}F]fluorobenzoate ([^{18}F]SFB). *Appl. Radio. Iso. 69,* 1218-1225.

8 Schirrmacher, E., Wangler, B., Cypryk, M., Bradtmoller, G., Schafer, M., Eisenhut, M., Jurkschat, K., Schirrmacher, R. (2007) Synthesis of *p*-(Di-*tert*-butyl[^{18}F]fluorosilyl)benzaldehyde ([^{18}F]SiFA-A) with high specific activity by isotopic exchange: a convenient labelling synthen for the ^{18}F-labeling of N-amino-*oxy* derivatized peptides. *Bioconjugate Chem. 18,* 2085-2089.

9 Li, Y., Liu, Z., Harwig, C. W., Pourghiasian, M., Lau, J., Lin, K. S., Schaffer, P., Benard, F., Perrin, D. M. (2013) ^{18}F-click labelling of a bombesin antagonist with an alkyne-^{18}F-$ArBF_3^-$: *in vivo* PET imaging of tumors expressing the GRP-receptor. *Am J Nucl Med Mol Imaging. 3,* 57-70.

10 McBride, W. J., D'Souza, C. A., Sharkey, R. M., Karacay, H., Rossi, E. A., Chang, C. H., Goldenberg, D. M. (2010) Improved ^{18}F labelling of peptides with a flouride-aluminum chelate complex. *Bioconjugate Chem. 21,* 1331-1340.

11 Ramenda, T., Bergmann, R., Wuest, F. (2007) Synthesis of ^{18}F-labelled neurotensin(8-13) via copper-mediated 1,3-dipolar [3+2]cycloaddition *Reaction. Lett. Drug. Des. Discov. 4,* 279-285.

12 Knight, J. C., Richter, S., Wuest, M., Way, J. D., Wuest, F. (2013) Synthesis and evaluation of an ^{18}F-labelled norbornene derivative for copper-free click chemistry reactions. *Org. Biomol. Chem. 11,* 3817-3825.

13 Campbell-Verduyn, L. S., Mirfeizi, L., Schoonen, A. K., Dierchx, R. A., Elsinga, P. H., Feringa, B. L. (2011) Strain-promoted copper-free ”click” chemistry for ^{18}F radiolabelling of bombesin. *Angew. Chem. Int. Ed. 50,* 11117-11120.

14 Way, J., Bouvet, V., Wuest F. (2013) Synthesis of 4-[^{18}F]fluorohalo-benzenes and palladium-mediated cross-coupling reactions for the synthesis of ^{18}F-labelled radiotracers. *Curr. Org. Chem. 17,* 2138-2152.

15 Wust, F. R.; Kniess, T. (2004) No-carrier added synthesis of ^{18}F-labelled nucleosides using Stille cross-coupling reactions with 4-[^{18}F]fluoroiodobenzene. *J. Labelled Compd. Radiopharm. 47*, 457-468.

16 Wust, F. R.; Kniess, T. (2003) Synthesis of 4-[^{18}F]fluoroiodobenzene and its application in Sonogashira cross-coupling reactions. *J. Labelled Compd. Radiopharm*. *46*, 699-713.

17 Way, J., Wang, M., Hamann, I., Wuest, M., Wuest F. (2014) Synthesis and evaluation of 2-amino-5-(4-[^{18}F]fluorophenyl)pent-4-ynoic acid ([^{18}F]FPhPA): A novel ^{18}F-labelled amino acid for oncologic PET imaging. *Nucl. Med. Biol. 41,* 660-669.

18 Gao, Z., Gouverneur, V., Davis, B. G. (2013) Enhanced aqueous Suzuki-Miyaura coupling allows site-specific polypeptide ^{18}F-labeling. *J. Am. Chem. Soc. 135,* 13612-13615.

19 Dibowski, H., Schmidten, F. P. (1998) Bioconjugation of peptides by palladium-catalyzed C-C cross-couplings in water. *Angew. Chem. Int. Ed. 37,* 476-478.

20 Bong, D. T., Ghadiri, M. R. (2001) Chemoselctive Pd(0)-catalyzed peptide coupling in water. *Org. Lett. 3,* 2509-2511.

21 Li, N., Lim, R. K. V., Edwardraja, S., Lin, Q. (2011) Copper-free Sonogashira cross-coupling for functionaliztion of alkyne-encoded proteins in aqueous medium and in bacterial Cells. *J. Am. Chem. Soc. 133,* 15316-15319.

22 Amatore, C., Blart, E., Genet, J. P., Jutand, A., Lemaire-Audoire, S., Savignac, M. (1995) New synthetic applications of water soluble acetate Pd/TPPTS catalysts generated *in situ*. Evidence of a true Pd(0) Species intermediate. *J. Org. Chem. 60,* 6829-6839.

23 Kiick, K. L., Saxon, E., Tirrell, D. A., Certozzi, C. R. (2002) Incorporation of azides into recombinant proteins for chemoselective modification by the Staudinger ligation. *PNAS. 99,* 19-24.

Chapter 6

Summary and outlook

Jenilee Way

6.1. Summary

The thesis deals with the development of novel radiolabelling methods based on Sonogashira cross-coupling reactions with 4-[^{18}F]fluoroiodobenzene ([^{18}F]FIB) as the coupling partner.

Based on a comprehensive review on the synthesis of various ^{18}F-labelled halobenzenes and their application in transition metal-mediated reactions for the preparation of PET radiotracers, the thesis defined three major goals:

(1) Development of an automated synthesis of 4-[^{18}F]fluoroiodobenzene.

(2) Application of 4-[^{18}F]fluoroiodobenzene ([^{18}F]FIB) in a Sonogashira cross-coupling reaction for the synthesis of a ^{18}F-labelled amino acid as an example of a low molecular weight compound.

(3) Application of 4-[^{18}F]fluoroiodobenzene ([^{18}F]FIB) in a Sonogashira cross-coupling reaction for the synthesis of a ^{18}F-labelled peptides as an example of a higher molecular weight compound.

We have successfully developed a fully automated synthesis for the preparation of 4-[^{18}F]fluoroiodobenzene **2** ([^{18}F]FIB) from commercially available precursor material **1**, as shown in *Figure 6.1.* This procedure was adapted from the manual synthesis recently published by Linjing *et al.*[1]. Our automated synthesis provided

[^{18}F]FIB in very high radiochemical yields of 89 ± 10 % (n=7) and high radiochemical purity of 97 ± 3 % within a reaction time of 59 ± 2 min including HPLC purification. HPLC purification of [^{18}F]FIB was fully optimized to allow for isolation of chemically pure radiotracer, as the precursor compound could sufficiently be separated from [^{18}F]FIB as the product of interest. [^{18}F]FIB was prepared at high specific activity of greater than 40 GBq/μmol. In a typical automated synthesis, 6.4 GBq of [^{18}F]FIB could be prepared starting from 10.4 GBq of n.c.a. [^{18}F]fluoride.

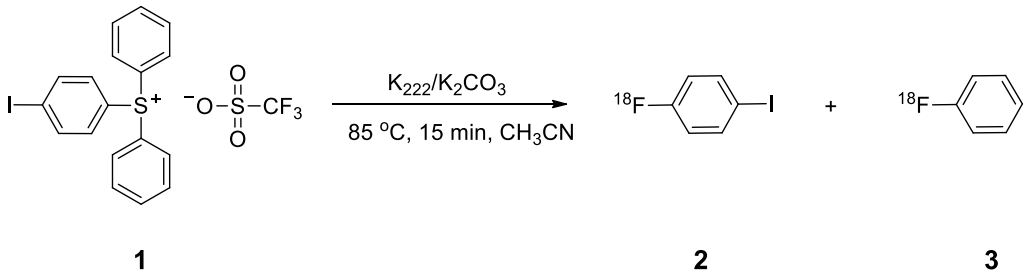

Figure 6.1. Synthetic procedure for the production of [^{18}F]FIB.

The automated synthesis of [^{18}F]FIB opened convenient availability of [^{18}F]FIB as a useful building block in ^{18}F radiochemistry.

[^{18}F]FIB was used for the radiosynthesis of 2-amino-5-(4-[^{18}F]fluorophenyl)pent-4-ynoic acid ([^{18}F]FPhPA) as novel amino acid radiotracer via the Sonogashira cross-coupling reaction with propargylglycine as commercially available starting material, as shown in *Figure 6.2*. Cross-coupling conditions were optimized by screening different reaction parameters. Overall the synthesis was found to proceed best at 55 °C for 30 min, with 1 mg of $Pd(OAc)_2$, CuI, and D/L-

propargylglycine in a 1 mL solution of acetonitrile:water (50:50) containing 25 μL of TEA.

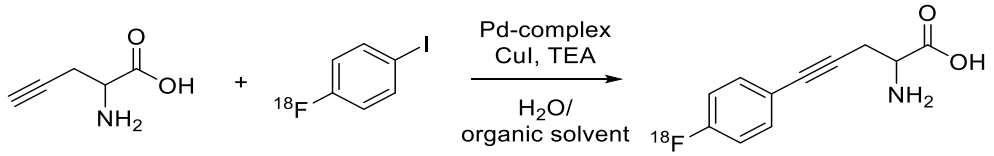

Figure 6.2. Synthetic procedure for the production of [^{18}F]FPhPA.

HPLC purification of the reaction mixture gave decay-corrected radiochemical yields of 29 ± 14% (n=11) with a high radiochemical purity of greater 95% within 56 ± 5 min based on [^{18}F]fluoride. In a typical experiment, 480 MBq of D/L-[^{18}F]FPhPA could be synthesized starting from 1200 MBq of 4-[^{18}F]fluoroiodobenzene. The specific activity of D/L-[^{18}F]FPhPA at the end-of-synthesis was determined from the quality control sample to be greater than 200 GBq/μmol.

Isolated D/L-[^{18}F]FPhPA, D-[^{18}F]FPhPA, and L-[^{18}F]FPhPA were used in *in vivo* and *in vitro* experiments using EMT6 cells. Radiopharmacological profile of L-[^{18}F]FPhPA was compared with clinically relevant amino acid radiotracer [^{18}F]FET. L-[^{18}F]FPhPA was shown to be transported predominately by the amino acid transporters LAT1 and ASCT2, with a comparable uptake in EMT6 tumors to that of [^{18}F]FET.

Amino acid radiotracer 2-amino-5-(4-[^{18}F]fluorophenyl)pent-4-ynoic acid ([^{18}F]FPhPA) displayed interesting radiopharmacological profile that warrants further investigation as PET radiotracer for molecular imaging of amino acid metabolism.

We also explored the Sonogashira cross-coupling reaction for the synthesis of ^{18}F-labelled peptides for the first time. A alkyne-containing bombesin derivative (pBBN) was used as coupling partner for Sonogashira reaction with [^{18}F]FIB, as shown in *Figure 6.3.* Synthesis of the desired product [^{18}F]FBpBBN was optimized through screening of different reaction conditions. Best results were obtained when the reaction was performed at 25 °C for 10 min, with 0.1 mg of $Pd(OAc)_2$ containing 1 mg TPPTS, and 1.0 mg CuI in a 1 mL solution of PBS buffer:acetonitrile (90:10) containing 50μL of TEA. HPLC purification of the reaction mixture gave the desired peptide in decay-corrected radiochemical yields of 71 ± 4% (n=3) with a high radiochemical purity of greater 95% within 30 ± 5 min based on [^{18}F]FIB. In a typical experiment, 27.3 MBq of [^{18}F]FBpBBN could be synthesized with specific activity of around 300 GBq/μmol.

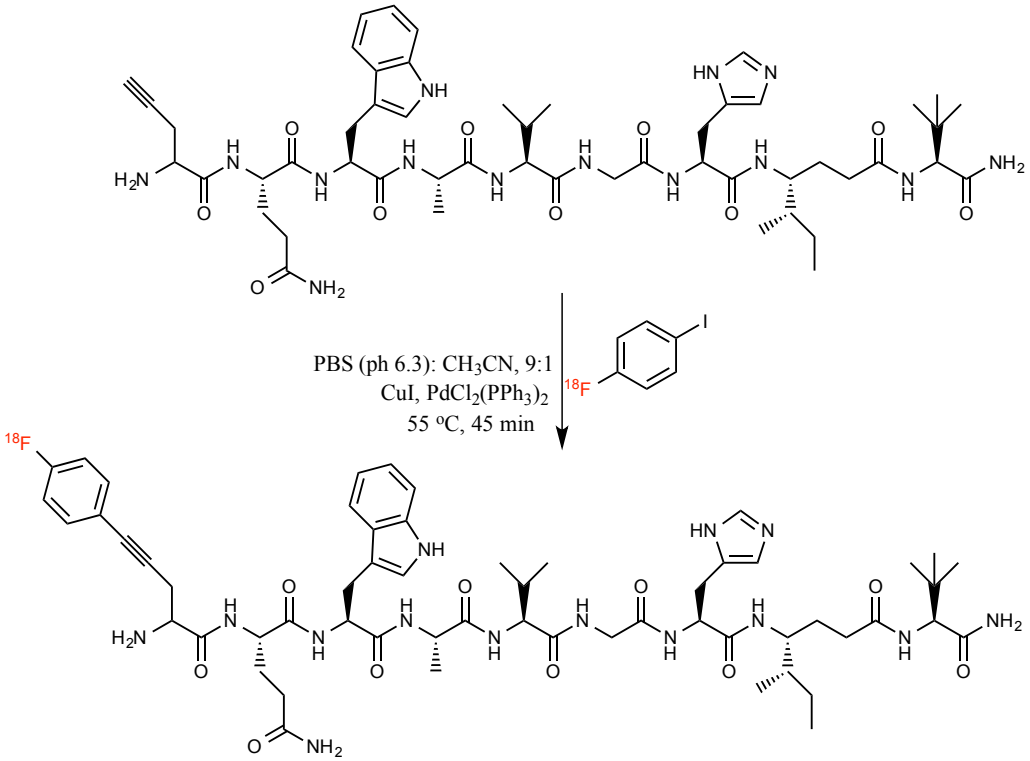

Figure 6.3. Synthetic procedure for the production of [^{18}F]FBpBBN.

To the best of our knowledge, this is the first example of a Sonogashira reaction to prepare ^{18}F-labelled peptides. The reaction proceeded under mild conditions compatible with the delicate structure of peptides. The described synthesis of ^{18}F-labelled peptides based on the Sonogashira cross-coupling reaction with [^{18}F]FIB allows for site-specific incorporation of fluorine-18 into peptides under mild conditions. Employed reaction conditions enable synthesis of radiolabelled peptides in automated synthesis units.

6.2. Outlook

The described Sonogashira cross-coupling reaction with [^{18}F]FIB is a reliable, robust, high yielding innovative radiolabelling technique for the convenient and site-specific incorporation of 4-[^{18}F]fluorophenyl groups into a given molecule. The mild reaction conditions are applicable to other biomacromolecules like oligonucleotides and proteins.

The favorable characteristics of the Sonogashira cross-coupling reaction with [^{18}F]FIB make this reaction an important and versatile novel labelling tool to further expand the arsenal of PET radiotracers.

6.3. References

1 Linjing, M., Fischer, C. R., Holland, J. P., Becaud, J., Schubiger, P. A., Schibli, R., Ametamey, S. M., Graham, K., Stellfeld, T., Dinkelborg, L. M., Lehnmann, L. (2012) ^{18}F-Radiolabeling of aromatic compounds using triarylsulfonium salts. *Eur. J. Org. Chem*. *5*, 889–892.

Appendix

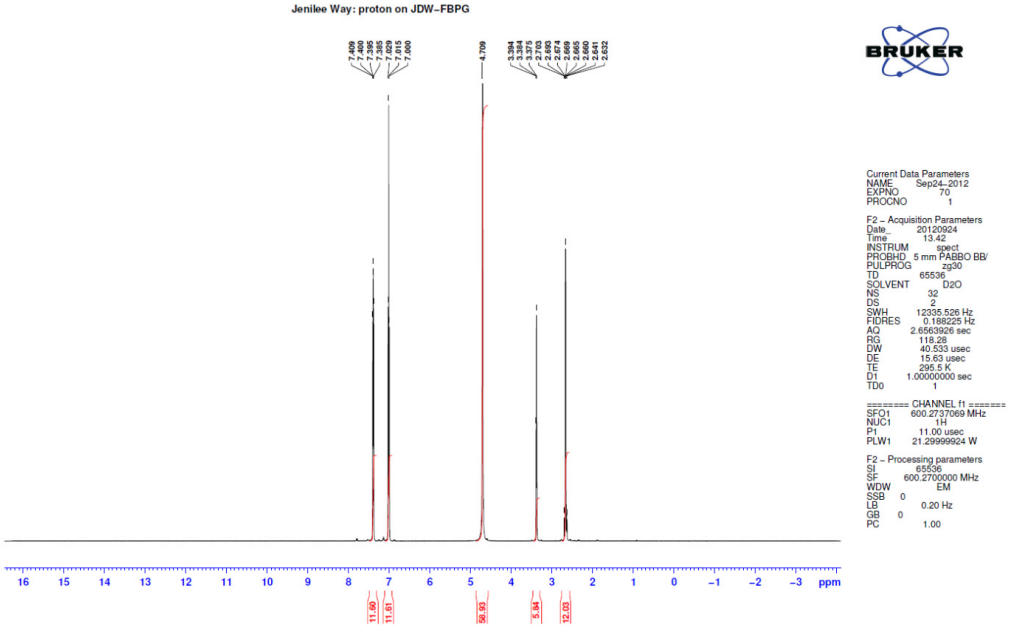

Figure 7.1. ^{1}H-NMR of [^{19}F]FPhPA.

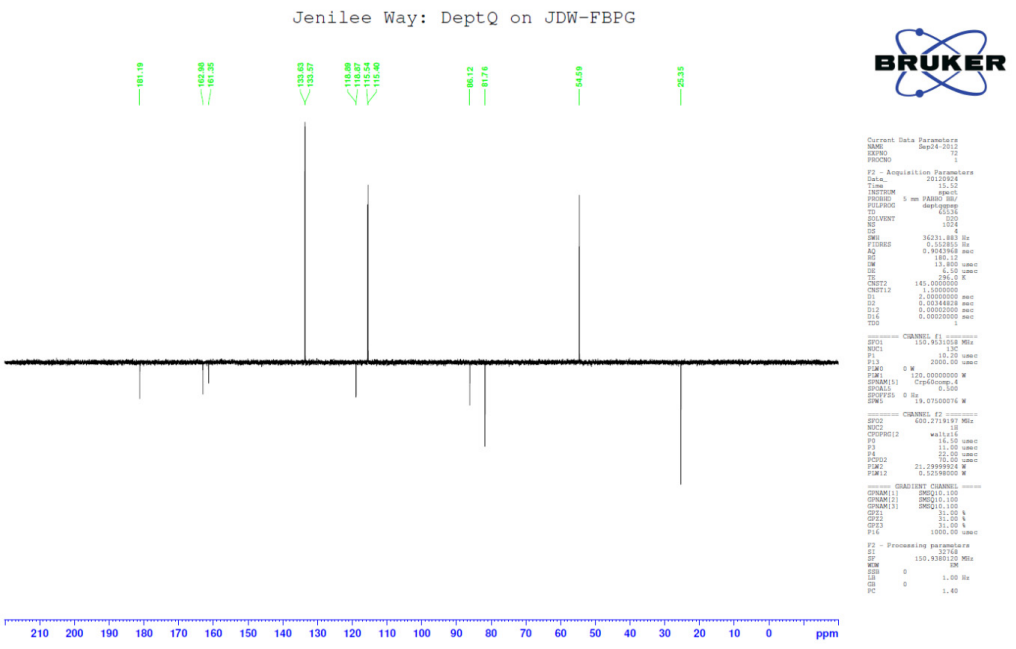

Figure 7.2. ^{13}*C-NMR of [*^{19}*F]FPhPA.*

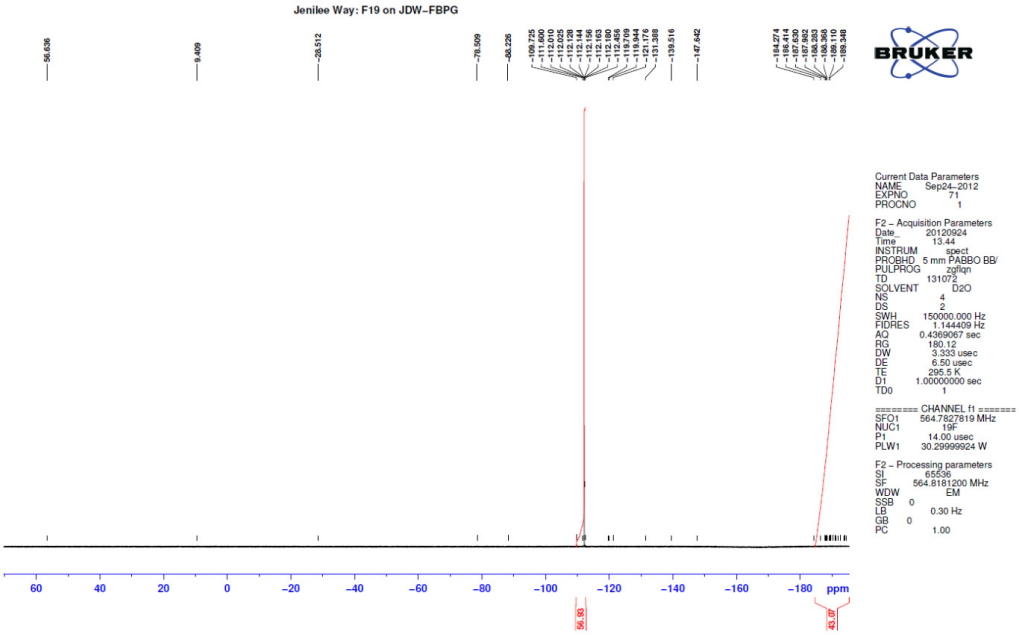

Figure 7.3. ^{19}*F-NMR of [*^{19}*F]FPhPA.*

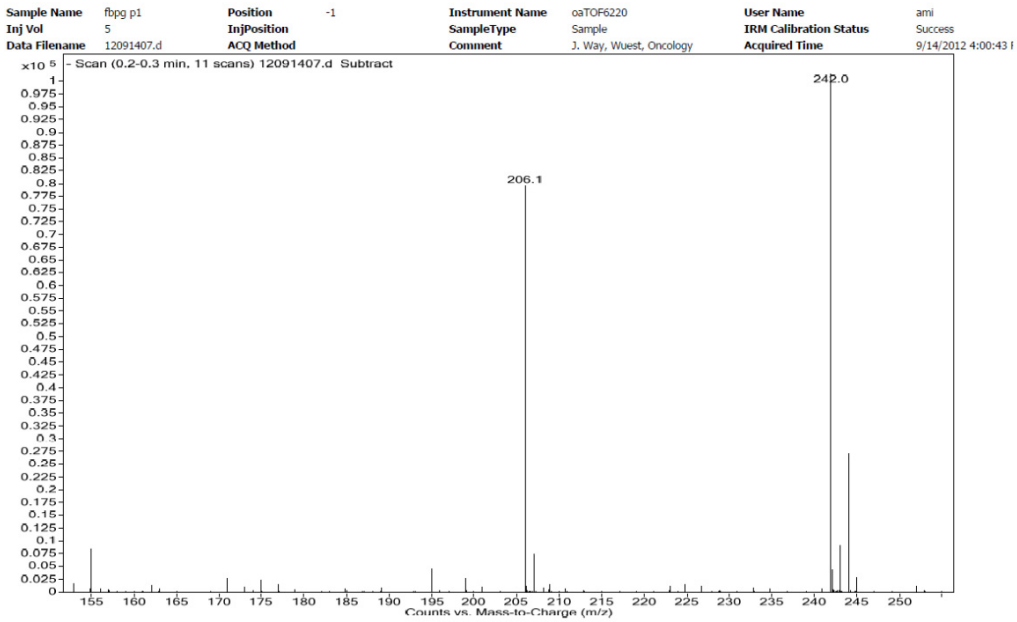

Figure 7.4. LR-MS of [^{19}F]FPhPA cold reference compound.

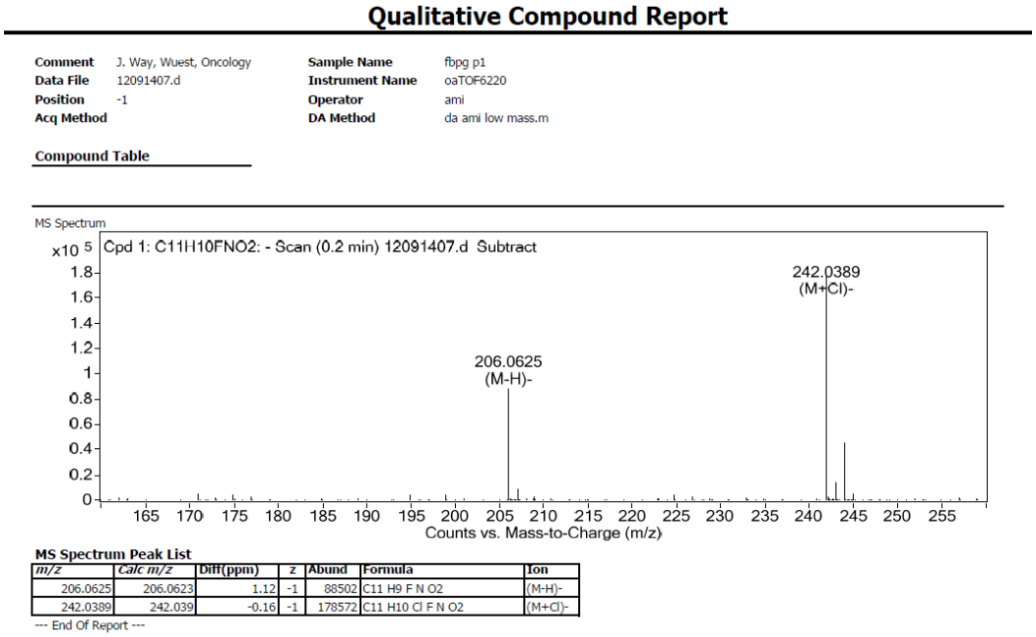

Figure 7.5. HR-MS of [^{19}F]FPhPA cold reference compound.

Qualitative Compound Report

Comment	J. Way, Wuest, Oncology	**Sample Name**	fbpbbno 413 p2
Data File	13040316.d	**Instrument Name**	oaTOF6220
Position	-1	**Operator**	ami
Acq Method		**DA Method**	da ami low mass.m

Compound Table

MS Spectrum

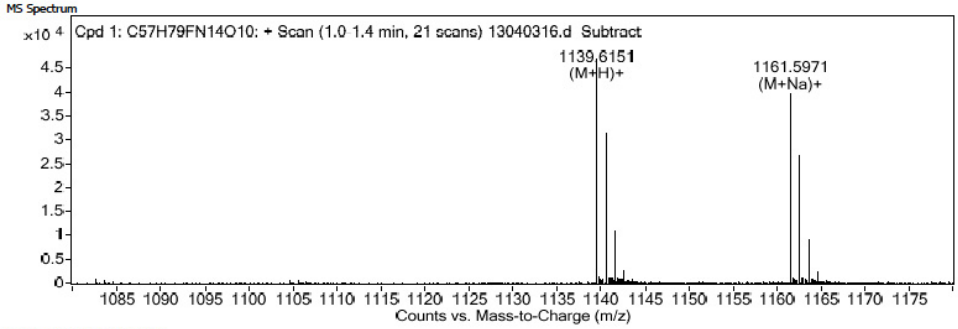

MS Spectrum Peak List

m/z	*Calc m/z*	Diff(ppm)	z	Abund	Formula	Ion
1139.6151	1139.616	-0.78		46917	C57 H80 F N14 O10	(M+H)+
1161.5971	1161.598	-0.75	1	39775	C57 H79 F N14 Na O10	(M+Na)+

--- End Of Report ---

Figure 7.6. HR-MS of [^{19}F]FBpBBN cold reference compound.

Sample Name	cb 58.3	**Position**	-1	**Instrument Name**	oaTOF6220	**User Name**	ami
Inj Vol	5	**InjPosition**		**SampleType**	Sample	**IRM Calibration Status**	Success
Data Filename	13062409.d	**ACQ Method**		**Comment**	C. Bergman, Wuest, Oncology	**Acquired Time**	6/24/2013 5:24

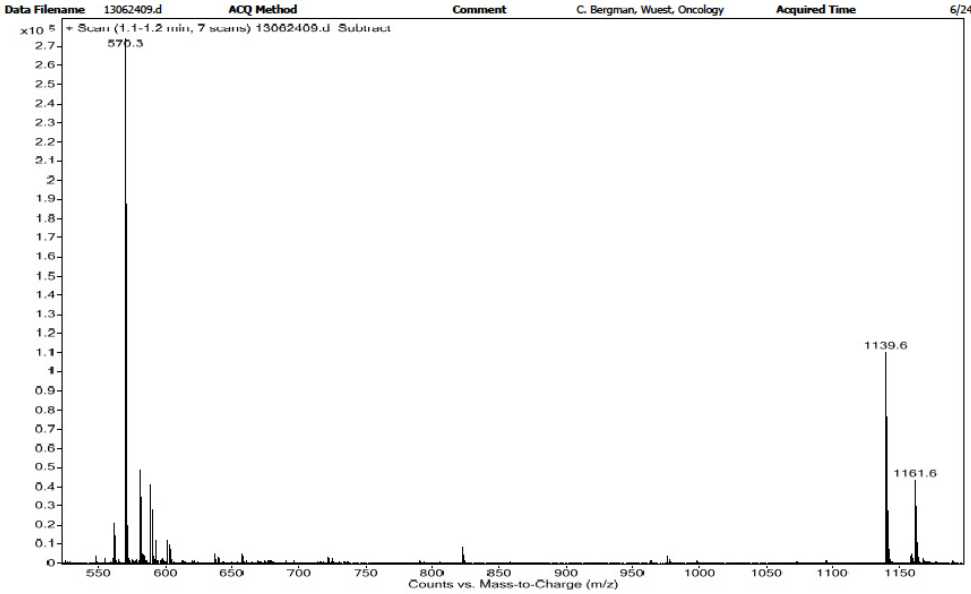

Figure 7.7. LR-MS of [^{19}F]FBpBBN cold reference compound.

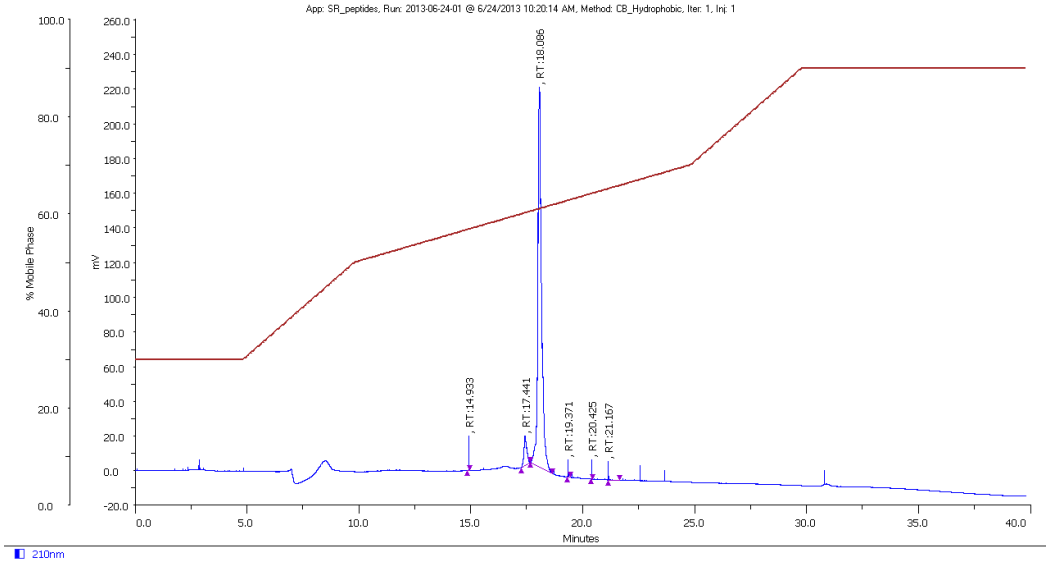

Figure 7.8. HPLC purification of [^{19}F]FBpBBN cold reference compound.

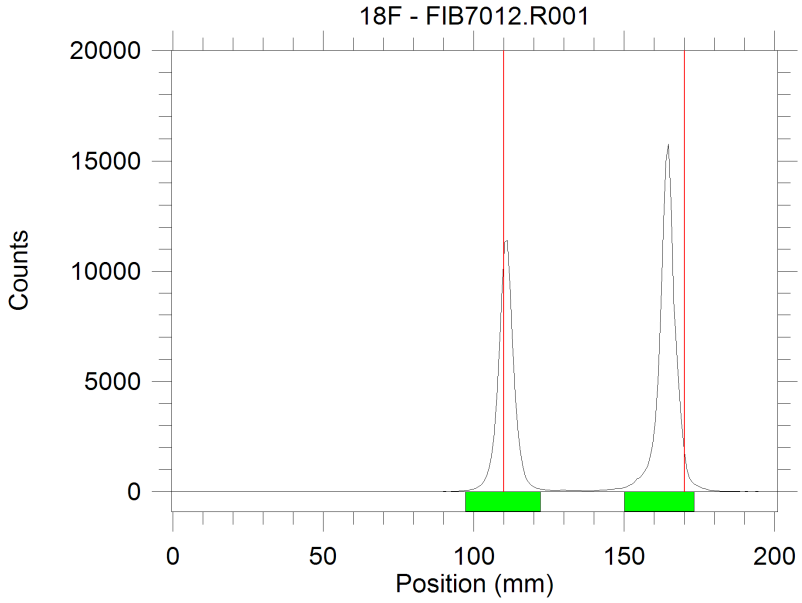

Figure 7.9. TLC analysis for the synthesis of 4-[^{18}F]fluoroiodobenzene.

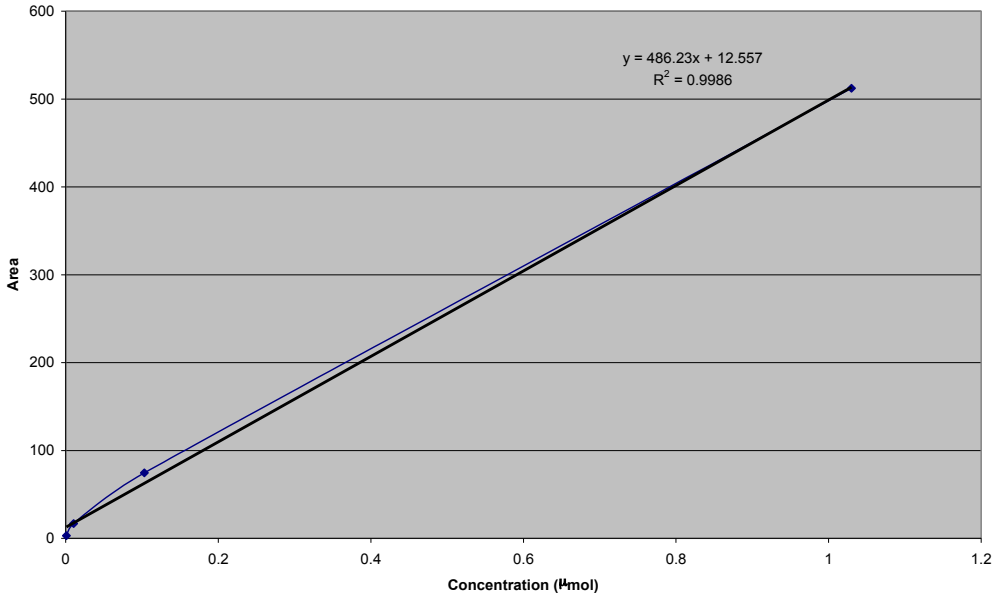

Figure 7.10. Specific activity curve for [^{19}F]fluoroiodobenzene.

Run ID	Activity (GBq)	Area	Calculated Concentration from Graph	Specific Activity (GBq/µmol)
08-01-2013-01	1	34	0.045	22
10-01-2013-01	1	25	0.026	38
18-01-2013-01	1	36	0.049	20
22-01-2013-01	1	22	0.019	54
25-01-2013-01	4	39	0.054	74
20-02-2013-01	1.7	31	0.037	46
12-03-2013-02	1.5	41	0.058	26
21-05-2013-01	2.8	54	0.086	32

Table 7.1. : Area under the UV trace for various [^{18}F]FIB production syntheses.

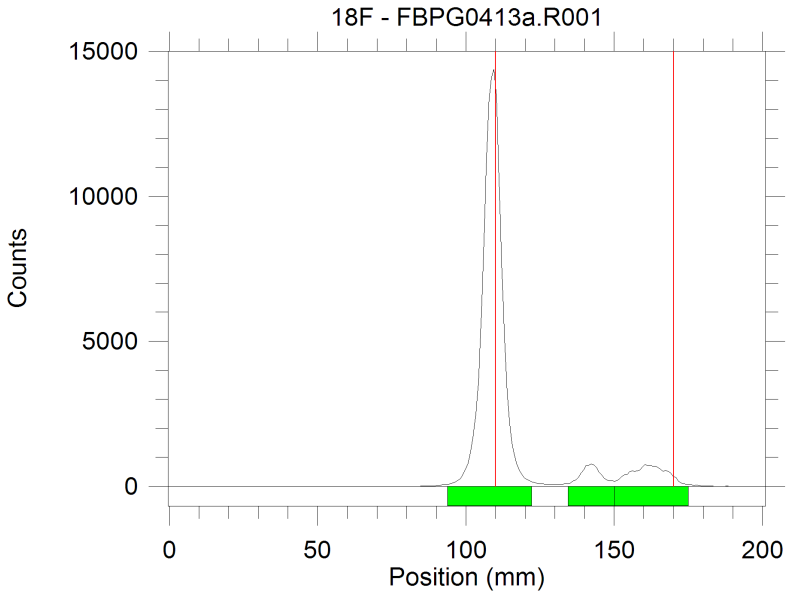

Figure 7.11. TLC analysis for the synthesis of 4-[^{18}F]FPhPA.

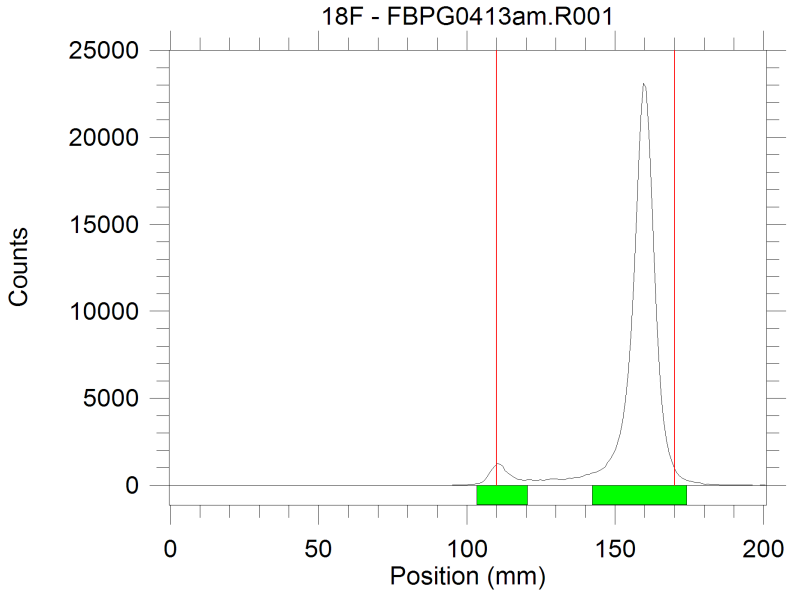

Figure 7.12. Secondary TLC analysis for the synthesis of 4-[^{18}F]FPhPA.

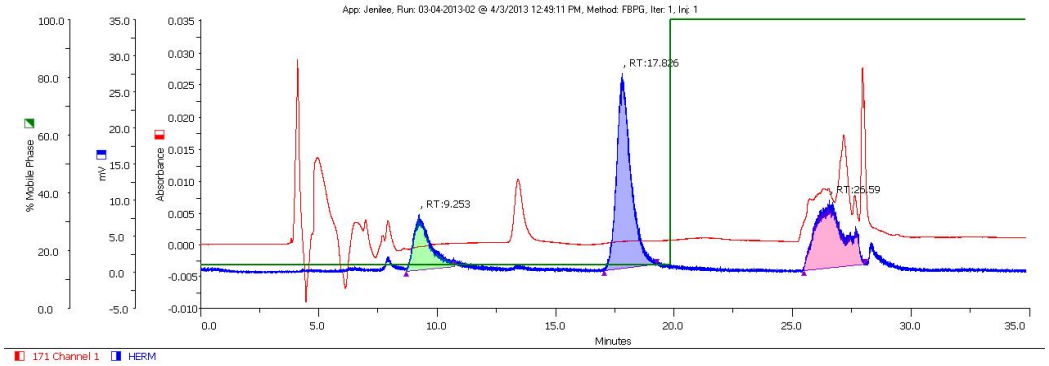

Figure 7.13. HPLC purification of [^{18}F]FPhPA.

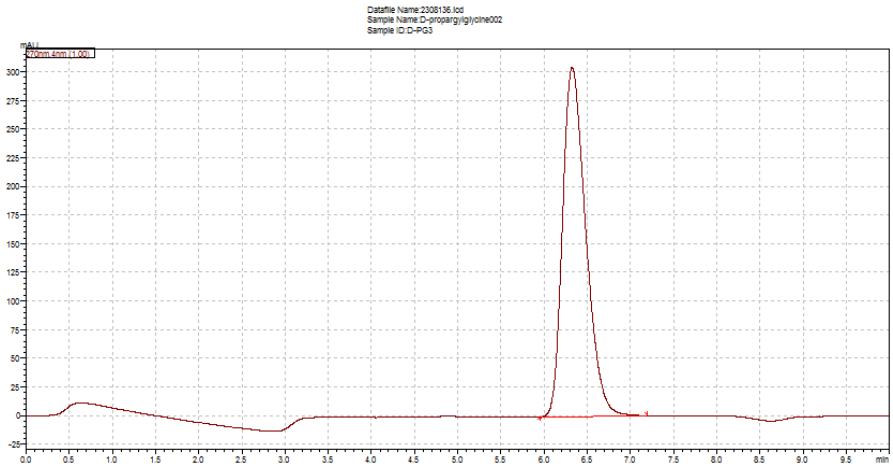

Figure 7.14.Chiral separation of D-propargylglycine.

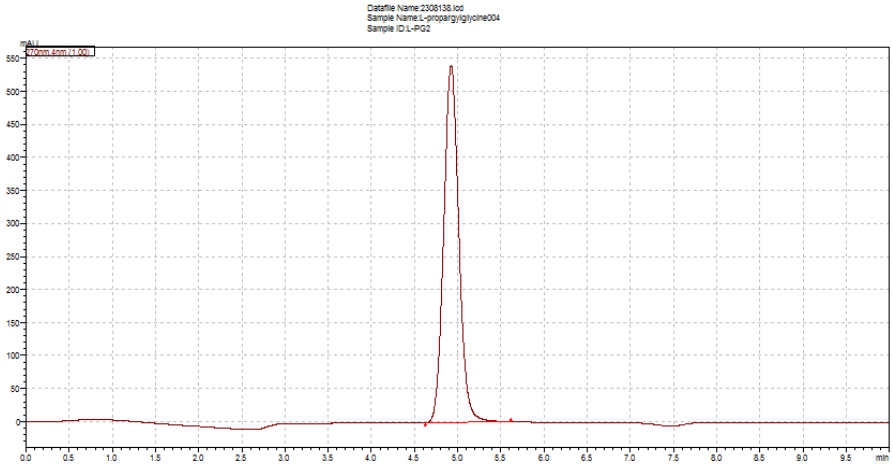

Figure 7.15. Chiral separation of L-propargylglycine.

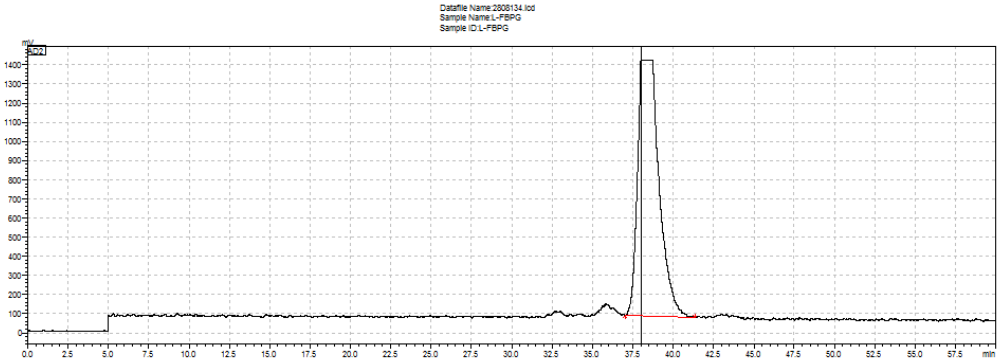

Figure 7.16. Chiral separation of L-[^{18}F]FPhPA.

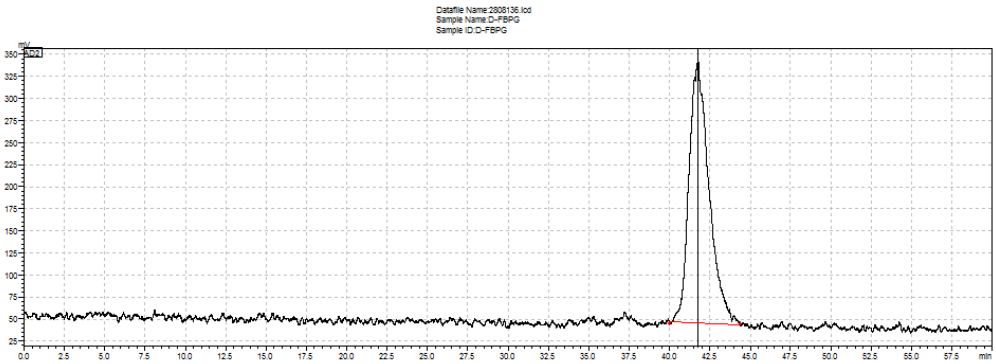

Figure 7.17. Chiral separation of D-[^{18}F]FPhPA.

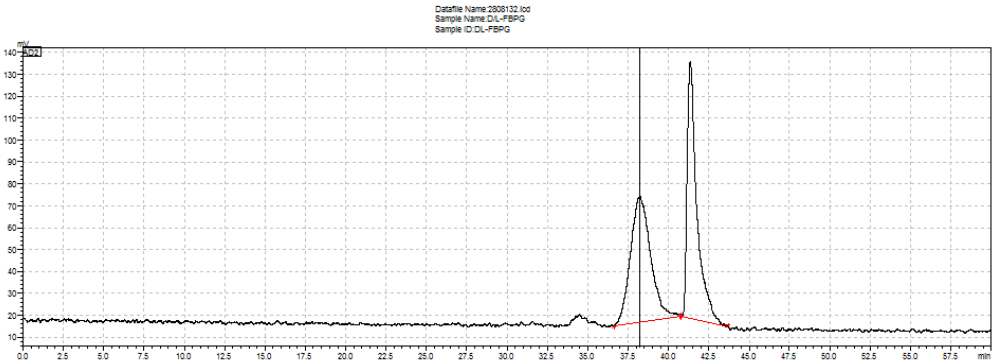

Figure 7.18. Chiral separation of D/L-[^{18}F]FPhPA.

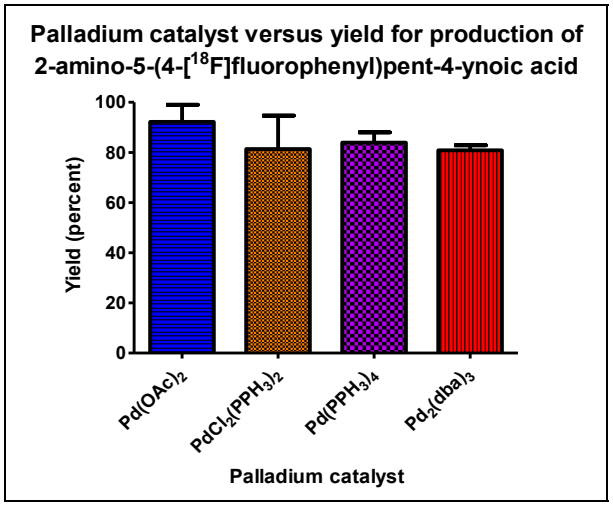

Figure 7.19. Palladium type versus yield for the synthesis of [^{18}F]FPhPA (n=3).

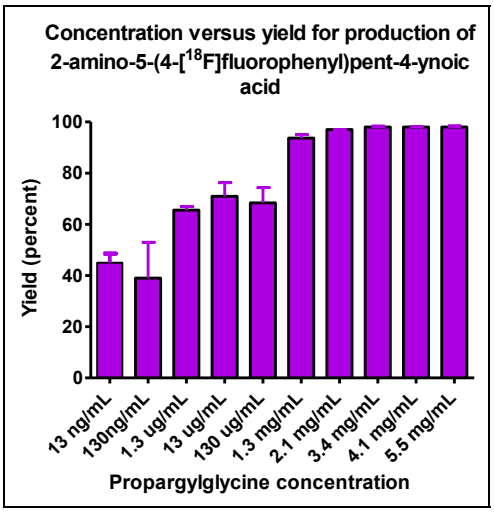

Figure 7.20. Propargylglycine concentration type versus yield for the synthesis of [^{18}F]FPhPA (n=3).

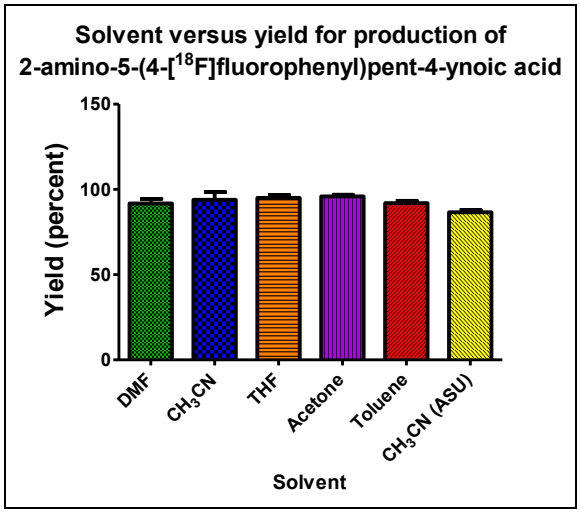

Figure 7.21. Solvent versus yield for the synthesis of [^{18}F]FPhPA (n=3).

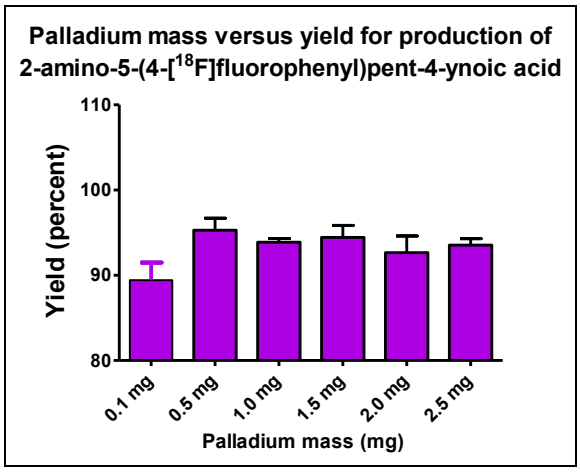

Figure 7.22. Palladium Mass versus yield for the synthesis of [^{18}F]FPhPA (n=3).

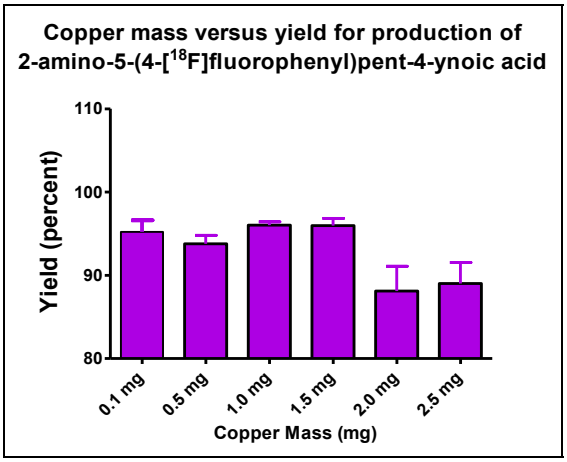

Figure 7.23. Copper Mass versus yield for the synthesis of [^{18}F]FPhPA (n=3).

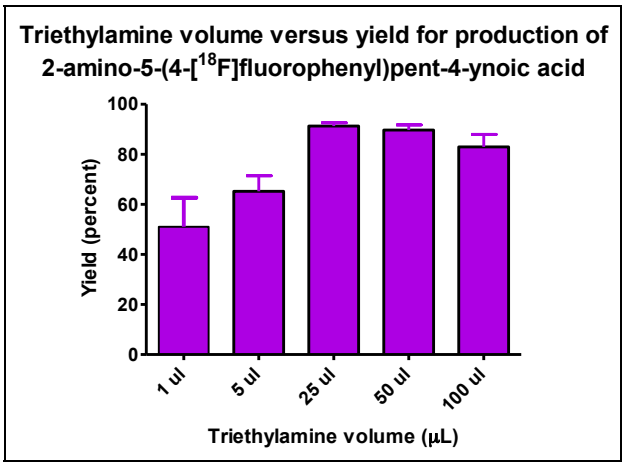

Figure 7.24. Triethylamine volume versus yield for the synthesis of [^{18}F]FPhPA (n=3).

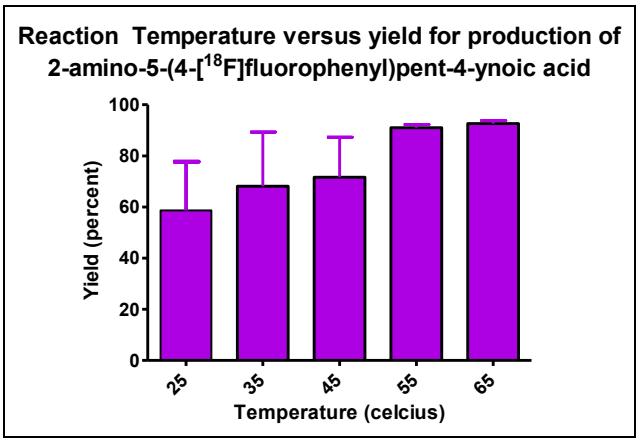

Figure 7.25. Temperature versus yield for the synthesis of [^{18}F]FPhPA (n=3).

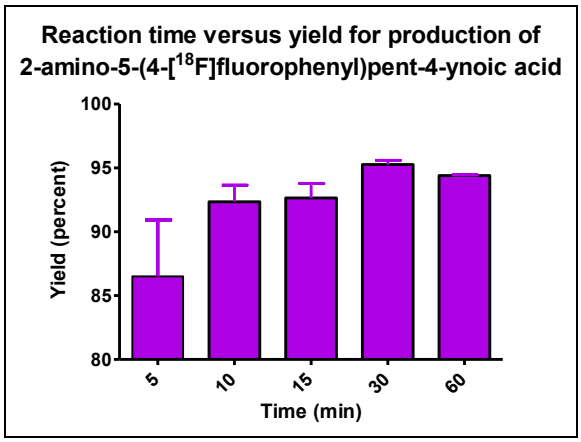

Figure 7.26. Time versus yield for the synthesis of [^{18}F]FPhPA (n=3).

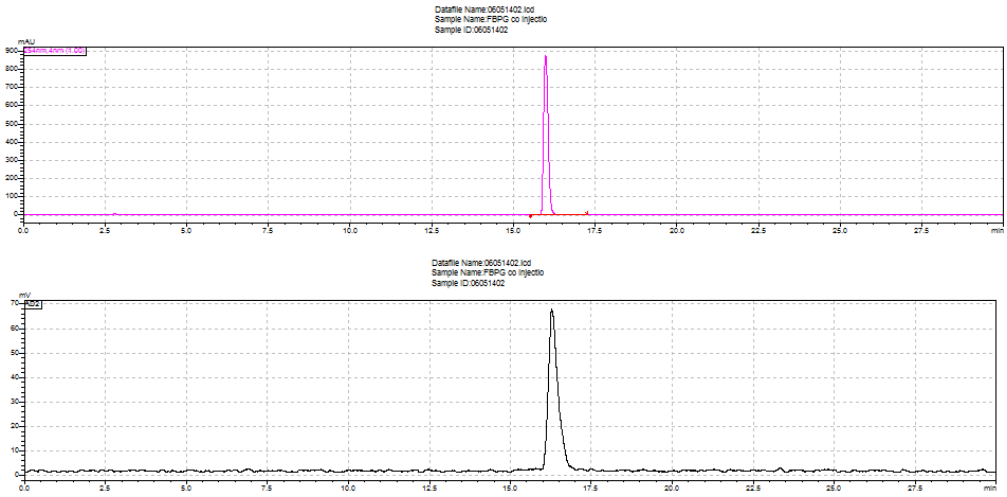

Figure 7.27. HPLC radiotrace of [^{18}F]FPhPA.

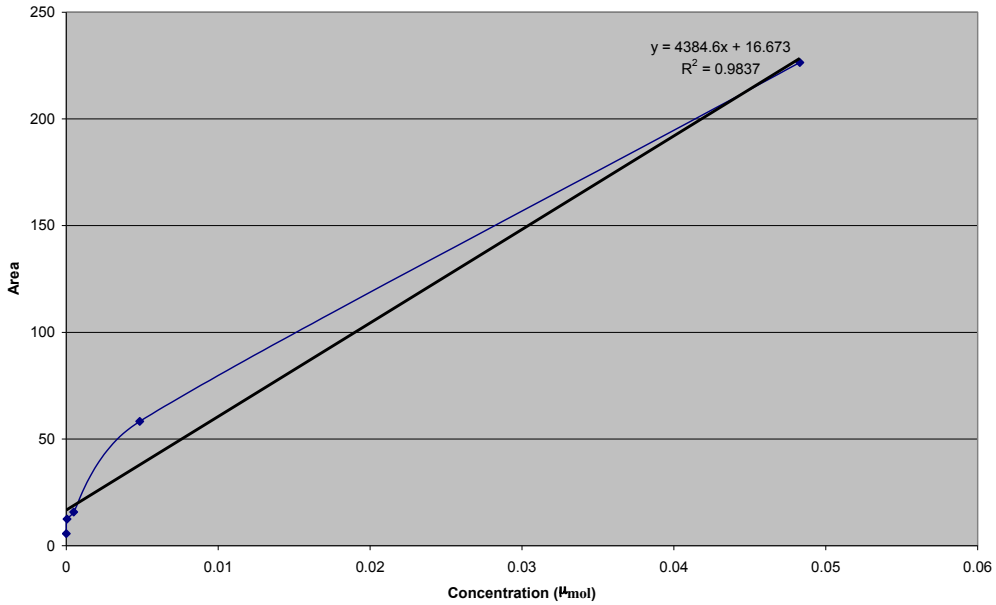

Figure 7.28. Specific activity curve of [^{18}F]FPhPA.

Run ID	Activity (GBq)	Area	Specific Activity (GBq/mmol)
28-08-2013-05	0.01197	0	2479
28-08-2013-06	0.00686	0	1421
28-08-2013-07	0.0101	0	2092

Table 7.2. *Area under the UV trace for various [^{18}F]FPhPA production syntheses.*

.

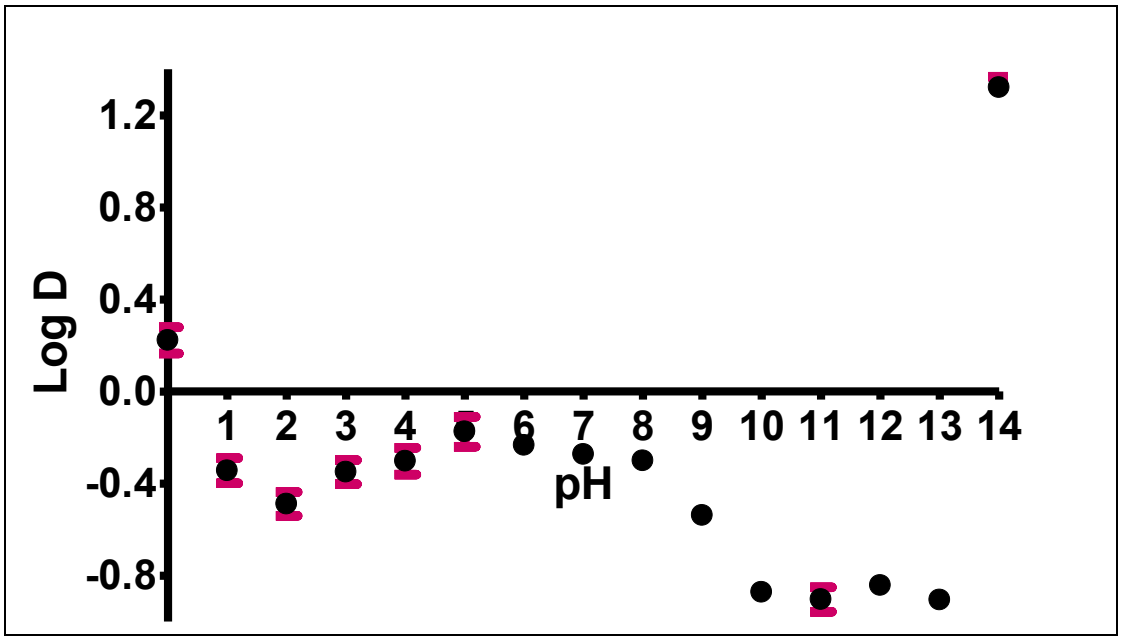

Figure 7.29. LogD of [^{18}F]FPhPA over the pH range of 0 to 14.

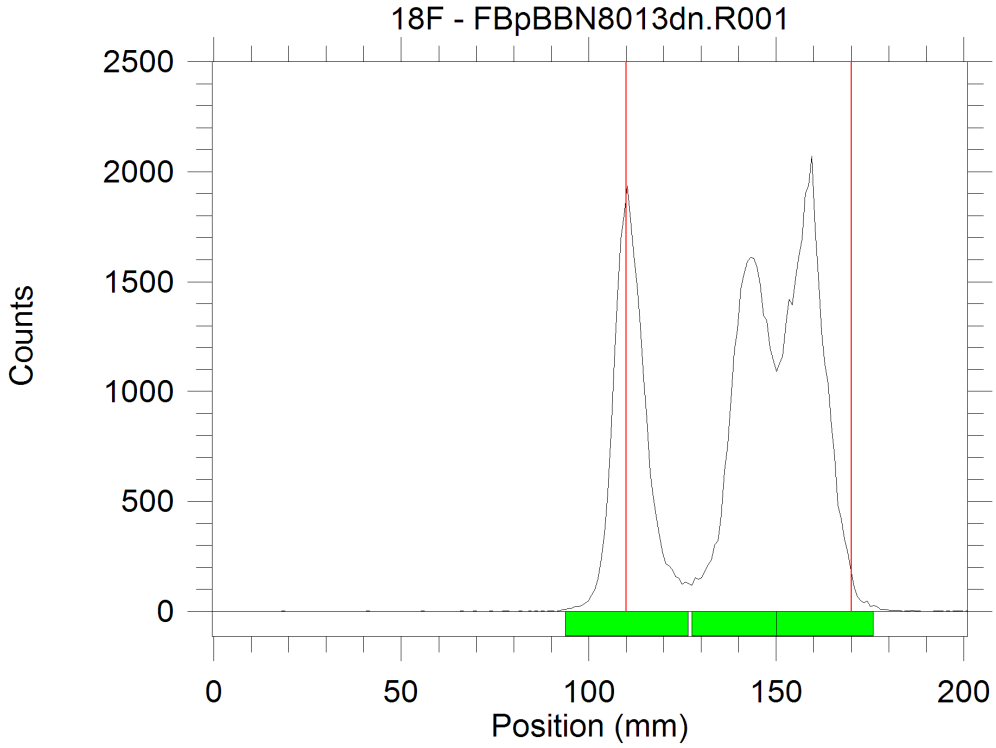

Figure 7.30: TLC analysis for the synthesis of 4-[^{18}F]FBpBBN.

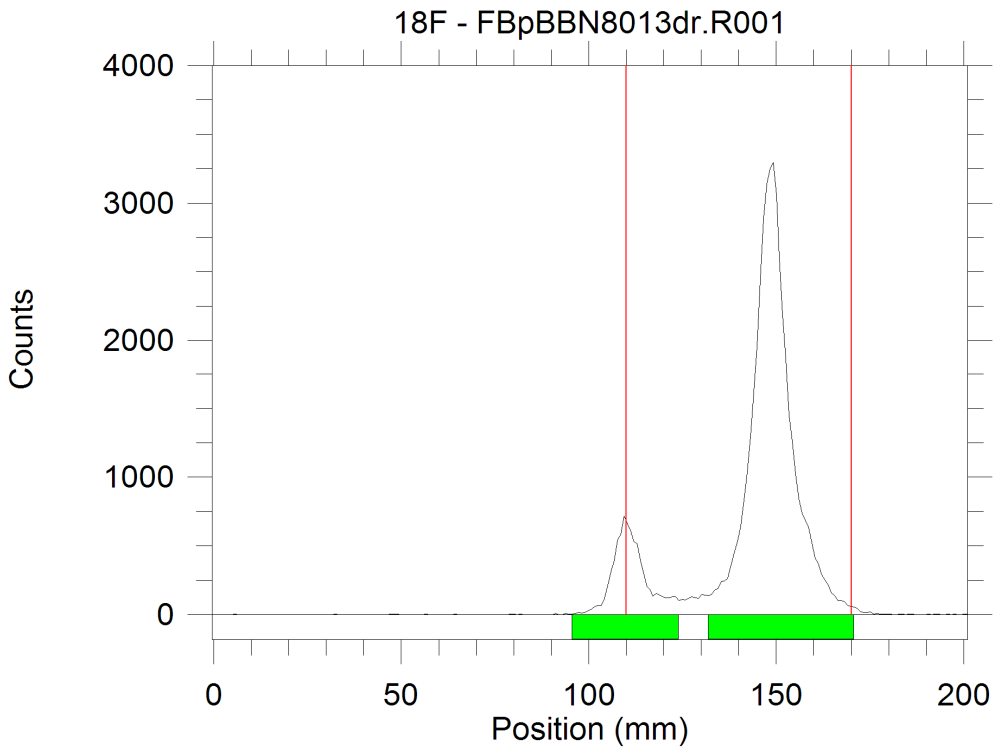

Figure 7.31. Secondary TLC analysis for the synthesis of 4-[^{18}F]FBpBBN.

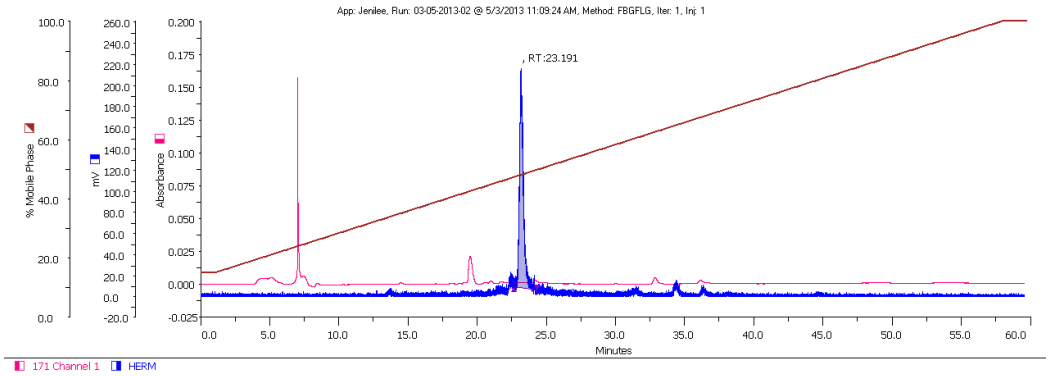

Figure 7.32: HPLC purification of [^{18}F]FBpBBN.

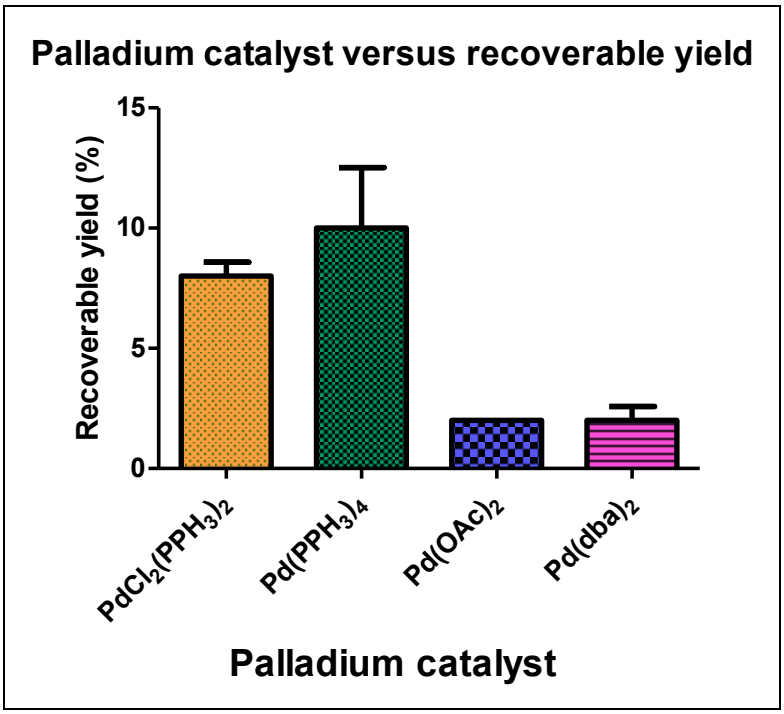

Figure 7.33. Recoverable radiochemical yield versus palladium catalyst for the synthesis of [^{18}F]FBpBBN (n=3).

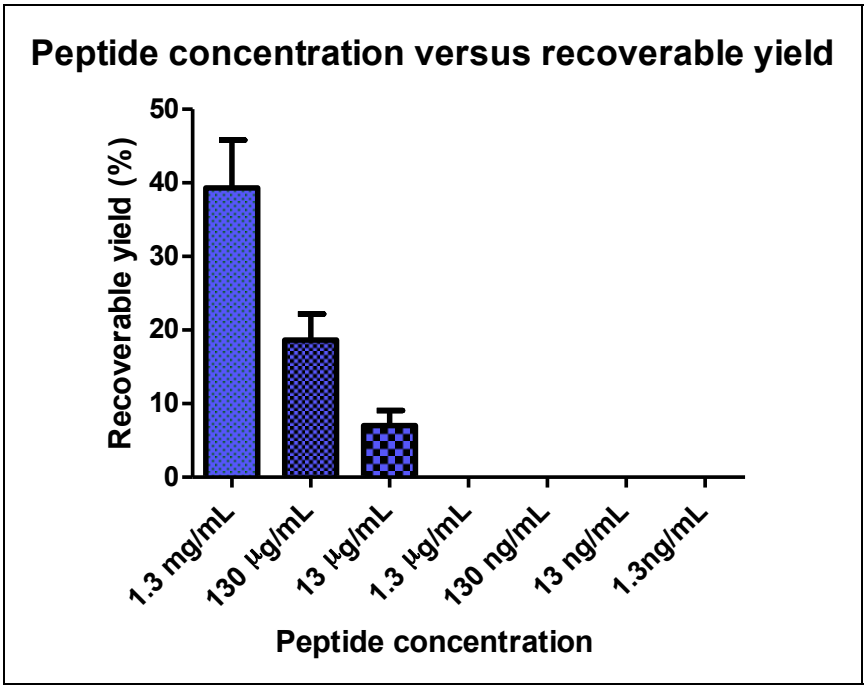

Figure 7.34. Recoverable rcy. versus peptide concentration for the synthesis of [^{18}F]FBpBBN (n=3).

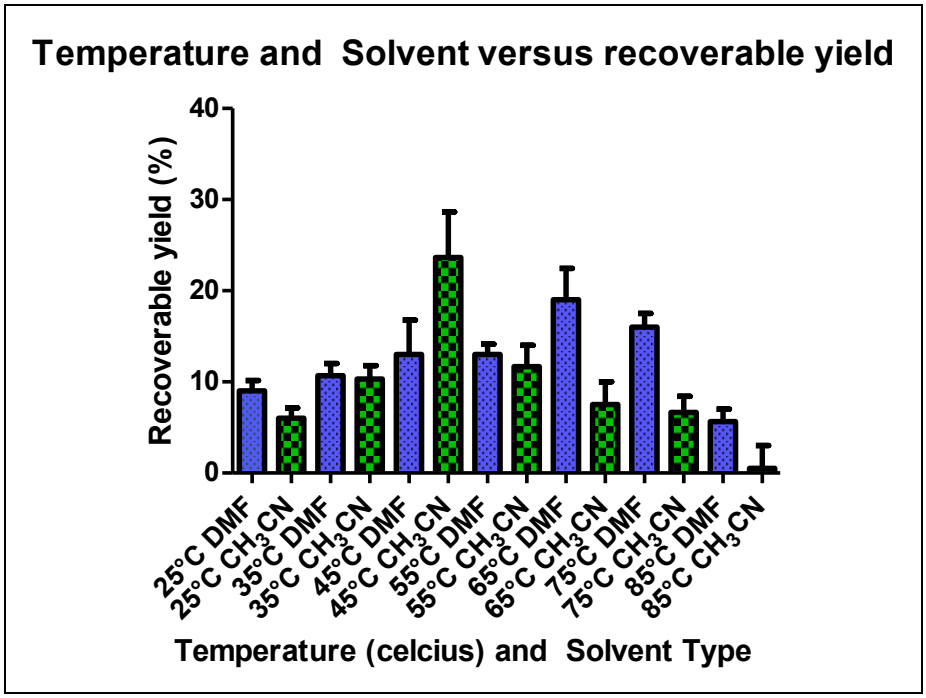

Figure 7.35. Recoverable rcy. versus temperature and solvent for the synthesis of [^{18}F]FBpBBN (n=3).

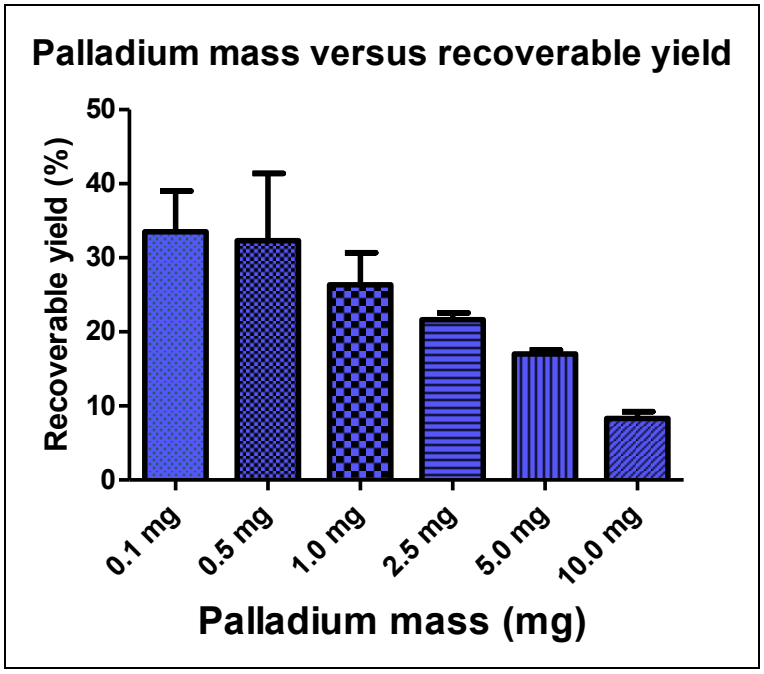

Figure 7.36. Recoverable rcy. versus palladium catalyst mass for the synthesis of [^{18}F]FBpBBN (n=3).

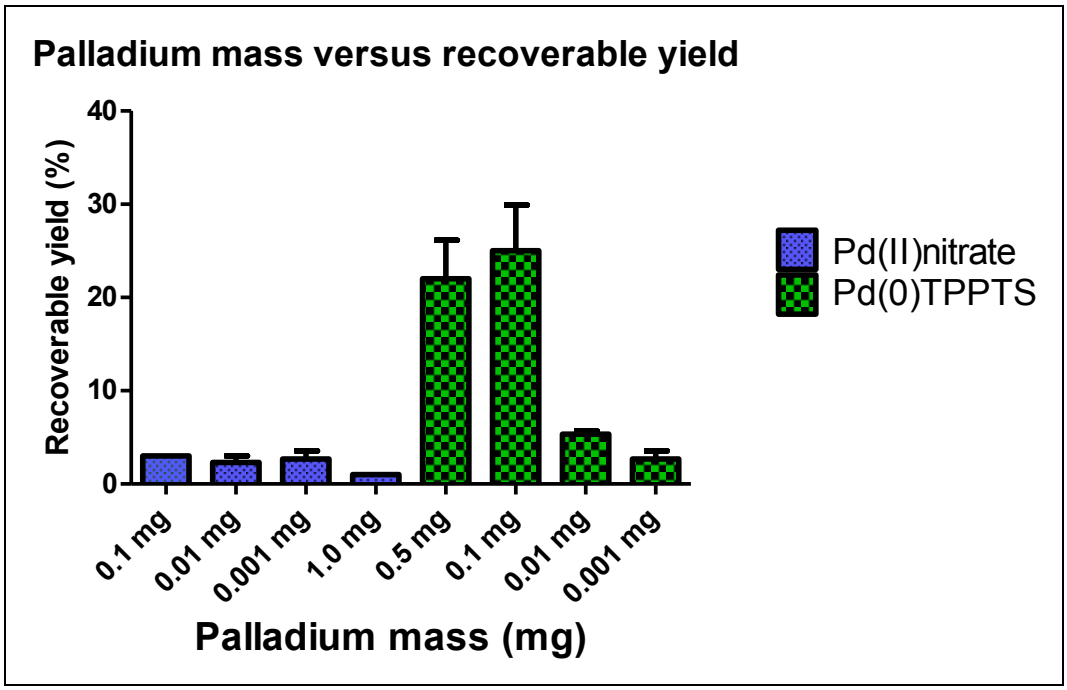

Figure 7.37. Recoverable rcy. versus water soluble palladium catalyst for the synthesis of [^{18}F]FBpBBN (n=3).

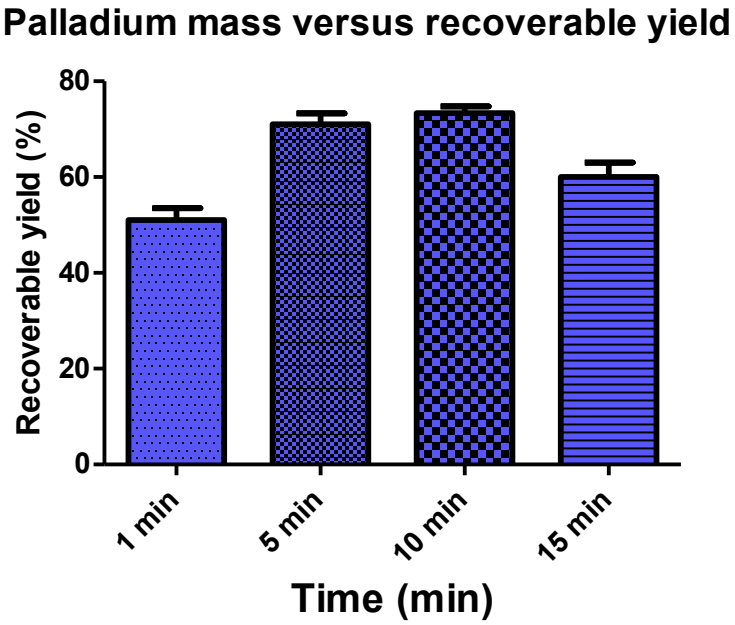

Figure 7.38. Recoverable rcy. versus time of reaction for the synthesis of [^{18}F]FBpBBN (n=3).

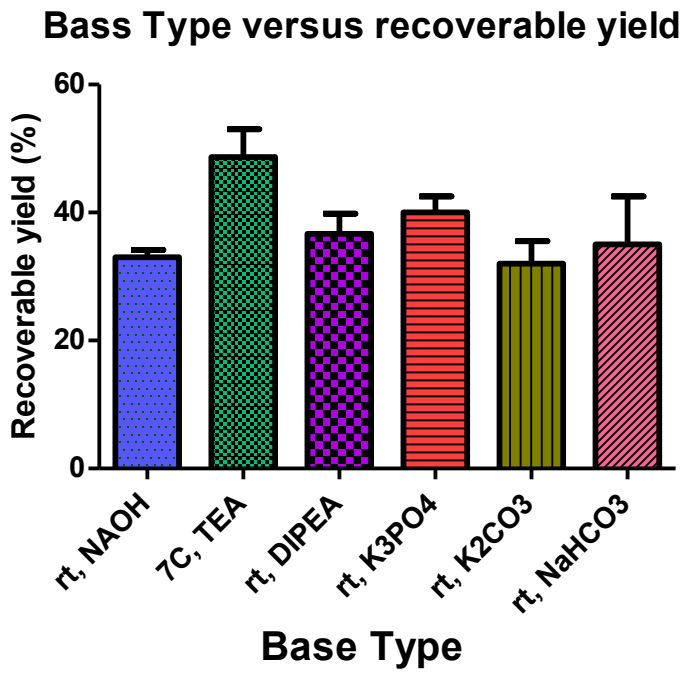

Figure 7.39. Recoverable rcy. versus temperature and base of reaction for the synthesis of [^{18}F]FBpBBN (n=3).

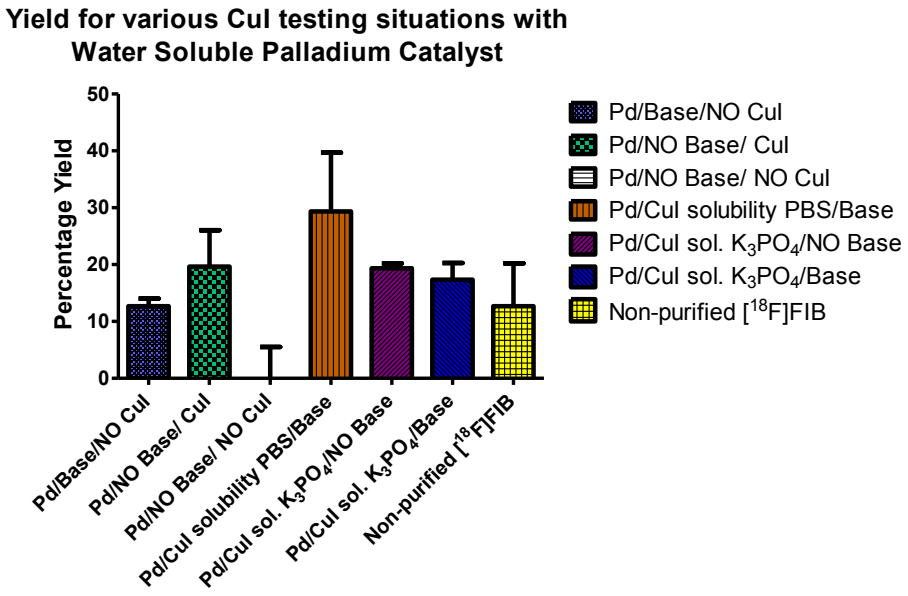

Figure 7.40. Rcy. versus CuI, Pd and base of reaction for the synthesis of [^{18}F]FBpBBN (n=3).

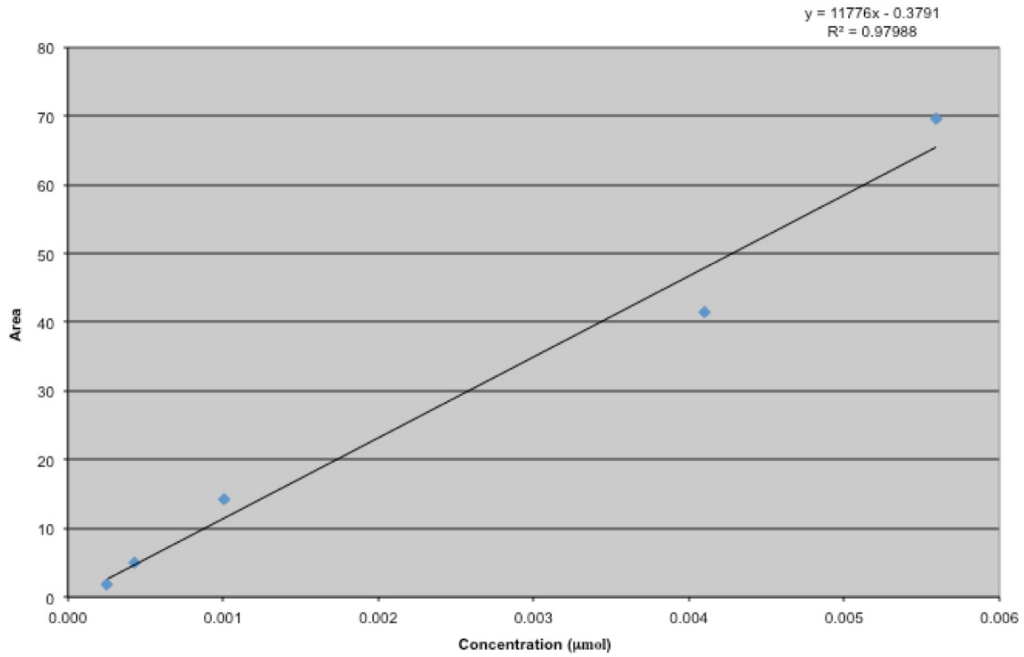

Figure 7.41. Specific activity curve of [^{18}F]FBpBBN.

Run ID	Activity (GBq)	Area	Specific Activity (GBq/mmol)
11-03-2014-03	0.00316	0	98
10-03-2014-02	0.00774	0	240
17-03-2014-02	0.0273	0	848

Table 7.3. *Area under the UV trace for various [^{18}F]FBpBBN production syntheses.*

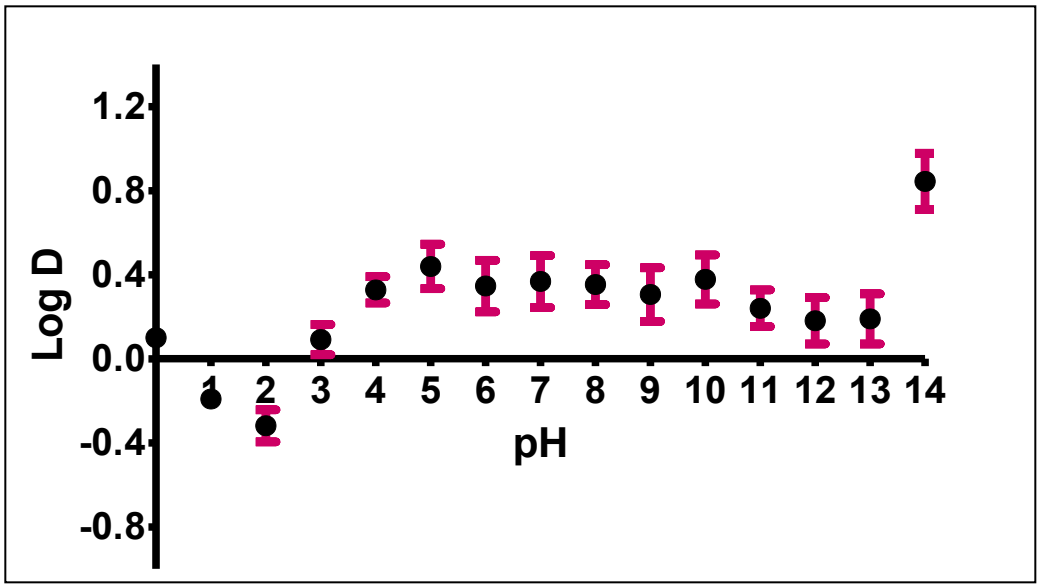

Figure 7.42. LogD of [^{18}F]FBpBBN over the pH range of 0 to 14.

Bibliography

Alauddin, M. M. (2012) Positron emission tomography (PET) imaging with ^{18}F-based radiotracers. *Am. J. Nucl. Med. Mol. Imaging. 2,* 55-76.

Allain-Barbier, L.; Lasne, M-C.; Perrio-Huard C.; Mureau, B.; Barre, L. (1998) Synthesis of 4-[^{18}F]fluorophenyl -alkenes and -arenes via palladium-catalyzed coupling of 4-[^{18}F]fluoroiodobenzene with vinyl and aryl tin reagents. *Acta Chem. Scand. 52*, 480-489.

Amatore, C., Blart, E., Genet, J. P., Jutand, A., Lemaire-Audoire, S., Savignac, M. (1995) New synthetic applications of water soluble acetate Pd/TPPTS catalysts generated *in situ*. Evidence of a true Pd(0) Species intermediate. *J. Org. Chem. 60,* 6829-6839.

Anagnostopoulos, C., Georgakopoulos, A., Pianou, N., Nekolla, S. G. (2013) Assessment of myocardial perfusion and viability by positron emission tomography. *Int. J. Cardiol. 167*, 1737-1749.

Basuli, F.; Wu, H.; Griffiths, G. (2011) Synthesis of meta-[^{18}F]fluorobenzadehyde and meta-[^{18}F]fluobenzylbromide from phenyl(3-Formylphenyl)iodonium salt precursors. *J. Labelled Compd. Radiopharm. 54*, 224-228.

Berridge, M.; Crouzel, C.; Comar, D. (1982) No-carrier-added ^{18}F-fluoride in organic solvents production and labelling results. *J. Labelled Compd. Radiopharm. 19*, 1639-1640.

Bierry, G., Dietemann, JL. (2013) Imaging evaluation of inflammation in the musculoskeletal system: current concepts and perspectives. *Skeletal Radiol*. *42*, 1347-1359.

Blodgett, T. M., Meltzer, C. C., Townsend, D. W. (2007) PET/CT: form and function. *Radiology 242*, 360-385.

Bong, D. T., Ghadiri, M. R. (2001) Chemoselctive Pd(0)-catalyzed peptide coupling in water. *Org. Lett. 3,* 2509-2511.

Bouvet, V.; Wuest, M.; Tam, P. H.; Wang, M.; Wuest, F. (2012) Microfluidic technology: an economical and versatile approach for the synthesis of *O*-(2-[^{18}F]fluoroethyl)-L-tyrosine ([^{18}F]FET). *Bioorg. Med. Chem. Lett. 22*, 2291-2295.

Brinkman, G. A. (1981) Reactions of radioactive recoil atoms with arenes. *Chem. Rev. 81,* 270.

Bröer, S. (2009) The role of the neutral amino acid transporter B0AT1 (SLC6A19) in Hartnup disorder and protein nutrition. *IUBMB Life. 61*, 591-599.

Campbell-Verduyn, L. S., Mirfeizi, L., Schoonen, A. K., Dierchx, R. A., Elsinga, P. H., Feringa, B. L. (2011) Strain-promoted copper-free ”click” chemistry for ^{18}F radiolabelling of bombesin. *Angew. Chem. Int. Ed. 50,* 11117-11120.

Cardinale, J.; Ermert, J.; Kuegler, F.; Fabian, H.; Andreas, C.; Heinz, H. (2011) P-390 studies on Pd-catalysed nucleophilic ^{18}F-fluorination of aryl triflates. *J. Labelled Compd. Radiopharm. 54*, S479.

Caroll, M. A.; Nairne, J.; Smith, G.; Widdowson, D. A. (2007) Radical scavengers: A practical solution to the reproducibility issue in the fluoridation of diaryliodonium salts. *J. Fluor. Chem. 128*, 127–132.

Carroll, M. A.; Martín-Santamaría, S.; Pike, V. W.; Rzepa, H. S.; Widdowson, D. A. (1999) An ab initio and MNDO-d SCF-MO computational study of stereoelectronic control in extrusion reactions of R_2I–F iodine(III) intermediates. *J. Chem. Soc. Perkin Trans. 2*, 2707–2714.

Chun, J. H.; Lu, S.; Pike, V. W. (2011) Rapid and efficient radiosynthesis of *meta*-substituted [^{18}F]fluoroarenes from [^{18}F]fluoride ion and diaryliodonium tosylates within a microreactor. *Eur. J. Org. Chem*., 4439-4447.

Chun, J. H.; Lu. S.; Lee, Y. S.; Pike, V. W. (2010) Fast and high yield microreactor syntheses of *ortho*-substituted [^{18}F]fluoroarenes from reactions of [^{18}F]fluoride ion with diaryliodonium salts. *J. Org. Chem. 75*, 3332-3338.

Coenen, H. H.; Moerlein, S. M. (1987) Regiospecific aromatic fluorodemetallation of group IVb metalloarenes using elemental fluorine and acetyl hypofluorite. *J. Fluor. Chem. 36*, 63-75.

Correia, J. D. G., Paulo, A., Santos, R., Santos, I. (2011) Radiometallated peptides for molecular imaging and targeted therapy. Dalton Trans. 40, 6144-6167.

Dibowski, H., Schmidten, F. P. (1998) Bioconjugation of peptides by palladium-catalyzed C-C cross-couplings in water. *Angew. Chem. Int. Ed. 37,* 476-478.

DiRaddo, P.; Diksic, M.; Jolly, D. (1984) The ^{18}F radiofluorination of arylsilanes. *J. Chem. Soc. Chem. Commun*. 159-160.

Duelli, R.; Enerson, B. E.; Gerhart, D. Z.; Drewes, L. R. (2000) Expression of large amino acid transporter LAT1 in rat brain endothelium. *J. Cereb. Blood Flow Metab. 20*, 1557-1562.

Erba, P. A., Sollini, M., Lazzeri, E., Mariani, G. (2013) FDG-PET in cardiac infections. *Semin. Nucl. Med. 43*, 377-395.

Ermert J.; Hocke, C.; Ludwig T.; Gail, R.; Coenen, R. R. (2004) Comparison of pathways to the versatile synthon of no-carrier-added 1-bromo-4-[^{18}F]fluorobenzene. *J. Labelled Compd. Radiopharm. 47*, 429-441.

Fani, M., Maecke, H. R. (2012) Radiopharmaceutical development of radiolabelled peptides. *Eur. J. Nucl. Med. Mol. Imaging. 39,* S11–S30.

Fischer, C. R.; Mu, L.; Becaud, J.; Schubiger, P. A.; Schibli, R.; Ametamey, S. M.; Graham, K. Stellfeld, T.; Dinkelborg, L. M.; Lehmann, L. (2011) ^{18}F-labelling of unactivated aromatic compounds using triarylsulfonium salts. *J. Labelled Compd. Radiopharm. 54*, S71.

Forngren, T.; Anderson, Y.; Lamm, B.; Langstrom, B. (1998) Synthesis of [4-^{18}F]-1-bromo-4-fluorobenzene and its use in palladium-promoted cross-coupling reactions with organostannanes. *Acta Chem. Scand. 52*, 475-479.

Fuchs, B. C.; Bode, B. P. (2005) Amino acid transporters ASCT2 and LAT1 in cancer: partners in crime? S*emin. Cancer Biol. 15*, 254-266.

Fuchs, B. C.; Finger, R. E.; Onan, M. C.; Bode, B. P. (2007) ASCT2 silencing regulates mammalian target-of-rapamycin growth and survival signaling in human hepatoma cells. *Am. J. Physiol. Cell Physiol. 293*, C55-C63.

Fukuda, H., Kubota, K., Matsuzawa, T. (2013) Pioneering and fundamental achievements on the development of positron emission tomography in oncology. *Tohoku. J. Exp. Med. 230*, 155-169.

Gail, R.; Coenen, H. H. (1994) A one step preparation of the n.c.a. fluorine-18 labelled synthons: 4-fluorobromobenzene and 4-fluoroiodobenzene. *Appl. Radiat. Isot. 45*, 105-111.

Gail, R.; Hocke, C.; Coenen, H. H. (1995) Direct n.c.a. ^{18}F-fluorination of halo- and alkylarenes via corresponding diphenyliodonium salts. *J. Labelled Compd. Radiopharm. 40*, 50-53.

Gao, Z., Gouverneur, V., Davis, B. G. (2013) Enhanced aqueous Suzuki-Miyaura coupling allows site-specific polypeptide ^{18}F-labeling. *J. Am. Chem. Soc. 135,* 13612-13615.

Gillings, N. (2013) Radiotracers for positron emission tomography imaging. *Magn. Reson. Mater Phy*. *26*, 149-158.

Gliddon, C. M.; Shao, Z.; LeMaistre, J. L.; Anderson, C. M. (2009) Cellular distribution of the neutral amino acid transporter subtype ASCT2 in mouse brain. *J. Neurochem. 108*, 372-383.

Grushin, V. V. (1992) Carboranylhalonium ions: from striking reactivity to a unified mechanistic analysis of polar reactions of diarylhalonium compounds. Acc. Chem. Res. 25, 529–536.

Hackel, B. J., Kimura, R. H., Miao, Z., Liu, H., Sathirachinda, A., Cheng, Z., Chin, F. T., Gambhir, S. S. (2013) ^{18}F-Fluorobenzoate-Labelled Cystine Knot Peptides for PET Imaging of Integrin $a_v\beta_6$. *J. Nucl. Med. 54,* 1101-1105.

Hayempour, B. J., Alavi, A. (2013) Neuroradiological advances detect abnormal neuroanatomy underlying neuropsychological impairments: the power of PET imaging. *Eur. J. Nucl. Med. Mol. Imaging. 40*, 1462-1468.

Hediger, M. A.; Romero, M. F.; Peng, J. B.; Rolfs, A.; Takanaga, H.; Bruford, E. A. (2004) The ABCs of solute carriers: physiological, pathological and therapeutic implications of human membrane transport proteins. *Pflugers Arch. 447*, 465-468.

Huang, C.; McConathy, J. (2013) Fluorine-18 labelled amino acids for oncologic imaging with positron emission tomography. *Curr. Top Med. Chem. 13*, 871-891.

Ishiwata, K.; Kubota, K.; Murakami, M.; Kubota, R.; Senda, M. (1993) A comparative study on protein incorporation of L-[methyl-^{3}H]methionine, L-[1-^{14}C]leucine and L-2-[^{18}F]fluorotyrosine in tumor bearing mice. *Nucl. Med. Biol. 20*, 895-899.

Ismail, F. M. D. (2002) Important fluorinated drugs in experimental and clinical use. *J. Fluorine Chem. 118*, 27-33.

Jager, P. L.; Vaalburg, W.; Pruim, J.; de Vries, E. G.; Langen, K. J.; Piers, D. A. (2001) Radiolabelled amino acids: basic aspects and clinical applications in oncology. *J. Nucl. Med. 42*, 432-445.

Kaira, K.; Oriuchi, N.; Shimizu, K.; Tominaga, H.; Yanagitani, N.; Sunaga, N.; Ishizuka, T.; Kanai, Y.; Mori, M.; Endo, K. (2009) ^{18}F-FMT uptake seen within primary cancer on PET helps predict outcome of non-small cell lung cancer. *J. Nucl. Med. 50*, 1770-1776.

Kapty, J., Kniess, T., Wuest, F., Mercer, J. R. (2011) Radiolabelling of phosphatidylserine-binding peptides with prosthetic groups N-[6-(4-[^{18}F]fluorobenzylidene)aminoxyhexyl]maleimide ([^{18}F]FBAM) and N-succinimidyl-4-[^{18}F]fluorobenzoate ([^{18}F]SFB). *Appl. Radio. Iso. 69,* 1218-1225.

Keidar, Z., Nitecki, S. (2013) FDG-PET in prosthetic graft infections. *Semin. Nucl. Med. 43*, 396-402.

Keiding, S., Pavese, N. (2013) Brain metabolism in patients with hepatic encephalopathy studied by PET and MR. *Arch. Biochem. Biophys. 536*, 131-142.

Kiick, K. L., Saxon, E., Tirrell, D. A., Certozzi, C. R. (2002) Incorporation of azides into recombinant proteins for chemoselective modification by the Staudinger ligation. *PNAS. 99,* 19-24.

Kilbourn, M. R.; Welch, M. J.; Dence, C. S.; Tewson, T. J.; Saji, H.; Maeda M. (1984) Carrier-added and no-carrier-added syntheses of [^{18}F]spiroperidol and [^{18}F]haloperidol. *Int. J. Appl. Radiat. Isot. 35,* 591-598.

Knight, J. C., Richter, S., Wuest, M., Way, J. D., Wuest, F. (2013) Synthesis and evaluation of an ^{18}F-labelled norbornene derivative for copper-free click chemistry reactions. *Org. Biomol. Chem. 11,* 3817-3825.

Knochel, A.; Zwernemann, O. (1991) Aromatic n.c.a. labelling with ^{18}F by modified Balz-Schiemann decomposition. *Appl. Radiat. Isot. 42*, 1077-1080.

Kouijzer, I. J. E., Bleeker-Rovers, C. P., Oyen, W. J. G. (2013) FDG-PET in fever of unknown origin. *Semin. Nucl. Med. 43*, 333-339.

Krasikova, R. (2007) Synthesis modules and automation in F-18 labelling. *Ernst Schering Res. Found Workshop 62*, 289-316.

Langen, K. J.; Bröer, S. (2004) Molecular transport mechanisms of radiolabelled amino acids for PET and SPECT. *J. Nucl. Med. 45*, 1435-1436.

Langen, K. J.; Hamacher, K.; Weckesser, M.; Floeth, F.; Stoffels, G.; Bauer, D.; Coenen, H. H.; Pauleit, D. (2006) *O*-(2-[^{18}F]fluoroethyl)-L-tyrosine: uptake mechanisms and clinical applications. *Nucl Med Biol. 33*, 287-294.

Lazarova, N.; Siméon, F. G.; Musachio, J. L.; Lu, S. Y.; Pike, V. W. (2007) Integration of a microwave reactor with Synthia to provide a fully automated radiofluorination module. *J. Labelled Compd. Radiopharm. 50*, 463–465.

Lee, E.; Kamlet, A. S.; Powers, D. C.; Neumann, C. N.; Boursalian, G. B.; Furuya, T.; Choi, D. C.; Hooker, J. M.; Ritter, T. (2001) A fluoride-derived electrophilic late-stage fluorination reagent for PET imaging. *Science 334*, 639-642.

Li, L., Hopkinson, M. N., Yona, R. L., Bejot, R., Bee, A. D., Gouverneur, V. (2011) Convergent ^{18}F radiosynthesis: a new dimension for radiolabelling. *Chem. Sci. 2*, 123-131.

Li, N., Lim, R. K. V., Edwardraja, S., Lin, Q. (2011) Copper-free Sonogashira cross-coupling for functionaliztion of alkyne-encoded proteins in aqueous medium and in bacterial Cells. *J. Am. Chem. Soc. 133,* 15316-15319.

Li, Y., Liu, Z., Harwig, C. W., Pourghiasian, M., Lau, J., Lin, K. S., Schaffer, P., Benard, F., Perrin, D. M. (2013) ^{18}F-click labelling of a bombesin antagonist with an alkyne-^{18}F-$ArBF_3^-$: *in vivo* PET imaging of tumors expressing the GRP-receptor. *Am J Nucl Med Mol Imaging. 3,* 57-70.

Linjing, M., Fischer, C. R., Holland, J. P., Becaud, J., Schubiger, P. A., Schibli, R., Ametamey, S. M., Graham, K., Stellfeld, T., Dinkelborg, L. M., Lehnmann, L. (2012) ^{18}F-Radiolabeling of aromatic compounds using triarylsulfonium salts. *Eur. J. Org. Chem*. *5*, 889–892.

Littich, R., Scott, P. J. H. (2013) Novel strategies for fluorine-18 radiochemistry. *Angew. Chem. Int. Ed. 51*, 1106-1109.

Lozza, C., Navarro-Teulon, I., Pelegrin, A., Pouget, J. P., Vives, E. (2013) Peptides in receptor-mediated readiotherapy: from design to the clinical aplication in cancer. *FONC. 247,* 1-13.

Lu, S. Y., Pike, V. W. (2007) Micro-reactors for PET tracer labelling. *Ernst Schering Res. Found Workshop. 62*, 271-287.

Mackenzie, B.; Erickson, J. D. (2004) Sodium-coupled neutral amino acid (System N/A) transporters of the SLC38 gene family. *Pflugers Arch*. *447,* 784-795.

Marriere, E.; Chazalviel, L.; Dhilly, M.; Toutain, J.; Perrio, C.; Dauphin, F.; Lasne, M. C. (1999) Synthesis of [^{18}F]RP 62203, a potent and selective serotonin 5-HT_{2A} receptor antagonist and biological evaluations with *ex-vivo* autoradiography. *J. Labelled Compd. Radiopharm. 42*, S69-S71.

Marriere, E.; Rouden, J.; Tadino, V.; Lasne, M. C. (2000) Synthesis of analogues of ()-cystine for *in vivo* studies of nicotinic receptors using positron emission tomography. *Organic Letters 8*, 1121-1124.

Martín-Santamaría, S.; Carroll, M. A.; Carroll, C. M.; Carter, C. D.; Pike, V. W.; Rzepa, H. S.; Widdowson, D. A. (2000) Fluoridation of heteroaromatic iodonium salts—experimental evidence supporting theoretical prediction of the selectivity of the process. *Chem. Commun.,* 649–650.

Martín-Santamaría, S.; Carroll, M. A.; Pike, V. W.; Rzepa, H. S.; Widdowson, D. A. (2000) An ab initio and MNDO-d SCF–MO computational study of the extrusion reactions of R2I–F iodine(III) via dimeric, trimeric and tetrameric transition states. *J. Chem. Soc. Perkin Trans. 2,* 2158– 2161.

McBride, W. J., D'Souza, C. A., Sharkey, R. M., Karacay, H., Rossi, E. A., Chang, C. H., Goldenberg, D. M. (2010) Improved ^{18}F labelling of peptides with a flouride-aluminum chelate complex. *Bioconjugate Chem. 21,* 1331-1340.

McConathy, J.; Goodman, M. M. (2008) Non-natural amino acids for tumor imaging using positron emission tomography and single photon emission computed tomography. *Cancer Metastasis Rev. 27*, 555-573.

Millar, B. C., Prendergast, B. D., Alavi, A., Moore, J. E. (2013) ^{18}FDG-positron emission tomography (PET) has a role to play in the diagnosis and therapy of infective endocarditis and cardiac device infection. *Int. J. Cardiol. 167,* 1724-1736.

Milstein, D.; Stille, J. K. (1979) Palladium-catalyzed coupling of tetraorganotin compounds with aryl and benzyl halides. Synthetic utility and mechanism. *J. Am. Chem. Soc. 17*, 4994-4998.

Nicklin, P.; Bergman, P.; Zhang, B.; Triantafellow, E.; Wang, H.; Nyfeler, B.; Yang, H.; Hild, M.; Kung, C.; Wilson, C.; Myer, V. E.; MacKeigan, J. P.; Porter, J. A.; Wang, Y. K.; Cantley, L. C.; Finan, P. M.; Murphy L. O. (2009) Bidirectional transport of amino acids regulates mTOR and autophagy. *Cell. 136*, 521-534.

Oka, S.; Okudaira, H.; Yoshida, Y.; Schuster, D. M.; Goodman, M. M.; Shirakami, Y. (2012) Transport mechanisms of trans-1-amino-3-fluoro[1-(14C)]cyclobutane-carboxylic acid in prostate cancer cells. Nucl. Med. Biol. 39, 109-119.

Ono, M.; Oka, S.; Okudaira, H.; Schuster, D. M.; Goodman, M. M.; Kawai, K.; Shirakami, Y. (2013) Comparative evaluation of transport mechanisms of trans-1-amino-3-[^{18}F]fluorocyclobutanecarboxylic acid and L-[methyl-^{11}C]methionine in human glioma cell lines. *Brain Res. 1535*, 24-37.

Pagani, M., Stone-Elander, S., Larsson, S. A. (1997) Alternative positron emission tomography with non-conventional positron emitters: effects of their physical properties on image quality and potential clinical applications. *Eur. J. Nucl. Med. 24*, 1304-1327.

Palestro, C. J. (2013) FDG-PET in musculoskeletal infections. *Semin. Nucl. Med. 43*, 367-376.

Park, B. K., Kitteringham, N. R., O'Neill, P. M. (2001) Metabolism of fluorine-containing drugs. *Annu. Rev. Pharmacol. Toxicol. 41*, 443.

Qaim, S. M. (2003) *Cyclotron production of medical radionuclides.* In: Vertes, A., Nagy, S., Klencsar, Z. Handbook of Nuclear Chemistry, Volume 4, Radiochemistry and Radiopharmaceutical Chemistry in Life Science. Kluwer Academic Publishers, 47-79.

Ramenda, T., Bergmann, R., Wuest, F. (2007) Synthesis of ^{18}F-labelled neurotensin(8-13) via copper-mediated 1,3-dipolar [3+2]cycloaddition *Reaction. Lett. Drug. Des. Discov. 4,* 279-285.

Richter, S., Wuest, M., Krieger, S. S., Rogers, B. E., Friebe, M., Bergmann, R., Wuest, F. (2013) Synthesis and radiopharmacological evaluation of a high-affinity and metabolically stabilized ^{18}F-labelled bombesin analoque for molecular imaging of gastrin-releasing peptide receptor-expressing prostate cancer. *Nucl. Med. Biol. 40,* 1025-1034.

Ross, T. L.; Ermert, J.; Hocke, C.; Coenen, H. H. (2007) Nucleophilic ^{18}F-fluorination of heteroaromatic iodonium salts with no-carrier-added [^{18}F]fluoride. *J. Am. Chem. Soc. 129*, 8018–8025.

Sathekge, M., Maes, A., VandeWiele, C. (2013) FDG-PET imaging in HIV infection and tuberculosis. *Semin. Nucl. Med. 43*, 349-366.

Satyamurthy, N.; Barrio, J. R. (2010) Nucleophilic fluorination of aromatic compounds. *Patent: WO 2010/008522* A2.

Schirrmacher, E., Wangler, B., Cypryk, M., Bradtmoller, G., Schafer, M., Eisenhut, M., Jurkschat, K., Schirrmacher, R. (2007) Synthesis of *p*-(Di-*tert*-butyl[^{18}F]fluorosilyl)benzaldehyde ([^{18}F]SiFA-A) with high specific activity by isotopic exchange: a convenient labelling synthen for the ^{18}F-labeling of N-amino-*oxy* derivatized peptides. *Bioconjugate Chem. 18,* 2085-2089.

Schubiger, P. A.; Lehmann, L.; Friebe, M. (Eds). (2007). *Ernst Schering Research Foundation Workshop 6:* PET Chemistry (1st edn.). Springer, Berlin, Germany.

Selivanova, S. V.; Combe, F.; Schubiger, A. P.; Ametamey, S. M. (2011) P-423 palladium catalyzed nucleophilic radiofluorination of aromatic compounds. *J. Labelled Compd. Radiopharm*. *54*, S512.

Shah, A.; Widdowson, D. A.; Pike V. W. (1995) Synthesis of substituted diaryliodonium salts and investigation of their reactions with no-carrier added [^{18}F]fluoride. *J. Labelled Compd. Radiopharm. 40*, 65-67.

Shiue, C-Y.; Watanabe, M.; Wolf, A. P.; Fowler, J. S.; Salvadori P. (1984) Application of the nucleophilic substitution reaction to the synthesis of no-carrier-added [^{18}F]fluorobenzene and other 18F-labelled aryl fluorides. *J. Labelled Compd. Radiopharm. 21,* 533-547.

Sonogashira, K.; Tohda, Y.; Hagihara, N. (1975) A convient synthesis of acetylenes: catalytic substitutions of acetylenic hydrogen with bromoalkenes, iodoarenes, and bromopyridines. *Tetrahedron Letters 50*, 4467-4470.

Sossi, V., Ruth, T. J. (2005) Micropet imaging: *in vivo* biochemistry in small animals. *J. Neural Transm. 112*, 319-330

Speranza, M.; Shiue, C.-Y.; Wolf, A. P.; Wilbur, D. S.; Angelini, G. (1985) Electrophilic radiofluorination of aryltrimethylsilanes as a general route to ^{18}F-labelled aryl fluorides. *J. Fluor. Chem. 30*, 97-107.

Steiniger, B.; Wuest, F. R. (2006) Synthesis of ^{18}F-labelled biphenyls via Suzuki cross-coupling with 4-[^{18}F]fluoroiodobenzene. *J. Labelled Compd. Radiopharm. 49*, 817-827.

Strauss, L. G., Conti, P. S. (1991) The Applications of PET in clinical oncology. *J. Nucl. Med. 32*, 623-648.

Surti, S,; Kuhn, A.; Werner, M. E.; Perkins, A. E.; Kolthammer, J.; Karp, J. S. (2007) Performance of philips gemini TF PET/CT scanner with special consideration for its time-of-flight imaging capabilities. *J. Nucl. Med. 48,* 471-480.

Surti, S., Karp, J. S., Popescu, L. M., Daube-Witherspoon, M. E., Werner, M. (2006) Investigation of time-of-flight benefit for fully 3-D PET. *IEEE Trans. Med. Imaging. 25*, 529-538.

Surti, S., Kuhn, A., Werner, M. E., Perkins, A. E., Kolthammer, J., Karp, J. S. (2008) The benefit of time-of-flight in PET imaging: experimental and clinical results. *J. Nucl. Med. 49*, 462-470.

Suzuki, A. (2002) Cross-coupling reaction via organoboranes. *Journal of Organometallic Chemistry 653*, 83-90.

Talukder, J. R.; Kekuda, R.; Saha, P.; Sundaram, U. (2008) Mechanism of leukotriene D4 inhibition of Na-alanine cotransport in intestinal epithelial cells. *Am. J. Physiol. Gastrointest. Liver Physiol. 295*, G1-G6.

Utsunomiya-Tate, N.; Endou, H.; Kanai, Y. (1996) Cloning and functional characterization of a system ASC-like Na+-dependent neutral amino acid transporter. *J. Biol. Chem*. *271*, 14883-14890.

Valk, P. E., Delbeke, D., Bailey, D. L., Townsend, D. W., Maisey, M. N. (2006) *Positron emission tomography: clinical practice*. Springer-Verlag London Ltd.

Vicente, A. M. G., Castrejón, A. S. (2013) New perspectives of PET/CT in oncology. *Méd. Nucl. 37,* 88-92.

Vos, F. J., Bleeker-Rovers, C. P., Oyen, W. J. G. (2013) The use of FDG-PET/CT in patients with febrile neutropenia. *Semin. Nucl. Med. 43*, 340-348.

Wang, L.; Zha, Z.; Qu, W.; Qiao, H.; Lieberman, B. P.; Plössl, K.; Kung, H. F. (2012) Synthesis and evaluation of ^{18}F labelled alanine derivatives as potential tumor imaging agents. *Nucl. Med. Biol. 39*, 933-943.

Watson, D. A.; Su, M.; Teverovskiy, G.; Zhang, Y.; Garcia-Fortanet, J.; Kinzel, T.; Buchwald, S. L. (2009) Formation of ArF from LPdAr(F): catalytic conversion of aryl triflates to aryl fluorides. *Science 325*, 1661-1664.

Way, J. D.; Wuest, F. (2014) Automated radiosynthesis of no-carrier added 4-[^{18}F]fluoroiodobenzene: A versatile building block in ^{18}F radiochemistry. *J. Labelled Compds. Radiopharm. 57*, 104-109.

Way, J., Bouvet, V., Wuest F. (2013) Synthesis of 4-[^{18}F]fluorohalo-benzenes and palladium-mediated cross-coupling reactions for the synthesis of ^{18}F-labelled radiotracers. *Curr. Org. Chem. 17,* 2138-2152.

Way, J., Wang, M., Hamann, I., Wuest, M., Wuest F. (2014) Synthesis and evaluation of 2-amino-5-(4-[^{18}F]fluorophenyl)pent-4-ynoic acid ([^{18}F]FPhPA): A novel ^{18}F-labelled amino acid for oncologic PET imaging. *Nucl. Med. Biol. 41,* 660-669.

Way, J.; Bouvet, V.; Wuest, F. (2013) Application of palladium-mediated cross-coupling reactions for the synthesis of ^{18}F-labelled compounds. *Curr. Org. Chem. 17*, 2138-2152.

Wester, H. J.; Herz, M.; Weber, W.; Heiss, P.; Senekowitsch-Schmidtke, R.; Schwaiger, M.; Stocklin, G. (1999) Synthesis and radiopharmacology of *O*-(2-[^{18}F]fluoroethyl)-L-tyrosine for tumor imaging. *J. Nucl. Med. 40*, 205-212.

Wilson, A. A.; Jin, L.; Garcia, A.; DaSilva, J. N.; Houle, S. (2001) An admonition when measuring the lipophilicity of radiotracers using counting techniques. *Appl. Radiat. Isot. 54*, 203-208.

Wuest, F. (2007) Fluorine-18 labelling of small molecules: the use of ^{18}F-labelled aryl fluorides derived from no-carrier-added [^{18}F]fluoride as labelling precursors. *Ernst. Schering Res. Found. Workshop. 62*, 51-78.

Wuest, F.; Berndt, M.; Kniess, T. (2008) Palladium-mediated cross-coupling reactions with [^{11}C]methyl iodide and 4-[^{18}F]fluorohalobenzenes for the synthesis of positron emission tomography (PET) radiotracers. Research Signpost. *Recent Advances of Bioconjugation Chemistry in Molecular Imaging. X. Chen (Ed.),* 155-173.

Wust, F. R.; Hohne, A.; Metz, P. (2005) Synthesis of ^{18}F-labelled cyclooxygenase-2 (COX-2) inhibitors via Stille reaction with 4-[^{18}F]fluoroiodobenzene as radiotracers for positron emission tomography (PET). *Org. Biomol. Chem. 3*, 503-507.

Wust, F. R.; Kniess, T. (2003) Synthesis of 4-[^{18}F]fluoroiodobenzene and its application in Sonogashira cross-coupling reactions. *J. Labelled Compd. Radiopharm*. *46*, 699-713.

Wust, F. R.; Kniess, T. (2004) No-carrier added synthesis of ^{18}F-labelled nucleosides using Stille cross-coupling reactions with 4-[^{18}F]fluoroiodobenzene. *J. Labelled Compd. Radiopharm. 47*, 457-468.

Wust, F. R.; Kniess, T. (2005) *N*-Arylation of indoles with 4-[^{18}F]fluoroiodobenzene: synthesis of ^{18}F-labelled s_2 receptors ligands for positron emission tomography (PET). *J. Labelled Compd. Radiopharm. 48*, 31-43.

Zaidi, H. (2006) Recent developments and future trends in nuclear medicine instrumentation. *Z. Med. Phys*. *16*, 5-17.

Zhang, M. R.; Kumata, K.; Suzuki, K. (2007) A practical route for synthesizing a PET ligand containing [^{18}F]fluorobenzene using reaction of phenyliodonium salt with [^{18}F]F^{-}. *Tetrahedron Lett. 48*, 8632-8635.